Identification and characterization of HIRIP3 as a novel histone H2A chaperone

Maria Ignatyeva

UNIVERSITÉ DE STRASBOURG

ÉCOLE DOCTORALE DES SCIENCES DE LA VIE ET DE LA SANTE

[Institut de génétique et de biologie moléculaire et cellulaire (IGBMC) - UM 41/UMR 7104/UMR_S 964]

THÈSE présentée par :

[Maria IGNATYEVA]

soutenue le : **31 Mai 2017**

pour obtenir le grade de : **Docteur de l'université de Strasbourg**

Discipline/ Spécialité : Aspects Moleculaires et Cellulaires Biologie

Identification et caractérisation de HIRIP3 comme nouveau chaperon d'histone H2A

[Identification and characterization of HIRIP3 as a novel histone H2A chaperone]

THÈSE dirigée par :
[M. HAMICHE Ali] Directeur de recherches, Université de Strasbourg

RAPPORTEURS :
[Mme. AMEYAR-ZAZOUA Maya] Chercheur statutaire, Institut Necker Enfants Malades
[M. THIRIET Christophe] Directeur de recherches, Université de Nantes

---

AUTRES MEMBRES DU JURY :
[M. DAVIDSON Irwin] Directeur de recherches, Université de Strasbourg

TABLE OF CONTENTS

ACKNOWLEDGEMENT

I wish to thank my thesis director, Ali HAMICHE, for giving me the opportunity to pursue PhD thesis in his group. I'm grateful for his continuous support, motivation and guidance.

I would like to express my sincere gratitude to my thesis committee, Maya AMEYAR-ZAZOUA, Christophe THIRIET and Irwin DAVIDSON, for their expertise and evaluation of my work.

I would like to thank Christian BRONNER for his help with manuscript preparation and thesis revision. I'm highly grateful to all present and former laboratory members for the productive lab environment and their invaluable help: Philippe RAMAIN, Catherine RAMAIN, Isabelle STOLL, Khalid OUARARHNI, Chrysa LATRICK, Christophe PAPIN, Abdulkhaleg IBRAHIM, Muhammad Shuaib, Alexia VIDAL, Arslan IFTIKHAR and Hatem SALEM.

I would like to thank Stefan Dimitrov for kindly providing the anti-H2A.Z and anti-H2A antibodies used in this study.

I want to thank IGBMC cell medium preparation and antibody generation facilities, whose services I used during my study. I'm also grateful to IGBMC human resources and PhD Office for their help with administrative questions.

I gratefully acknowledge the staff of doctoral school of the University of Strasbourg for giving me all necessary assistance during my studies, especially Melanie MUSER and Geraldine SCHVERER.

Finally, I would like to sincerely thank all my friends and family for their support during my PhD study.

LIST OF ABBREVIATIONS

ACF – ATP-utilizing chromatin assembly and remodelling factor

ANP32E – acidic nuclear phosphoprotein 32 family member E

ARPs – actin related proteins

Asf1 – anti-silencing function protein 1

ATRX – α-thalassemia mental retardation X-linked protein

BAF – brahma-associated factor

BAP – brahma associated protein

BPTF – bromodomain PHD finger transcription factor

CAC – chromatin assembly complex

CAF-1 – chromatin assembly factor 1

CBP – CREB-binding protein

CHD – chromodomain Helicase DNA-binding

ChIP-seq – chromatin immunoprecipitation sequencing

CHRAC – chromatin accessibility complex

CRC – chromatin remodelling complexes

DAXX – death-associated protein 6

DMAP1– DNA methyltransferase-associated protein 1

DNMT1 – DNA methyltransferase 1

DSB – double-strand break

FACT – facilitates chromatin transcription.

GAS41– glioma amplified sequence 41

HIRA – histone cell cycle regulation-defective homolog A

HIRIP3 – HIRA-interacting protein 3

HSA – helicase-SANT-associated

HSP70 – heat shock protein family 70

INO80 – inositol requiring 80

ISWI – imitation SWItch

MCS – multiple cloning site

NoRC – nucleolar remodelling complex

NURF – nucleosome remodelling factor

PCNA – polymerase sliding clamp proliferating cell nuclear antigen

PTM – post translational modification

PTMs – Post-translational modifications

RBPs – recombinant baculovirus particles

RC – replication coupled

RCAF – replication-coupling assembly factor

RI – replication independent

RSC – Chromatin structure remodelling

RSF – remodelling and spacing factor

SLBP – stem-loop binding protein

SLBP – stem-loop binding protein

SRCAP – SNF2-related-CBP activator protein

SWI/SNF – SWItch/Sucrose-Non-Fermenting

SWR1 – Swi2/Snf2-Related 1

TAP – Tandem affinity purification

TF – transcription factor

ToRC – Toutatis-containing chromatin remodelling complex

XNP – X-linked nuclear protein

LIST OF FIGURES

LIST OF TABLES

1 FOREWORD

The genome of eukaryotic cells is packaged into chromatin, a highly organised complex of DNA and proteins. Chromatin functions as a scaffold for all processes of DNA metabolism, such as replication, repair and transcription. High order chromatin structure stability ensures normal cell cycle progression[1], differentiation during development[2] and epigenetic inheritance[3]. There are growing evidence linking deregulated histone synthesis and deposition with human cancers and other diseases[1,4]. The establishment of chromatin and its following maintenance requires processes of replication-coupled and replication-independent chromatin assembly. There are extensive number of factors involved into chromatin assembly, with ATP-dependent assembly factors and histone chaperones groups being most prominent[5]. Our understanding of chromatin assembly dynamics relies on identification of its factors and their functions and interactions. This project is dedicated to characterization of two factors of chromatin assembly machinery.

The first factor studied in this work was HIRIP3, a mammalian protein homologous to yeast H2A.Z-depositing chaperone Chz1[6]. We aimed to test whether HIRIP3 has characteristics of histone chaperone itself. At first we used TAP (Tandem affinity purification)-TAG purification approach to characterize HIRIP3 complex *in vivo* and established its interacting partners, including histones. Afterword, we moved to *in vitro E. coli* expression system to characterize the structural specificity of HIRIP3 interaction with histones. We have characterized HIRIP3 as a novel histone chaperone specific for H2A, that utilizes its CHZ motif-containing 403-527 region to interact with H2A C-terminal alphaC helix.

The second part of this work was the continuation of the studies on YL1 carried out previously in our laboratory, for which we have shown to be a H2A.Z-specific deposition histone chaperone belonging to the SRCAP complex[7]. SRCAP complex is a mammalian chromatin remodelling complex consisting of 10 subunits, including ATPases, actin-related proteins, histone chaperone and transcriptional co-activators. The interplay and functional connection between its subunits is still not elucidated. In this study we aimed to decipher the interaction network within the SRCAP complex and to identify functional sub-complexes within it. At first, we have identified YL1 interaction with TIP49A and TIP49B ATPases. Using YL1 and TIP49A/B proteins as a functional core, we have identified and reconstituted YL1, SRCAP, TIP49A, TIP49B, H2A.Z/H2B complex using baculovirus expression system.

This sub-complex contained all factors sufficient for chromatin remodelling activity of SRCAP complex, thus acting as a functional module.

2 RÉSUMÉ EN FRANÇAIS

La chromatine est un complexe d'ADN et de protéines qui forme des chromosomes dans le noyau des cellules eucaryotes[8]. L'unité structurale répétitive de la chromatine est le nucléosome, qui est constitué de 145-147 pb d'ADN s'enroulant autour d'un octamère d'histones constitué d'un tétramère d'histone $(H3\text{-}H4)_2$ et de deux dimères d'histones H2A/H2B[9]. La chromatine fonctionne à la fois comme un échafaudage et un régulateur de tous les processus de métabolisme de l'ADN, tels que la réplication, la réparation et la transcription. Au cours de ces processus, la structure de la chromatine est soumise à une perturbation temporaire suivie d'une reformation en temps opportun, qui nécessite l'assemblage de la chromatine. L'assemblage de la chromatine est nécessaire pour la formation *de novo* de la chromatine et pour le recyclage/remplacement des histones qui se produit sur les nucléosomes existants. Il y a deux grands groupes de facteurs impliqués dans l'assemblage de la chromatine; les facteurs d'assemblage dépendant de l'ATP et les chaperons d'histones[5].

Les chaperons d'histone sont un groupe constitué de diverses protéines qui lient physiquement les histones. Leur structure est variée, avec des chaînes d' acide-aminés, fréquemment riches en acide glutamique et aspartique. Ces chaînes se retrouvent souvent près des extrémités C-terminales des chaperons. Les chaperons d'histone jouent un rôle critique dans toutes les étapes du cycle des histones. Ils protègent, notamment, les histones des interactions et des modifications non-spécifiques, facilitent le recrutement d'histones à la chromatine et sont impliqués dans l'incorporation, l'éviction et l'échange des nucléosomes[10].

L'assemblage de la chromatine est un processus clé dans l'organisation de la structure de la chromatine, dont la stabilité assure la progression normale du cycle cellulaire[1] et la différenciation au cours du développement[2]. La synthèse dérégulée des histones et l'assemblage non conforme de la chromatine pourraient contribuer à la tumorigénèse[1]. Il existe des preuves croissantes liant l'échec dans le dépôt de variants d'histone et l'apparition de cancers humains et d'autres maladies[4].

Afin d'améliorer les connaissances sur la dynamique des histones, nous devons identifier tous les facteurs impliqués dans la déposition / éviction des histones. En 2014, notre laboratoire a identifié le premier chaperon pour H2A.Z impliqué dans son éviction de la chromatine[11]. Récemment, notre laboratoire a encore découvert et caractérisé la protéine YL1 comme un

chaperon de déposition pour H2A.Z[7]. Pour étudier plus en profondeur le mécanisme de la dynamique de H2A.Z chez les mammifères, nous avons analysé la fonction de la protéine HIRIP3. HIRIP3 est une protéine de mammifère de 556 acides aminés homologue au chaperon de Chz1 de levure H2A.Z-déposant[6]. La structure cristalline confirme son interaction spécifique avec le dimère H2A.Z/H2B, le motif CHZ de Chz1 étant critique pour sa stabilisation[12]. Le motif CHZ est conservé parmi la famille Chz1 et il est situé dans la partie C-terminale de HIRIP3. HIRIP3 a été initialement découvert comme un partenaire interactif de HIRA[13]. HIRA est un chaperon histone qui incorpore le variant d'histone H3.3 aux sites de transcription active d'une manière indépendante de la réplication[14].

Compte tenu de cette information sur HIRIP3, j'ai tenté de déchiffrer son implication possible dans la dynamique des histones et de la placer dans le contexte de la machinerie de la chromatine.

Pour évaluer le rôle de HIRIP3 dans la dynamique de la chromatine, j'ai commencé à tester son interaction avec les dimères d'histones H2A/H2B et H2A.Z/H2B *in vitro*. L'interaction physique avec les histones est un indicateur important de l'activité de chaperon d'histone. Dans ce but, les plasmides exprimant des histones H2A/H2B ou H2A.Z/H2B marquées ont été co-exprimées avec HIRIP3 dans *E. coli* et testées pour l'interaction physique directe. HIRIP3 a montré une interaction avec H2A/H2B et H2A.Z/H2B avec presque la même affinité. Il est possible que HIRIP3 puisse fonctionner en liant H2A et H2A.Z, mais il est également possible qu'une seule paire d'interactions soit biologiquement pertinente, avec une spécificité acquise par interaction avec d'autres facteurs, des changements conformationnels ou des modifications post-traductionnelles des histones.

Pour tenter de répondre à la question de qui est le partenaire de dimère fonctionnel pour HIRIP3 *in vivo*, j'ai utilisé l'approche TAP-TAG pour purifier les protéines qui interagissent directement avec HIRIP3 *in vivo*. La lignée cellulaire HeLa exprimant de façon stable le HIRIP3 marqué a été générée en utilisant une approche de transduction rétrovirale. L'immunopurification en tandem de HIRIP3 à partir d'extraits nucléaires HeLa nous a permis d'identifier des protéines interagissant directement avec HIRIP3. La spectrométrie de masse et l'analyse par Western blot du complexe HIRIP3 purifié ont identifié des dimères d'histones H2A/H2B en tant que partenaires interagissant avec ce chaperon. De manière surprenante, on n'a pas trouvé les dimères H2A.Z/H2B pouvant potentiellement s'associer au complexe HIRIP3. Ceci implique que même si HIRIP3 a une affinité et peut lier les deux dimères *in vitro*, il interagit exclusivement avec les dimères H2A/H2B *in vivo*.

L'analyse par spectrométrie de masse du complexe HIRIP3 a également révélé la présence de la kinase CK2 dans le complexe. CK2 est une sérine/thréonine kinase omniprésente évolutive qui participe à une série complexe d'événements cellulaires, incluant la régulation des gènes, la progression du cycle cellulaire et le maintien de la viabilité cellulaire[15]. Un certain nombre de cibles potentielles pour CK2 ont un rôle dans le métabolisme de la chromatine[16]. En effet, il a été démontré que CK2 phosphoryle et interagit *in vitro* avec HIRIP3[17]. La présence de CK2 dans le complexe HIRIP3 pourrait jouer un rôle dans la phosphorylation de HIRIP3 ou avoir d'autres fonctions inconnues dans le contexte du complexe HIRIP3. Pour tester cette dernière possibilité, j'ai utilisé un test de phosphorylation pour tester si CK2 peut phosphoryler les dimères H2A/H2B. Dans ce but, j'ai généré deux mutants H2A non phosphorylables (S1A et S122A). L'essai de phosphorylation a révélé que CK2 peut phosphoryler l'histone H2A entière et le mutant S122A mais pas le mutant S1A. La mutation S1A a complètement supprimé la phosphorylation du H2A, ce qui indique que le site de la Serine 1 est critique pour la phosphorylation de l'histone H2A. Cette découverte implique une connexion fonctionnelle entre les dimères HIRIP3/CK2 et H2A/H2B qui est réalisée par la phosphorylation et donne un aperçu possible sur la dynamique d'interaction de HIRIP3 et H2A.

L'étape suivante consistait à caractériser davantage l'interaction HIRIP3 et H2A/H2B en cartographiant le domaine HIRIP3 impliqué dans la reconnaissance et la liaison avec les histones. Pour atteindre cet objectif, j'ai utilisé une structure basée sur l'analyse mutationnelle de HIRIP3. L'analyse de suppression a permis de déterminer le domaine minimal de HIRIP3 requis pour l'interaction avec l'histone H2A. L'analyse initiale a identifié une région entre 403-527 comme nécessaire pour l'interaction avec les dimères H2A/H2B. D'autres mutants de déletion ont identifié le motif CHZ de HIRIP3 comme requis pour l'interaction avec les dimères H2A/H2B.

L'étape suivante consistait à identifier le domaine H2A qui interagit avec HIRIP3. Pour ce faire, j'ai généré des troncatures de H2A à partir de l'extrémité C-terminale. Les troncatures ont été sélectionnées sur la base des données disponibles dans la littérature montrant l'importance de l'hélice alphaC de l'histone H2A pour l'interaction avec plusieurs chaperons d'histones. J'ai co-exprimé les mutants tronqués H2A avec la région 397-556 de HIRIP3, qui contient le motif CHZ, et testé leur interaction. Les acides aminés 98-111 de H2A se sont révélés être critiques pour l'interaction avec HIRIP3. Cette région contient l'hélice alphaC, qui s'est avérée nécessaire pour l'interaction avec un certain nombre de chaperons du groupe H2A, tels que YL1[7], Anp32E[11] et Chz1[18].

Ce travail montre que HIRIP3 de mammifère interagit avec H2A d'une manière similaire à la levure Chz1 pour H2A.Z, en utilisant le motif hautement conservé CHZ. La divergence des histones chaperonées par la protéine contenant des motifs CHZ peut être attribuée à des changements évolutifs dans la machinerie de la chromatine et à différentes exigences cellulaires entre la levure et les mammifères. En comparaison avec Chz1, HIRIP3 contient des régions N-terminales additionnelles, telles que des régions à polarisation Glu et Poly-ser. Ces régions peuvent contribuer à l'interaction plus grande entre HIRIP3 et H2A, comme montré dans notre étude, avec la région 403-527, critique pour l'interaction. Ils peuvent également servir d'échafaudage pour l'interaction avec d'autres protéines, telles que HIRA, qui a été montré pour interagir avec HIRIP3[13]. Ces régions supplémentaires peuvent également contenir des motifs qui pourraient être ciblés par des modifications post-traductionnelles telles que la phosphorylation par la kinase CK2, et pourraient donc contribuer à des interactions et à des fonctions HIRIP3 uniques. La phosphorylation par CK2 est connue pour réguler la localisation et la fonction des chaperons d'histones comme montré pour le chaperon Nap1[19].

En résumé, ce travail a été consacré à la compréhension de la fonction du chaperon d'histone HIRIP3. J'ai montré que HIRIP3 forme un complexe avec les dimères d'histones H2A/H2B à la fois *in vitro* et *in vivo*. HIRIP3 lie H2A domaine par son côté C-terminal, à travers son motif CHZ, qui est conservée au cours de l'évolution de la levure à l'homme. HIRIP3 interagit avec H2A d'une manière similaire à Chz1 de levure qui interagit avec H2A.Z en utilisant l'hélice alpha C localisée dans la région C-terminale. En conclusion, notre étude a établi HIRIP3 comme un nouveau chaperon H2A qui utilise le motif conservé de CHZ pour interagir avec H2A par son hélice alpha C-terminale.

3 INTRODUCTION

3.1 Nucleosome composition

Chromatin is a complex of DNA and proteins that forms chromosomes within the nucleus of eukaryotic cells[8]. The repeating structural unit of chromatin is nucleosome, which is comprised of 145–147 bp of DNA wrapped around a histone octamer in 1.65 turns of a flat, left-handed superhelix[9]. An octamer has a tripartite organisation, with a central $(H3–H4)_2$ tetramer flanked by two H2A–H2B dimers[20,21]. $(H3–H4)_2$ tetramer organizes the core of nucleosome, while H2A–H2B dimers are located on periphery and thus are more easily accessible. Linker histone H1 is located outside octamer, close to DNA entry/exist point in nucleosome. It is present in most, but not all, eukaryotic cell, with a frequency of approximately one molecule per nucleosome[22]. Histone octamers are linked together by linker DNA of 20-80 bp.

In mammals all histone genes are found in 2 histone clusters[23]. Their expression is dependent on cell cycle phase, with a 35 fold increase before S phase for canonical histones[24]. Unlike mRNA of other proteins, canonical histone mRNA is not polyadenylated. It possesses a conserved stem-loop, which is recognised by SLBPs (stem-loop binding proteins). SLBPs play major part in histone pre-mRNA processing and protection from degradation.

Histones are usually 9-14 kDa proteins, rich in arginine and lysine. There are a few exceptions with unconventional molecular weight, such as macroH2A, that contains an additional 30-kDa non-histone domain[25]. Histones possess two distinguished structural elements – histone fold and histone tails. Histone fold is a structured region, highly conserved among core histones[21]. This fold consists of three alpha-helices connected by two loops, L1 and L2. The histone tails are intrinsically disordered structures that protrude from the surface of nucleosome. This disorder helps connections with neighbouring nucleosomes or with nuclear factors. Histone tails also play an essential role in the folding of nucleosomal arrays into higher-order structures. Majority of studied histones post-translation modifications are located on those tails, with only a few identified on the core[26].

Nucleosomes are stabilised by a number of factors. First level is direct histone–histone and histone–DNA interactions. The tetramer structure is defined by interaction of H3-H4 pairs through a 4-helix bundle formed from both H3 histones[9]. The interaction between

tetramer and each H2A–H2B is facilitated through a second, homologous 4-helix bundle between H2B and H4 histone folds. Another source of stabilisation is the bridging of positively charged histone folds and negatively charged phosphate groups of DNA, with each histone-fold pair associated with 27–28 bp of DNA[27]. Water molecules also contribute to nucleosome stability by strengthening direct protein–DNA interactions and enabling formation of many additional interactions between more distantly related elements[28]. The presence of variant histones in nucleosome also has an impact on nucleosome stability. For example, incorporation of MacroH2A contribute to the rigidity of the nucleosome structure[29], while incorporation of H2A.bbd leads to its increased flexibility of the nucleosome[30]. Considering this information about nucleosomes, they can be characterised as a highly stable building blocks of chromatin that protect and organise DNA.

3.2 Chromatin organisation

Chromatin is organised in a way that allows both compaction of DNA in order to fit into the nucleus and accessibility of DNA for all the processes of the DNA metabolism. Chromatin was discovered to be hierarchically packaged into fibres of increased complexity[31] (Fig. 1). At the first level, nucleosomes together with linker histones and linker DNA form a 10-nm fibres that resemble "beads on a string" structures under microscope[32]. Those 10-nm fibres are further getting packaged into secondary level of compaction – 30-nm fibres. This compaction of chromatin is modulated by a number of factors: electrostatic interactions between nucleosomes[33], nucleosome repeat length[34], linker histones[34,35] and divalent cations[35] such as Mg^{2+} which reduce the repulsive forces between linker DNA. One of the key histone regions that is involved into compaction of chromatin, comprises of residues 14–19 of N-terminal tail of histone H4. Acetylation of histone H4 on lysine 16 can disrupt nucleosome-nucleosome contacts, inhibiting the formation of compacted 30-nm fibers[36]. H1 histone stabilizes the chromatin 30 nm fibre by acting on the path of DNA at the exit of the nucleosome[37]. It shields the excess negative charge of the linker DNA to promote the folding of the chromatin, while its depletion leads to the decondensation of chromatin[22].

There are a number of 30-nm chromatin fibres observed *in vitro*, such as solenoidal one-start helix[31], ribbon two-start helix[38] and other structures. They are topologically different, with 24- to 25-nm one-start helix having a zigzag arrangement of stacked nucleosome cores and 34-nm two-start helix having arrangement of interdigitated

nucleosomes from adjacent gyres[33]. The differences in observed structures are caused by the variations of linker histones amount, nucleosome repeat length and other conditions. Those structures obtained using electron microscopy and x-ray crystallography methods have established the notion that chromatin fibres possess intrinsic helical formation.

The third level of compaction – tertiary structure – is achieved with tail-mediated self-association of fibres. Thus 30-nm fibres are further condensed to interphase fibres or the even more highly compacted metaphase chromosome structures. In metazoan genomes each chromosome is located largely as an individual formation within chromatin, called chromatin territory[39]. Chromatin territories are highly interconnected within and between each other, which is achieved by remote intra- and interchromosomal contacts facilitated by active domains of each territory[40].

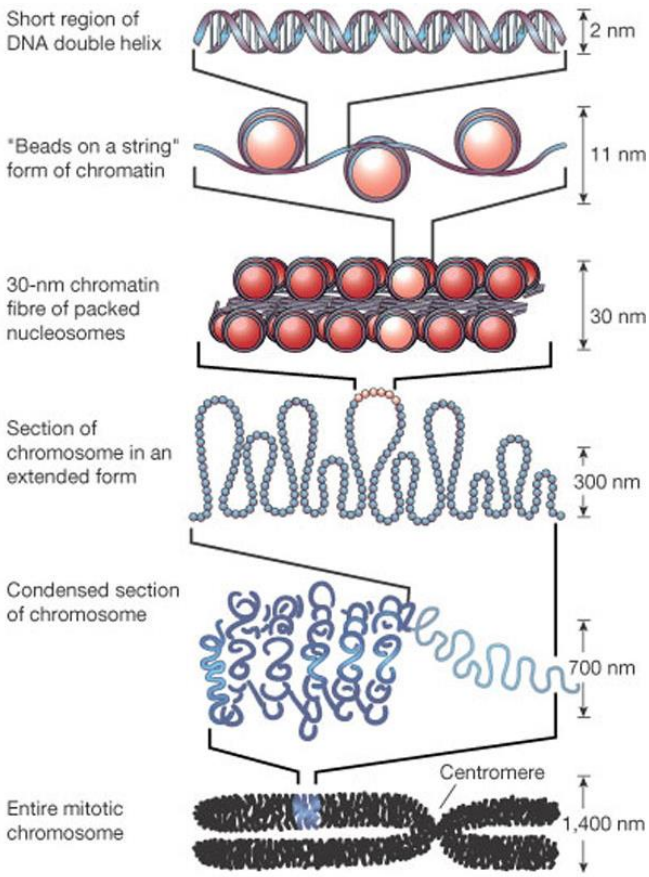

Figure 1. Hierarchical chromatin organisation.

The DNA helix is wrapping around the nucleosome to form a linear "beads on a string" resembling structures. These structures condense into 30-nm fibres that possess helical periodicity. Further condensation leads to a more rigid chromatin fibres, several hundred nanometres in diameter. Mitotic chromosomes are the final level of chromatin compaction in the cell.
(Modified from Felsenfeld et al., 2003[41]).

Recent studies, such as electron tomography assessed 3D structure of chromatin, reveal a prevalence of open, asymmetrical 3D zig-zag nucleosomal structures in nucleus[42,43]. These studies indicate the presence of highly dynamic chromatin, which is more compatible with 10-nm fibre than the rigid 30-nm one[44]. These 10-mm fibres possess highly dynamic, liquid-like system characterisrics[45], such as chromatin fluctuations. These fluctuations process may facilitate protein mobility, DNA exposure and interaction between close regions of chromatin[46]. Liquid-like chromatin is implicated to be a highly assessable substrate for the transcriptional regulatory machinery[42].

The diversity of observations of chromatin structures, such as hierarchical helix-repeating 30-nm fibres and dynamic and disordered 10-nm fibres rise a question of how those structures can coexist in nucleus. The presence of both types in the same cells was demonstrated, with transcriptionally inactive 30-nm and more structures located on periphery, while 10-nm dynamic transcriptionally active structures located in the center[47]. Such spatial positions are shared with another structure observed in chromatin, i.e., topologically associating domains (TADs)[48]. TADs are defined by boundaries consisting of housekeeping genes and insulator sites. In TADs, more active chromatin is shown to be located internally, while repressive chromatin on the periphery[49]. Active and inactive genes regions are spatially differentiated and are shown to cluster within nucleosome[29]. Taken together, these observations support the notion of compartmentalised high-order chromatin organisation, with non-randomly located and highly interconnected distinct regions[50,51].

3.3 Chromatin regulation

Chromatin is regulated by a number of diverse cellular processes, such as DNA methylation, RNA inhibition, histone PTM modifications, chromatin remodelling and assembly. Another layer of complexity comes from chromatin architectural proteins, such as polycomb group proteins or silencing proteins that can also affect chromatin structure and functions[52]. Chromatin is assuming different functional states defined by combinations of regulatory proteins, transcription factors, PTMs and other factors[49,53]. There is recognition of at least five chromatin types[49,54]: two distinct types of transcriptionally active chromatin that harbour different sets of genes, polycomb-repressed chromatin, HP1-repressed chromatin and null chromatin, a strongly repressive chromatin type that lacks HP1 or polycomb proteins.

The interplay between chromatin regulation factors regulate the diversity of processes and events occurring in cells.

3.3.1 Histone post-translational modifications

Post-translational modifications (PTMs) are various modifications of proteins that occurs during or after protein biosynthesis. Histone PTMs are introduction of various functional groups or moiety on the amino-terminal and carboxy-terminal histone tail residues[55]. Those modifications are introduced by the processes of acetylation and methylation of lysines and arginines, phosphorylation of serines and threonines, ubiquitylation and sumoylation of lysines and others processes. Additional level of complexity is achieved by the fact that lysine and arginine could accept more than one methyl group. More PTMs are identified every year, leading to possibility that nearly every solvent accessible histone residue may be a target for post-translational modification[55]. In yeast a number of histone PTMs are essential for viability[26]. The PTMs of histone residues have a big impact on chromatin structure and functions. PTMs act by either altering chromatin accessibility or folding, or altering binding of effector molecules[56].

Interplay between histone acetylation and deacetylation acts as a molecular switch between permissive and repressed chromatine[57]. Acetylation neutralize positive charge of target residue, which leads to destabilization of interaction between the histones and DNA[56]. This alters folding of nucleosome fibre, thus making chromosomal domains more accessible. Domain-wide acetylation helps both initiation of transcription and its elongation[58]. Acetylated lysines are recognised by bromodomains, that are often present in HATs and chromatin-associated proteins complexes[59]. Those lysines can also act as marks for bromodomain-containing transcription factors[60]. Acetylation is regulated by the opposing action of two families of enzymes, histone acetyltransferases (HATs) and histone deacetylases. There is an important role of acetylation of histones H3 and H4 in chromatin assembly. Disruption of acetylation on both histone tails lead to defects in nucleosome deposition and to a G2 cell-cycle arrest[61]. This acetylation is thought to mediate a reversible neutralization of the lysine charge that facilitates chromatin assembly[62].

Histone phosphorylation has diverse functions, such as DNA damage response, transcriptional activation and chromatin compaction[63]. Phosphorylation adds significant negative charge to the histone that can influence chromatin structure[56]. Phosphorylation of H4

and H2A-group of histones has a critical role during DNA repair[64,65], while phosphorylation of H3 group is necessary for the changes in chromatin structure for both genes activation and condensation during mitosis[66]. H3 phosphorylation and can temporarily relieve the silencing of specific genes, allowing transient transcription without affecting epigenetic memory[67]. Cell cycle progression is dependent on phosphorylation of histones, as shown for H3, H4 and H1 linker histones[66]. Its precise regulation is achieved by dynamic phosphorylation and dephosphorylation by the help of numerous identified kinases and phosphatases.

Histone methylation differs from acetylation and phosphorylation since it doesn't change the target charge, thus acting as a mark for other factors to carry out its function[56]. Histone lysine methylation can be involved in either activation or repression of transcription, depending on the sites of methylation. Thus, methylation of H3K4, H3K36, and H3K79 is associated with activation, whereas methylation of H3K9, H3K27, and H4K20 is associated with repression[68]. Methylation is shown to be involved into genome wide silencing. H3K9 methylation is a marker of both constitutive and facultative heterochromatin[69]. Histone methylation is carried out by histone lysine methyltransferases and arginine methyltransferases. For a long time it was considered that demethylation of histones is not naturally occurring[70], but in 2004 the first lysine demethylases have been discovered[71].

There are also number of other PTMs that affect chromatin structure and functions. Ubiquitylation adds a 76 amino acid long protein to the histone, that likely causes conformational changes in nucleosome[56]. Sumoylation introduces small ubiquitin-like modifier molecules to the histones and has a role in nucleocytoplasmic signalling, transport control and regulation of gene expression[72].

There are number of functional states and cellular events that correlate with a group of different histone PTMs. For example, transcriptional activation is associated with H4K8 and H3K14 acetylation and H3S10 phosphorylation, while transcriptional repression is associated with tri-methylation of H3K9 and the lack of H3 and H4 acetylation[55]. These examples implicate that in some cases histone modifications may propagate states as a group rather than alone. The idea that various PTMs, acting in a combinatorial or sequential fashion, together define specific chromatin states was described as the histone code hypothesis [73]. There are a large amount of proteins identified that establish, process and maintain histone code – writers, readers and erasers[74] of PTMs (Fig. 2). This machinery modify histone PTMs landscape in a highly dynamic reversible way, in order to modulate such processes of DNA metabolism, as transcription activation and repression, DNA replication and DNA repair.

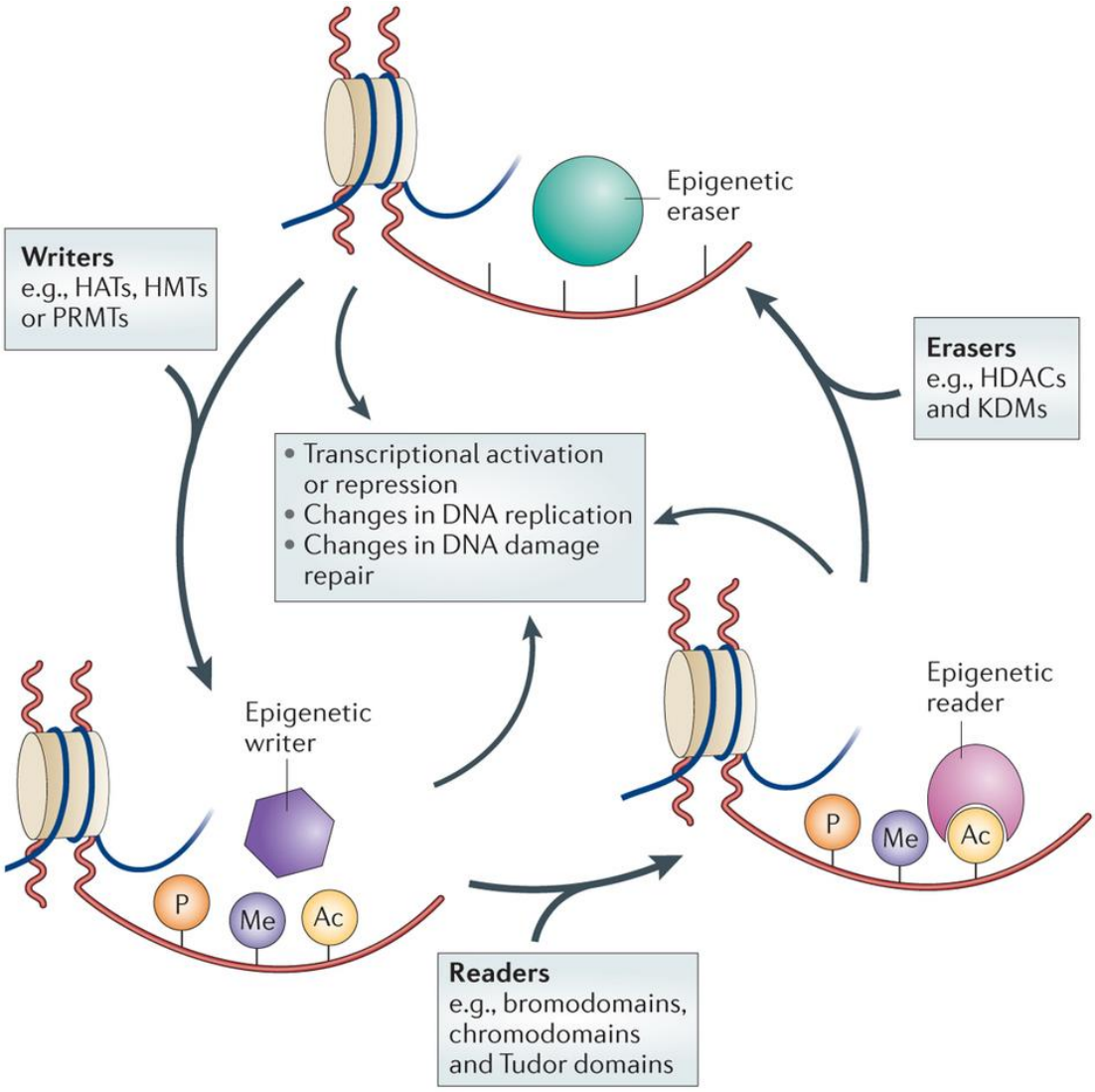

Figure 2. Interplay between writers, readers and erasers of PTMs.

Epigenetic writers such as histone acetyltransferases (HATs), histone methyltransferases (HMTs), protein arginine methyltransferases (PRMTs) and kinases create epigenetic marks on amino acid residues on histone tails. Epigenetic readers such as proteins containing bromodomains, chromodomains and Tudor domains recognise and bind to these epigenetic mark. Epigenetic erasers such as histone deacetylases (HDACs), lysine demethylases (KDMs) and phosphatases catalyse the removal of epigenetic marks. The interplay between those factors regulates processes of DNA metabolism.
(Modified from K. J. Falkenberg and R. W. Johnstone[75])

Nowadays histone code model is enriched by studies revealing complex crosstalk between histone PTMs. Some PTMs may either facilitate or block other PTMs on the same histone tail[60]. For example, there is a strong correlation between methylation of H3K4 and acetylation of H3K14[76]. It was demonstrated that trimethylated H3K4 binds PHD finger domain of Yng1, that is a part of NuA3 HAT, which subsequently acetylates H3K14[77]. As an

example of antagonising PTMs, it was shown that H3R2 methylation inhibits H3K4 trimethylation[78]. In conclusion, location, context and timing of PTMs are all playing important role for their total function[60].

3.3.2 Variant histones incorporation

Variant histones are sequential and functional variants of canonical histones. They are expressed throughout the whole cell cycle[79], with their mRNA polyadenylated[80]. Variant histones are incorporated during replication-independent chromatin assembly, necessary for DNA metabolism processes, such as transcription, repair and heterochromatin formation[81]. Variant histones, despite often having only a few amino acids difference with canonical ones, have a set of specialised functions. Incorporation of the same variant histone can contribute to antagonistic chromatin states based on the timing, location and presence of other factors. For example, while variant histone H3.3 maintains transcriptionally active chromatin states[82,83], it is also deposited into transcriptionally-repressed sites, such as pericentric[84] and other heterochromatin regions[85].

H2A group of variant histones is highly diverse and abundant. Some of the variants, namely H2A.Z and H2A.X are evolutionary conserved, while macroH2A and H2ABbd are vertebrate-specific[86,87]. The H2A variants are primarily distinguished by their N- and C-termini, which diverge in both length and sequence, as well as in their genomic distribution[88]. C-terminus of H2A, located at DNA entry/exit site, has the highest degree of diversity, leading to altered nucleosomal stability, dynamics, and interactions in variant histones[89].

H2A.Z is highly evolutionary conserved variant of canonical H2A histone. It is essential for early development of multicellular organisms[90]. H2A.Z-containing nucleosomes are structurally different from canonical H2A ones[91]. Those differences are mainly determined by alterations in C-terminal docking domain between H2A and H2A.Z (Fig. 3a). H2A.Z/H2B dimers possess an extended acidic patch that may act as an interaction interface for H4 tails or non-histone protein factors. H2A.Z docking domain residues His 112 and His 114 bind to and stabilize interactions with a metal ion, while the comparable region in H2A doesn’t make this interaction (Fig. 3b). The presence of metal ion in H2A.Z-containing nucleosomes may create a specific interaction interface for other nuclear proteins, such as assembly factors or chromatin remodelling factors. The residue substitutions and deletions in H2A.Z docking domain result into gap formation at the centre of H2A.Z-containing

nucleosome, which is filled with additional residues in H2A-containing nucleosome (Fig. 3b). Those structural differences result in altered, acidic surface that accounts for stability and binding differences between H2A.Z-containing octamers and octamers with canonical H2A. H2A.Z incorporation effect on the nucleosome structure stability remains controversial, with both destabilising[92] and stabilising[93,94] outcomes demonstrated.

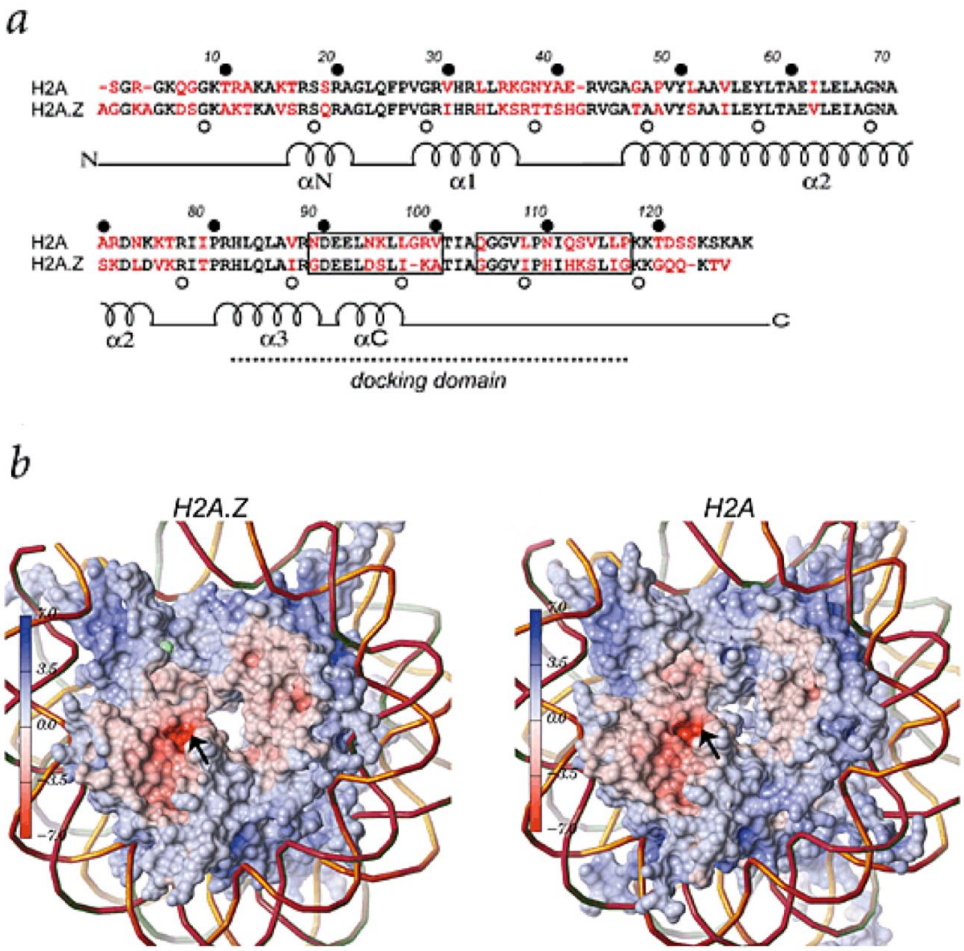

Figure 3. H2A and H2A.Z sequences and nucleosomes comparison

(a) Sequence alignment of *Xenopus laevis* H2A and mouse H2A.Z. Differences between the two amino acid sequences are indicated in red, the docking domain is indicated with a dashed line. Regions essential for the function of H2A.Z are boxed.
(b) Side-by-side comparison of H2A.Z-containing nucleosome and H2A-containing nucleosome X-ray crystallography assessed structures. Colour coding of nucleosomes indicate the electrostatic potential, which ranges from +7.0 (blue) to -7.0 (red) kcal mol^{-1} e^{-1}. The manganese ion is shown in green. The acidic patch is indicated by a black arrow. H2A.Z-containing nucleosome features gap in the centre, which is not present in H2A-containing nucleosome.
(Modified from R. Suto et al., 2000[91])

H2A.Z incorporation into nucleosomes has a vital role in transcription, with exact effect depending on chromatin context[95]. Based on surrounding chromatin type and marks it

could facilitate either gene activation or repression. H2A.Z containing nucleosomes are widely present in euchromatin and are found at nucleosome-depleted regions of active promoters and other regulatory regions[96,97]. Such positioning is necessary for the initial binding of the transcriptional machinery[98]. H2A.Z is also present at euchromatin and heterochromatin boundary, preventing the ectopic spread of silent heterochromatin[99]. H2A.Z is found at the promoters of silent genes occupied by the Polycomb-repressive complex 2[100]. H2A.Z is also shown to be targeting pericentric heterochromatin during early mammalian development, where it may act as a mark to distinguish constitutive from facultative heterochromatin[101].

The introduction of H2A.Z into chromatin is carried out by ATP-dependent complexes in a replication-independent manner in all eukaryotes. In yeast H2A.Z is bound by general Nap-1 and H2A.Z-specific Chz1 chaperones that translocate it to ATP-dependent SWR1 complex. SWR1 with the help of swc2 chaperone[102] catalyses replacement of H2A/H2B dimer with H2A.Z/H2B[103]. In *Drosophila*, TIP60 acetylates and exchanges phospho-H2Av with H2Av, by means of both histone acetyltransferase dTip60 as well as the adenosine triphosphatase Domino/p400[104]. In mammals SRCAP complex with the help of YL1 chaperone[7] facilitates ATP-dependent exchange of histone dimers containing H2B and H2A.Z into mononucleosomes[105]. The active eviction of H2A.Z from chromatin is also well defined and characterized. ANP32E chaperone, as part of P400/TIP60 complex, specifically removes H2A.Z from nucleosomes, including those at *cis*-regulatory sites[11]. The INO80 complex exchanges nucleosomal H2A.Z/H2B with free H2A/H2B dimers[106]. Those competing incorporation and eviction processes lead to constant dynamic exchange of H2A.Z in nucleosomes[79]. This cycling allows for precise regulation of H2A.Z localization in response to cellular requirements.

H2A.X is another conserved H2A variant, characterized by a C-terminal extension with the consensus SQ[E/D]Φ, where Φ represents a hydrophobic residue. H2A.X is extensively involved in DNA repair processes. In response to double-strand breaks, H2A.X is deposited to the affected nucleosomes, where it gets phosphorylated by DNA damage signalling kinases[64]. H2A.X phosphorylation is important mark for DNA repair and checkpoint factors recruitment, such as Rad50, Rad51 and BRCA1[64,107]. Loss of a single H2A.X allele leads to increased sensitivity to ionizing radiation and a higher occurrence of cancer in the absence of p53[108]. This phenotype is not recovered by H2A.X with substitution of the conserved serine phosphorylation site, implicating precise interplay between H2A.X histone incorporation and modification. The H2A.X -/- mice has a number of defects

including radiation sensitivity, growth retardation, immune deficiency and male's infertility[109]. These phenotypes are associated with chromosomal instability, repair defects and impaired recruitment of repair machinery. Together, these data establish H2A.X as a critical factor necessary for assembly and regulation of DNA-repair machinery in irradiation-induced foci.

H2A.Bbd (Barr body-deficient) is a histone variant specific to mammals only. It is highly specialized, being only 48% identical to canonical H2A. It lacks characteristic C-terminal tail of the H2A family and end sequence of the docking domain, which is important for interaction with H3[110]. H2A.Bbd was found to be largely excluded from inactive X chromosomes[111] and to be enriched in nucleosomes associated with transcriptionally active regions of the genome[111]. H2A.Bbd exchanges much more rapidly than H2A within the nucleosome, and nucleosomes containing H2A.Bbd are less stable than canonical ones[30]. This instability of H2A.Bbd contributes to disrupted chromatin structure at the sites of its incorporations. Such disruption leads to formation of more accessible chromatin, thus facilitating transcription.

MacroH2A is another highly divergent variant histone of H2A group. It contains additional large nonhistone macrodomain with possible enzymatic function[87]. Opposite to H2A.Bbd, it is mostly associated with condensed, inactive chromatin. MacroH2A is enriched on the heterochromatic inactive X chromosome[112] and the transcriptionally silent XY body during meiosis[113]. It is shown to act as a barrier to reprogramming of induced pluripotent stem cells[25]. The mechanism of this transcriptional silencing involves macroH2A interference with transcription factors binding and nucleosome remodelling by SWI/SNF chromatin remodelling factors[29]. In addition, the macroH2A nonhistone macrodomain may act as a roadblock for the passage of RNA polymerases, further establishing macroH2A as a transcription suppressor.

3.3.3 Chromatin remodelling complexes

Chromatin both protects DNA and impose constrains on it processing. In order to allow access to DNA for essential activities such as transcription, replication and repair, chromatin structure is being remodelled using energy of ATP. The factors involved in this process are chromatin remodelling complexes (CRCs) that mobilize, move and cycle nucleosomes[114].

CRCs are multi-molecular complexes of 300 kDa - 2 MDa molecular size. Their unifying characteristic is presence of protein with catalytic ATP-hydrolysing core, homologous to Snf2 family ATPase of the DEAD/H (SF2) superfamily of DNA-stimulated ATPases[115,116]. All of CRCs ATPases are evolutionary related to DNA and RNA helicases[114]. CRCs has a modular structure featuring diverse domains that allows high functional and context-wise specialisation[115].

CRCs are classified into different groups based on the domain organisation of ATPase-containing protein found in each complex (Fig. 4). Most of CRCs proteins belong to four major related families: SWI/SNF, ISWI, CHD/Mi-2 and SWR1/INO80[117-119]. There are number of differences between those families. Most importantly, they have different functional domains in addition to ATPase, such as SANT and SLIDE domain for ISWI-like, HSA and bromodomain for SWI/SNF group, chromodomains for CHD-like and HSA domain for SWR1/INO80[120]. These differences define CRCs subunit composition and functions. Secondly, the remodelling mechanisms are different between those families. While SWI/SNF family is more disruptive to DNA nucleosome interactions and may involve complete or partial disassembly of the histone octamer, ISWI family group action is often less invasive and may include nucleosome repositioning without its removal[121]. Thirdly, SNI/SNF complexes tend to be up to 2MDA and consist of 9–12 subunits, while the ISWI group of remodelling complexes are relatively small (300–650 kDa) containing 2–4 subunits[122]. At last, the substrate requirements for those families are different. The ATPase of CHD-family is stimulated by nucleosomal DNA, while ISWI and SWI/SNF are stimulated by free DNA, with ISWI being further stimulated by nucleosome tails[121].

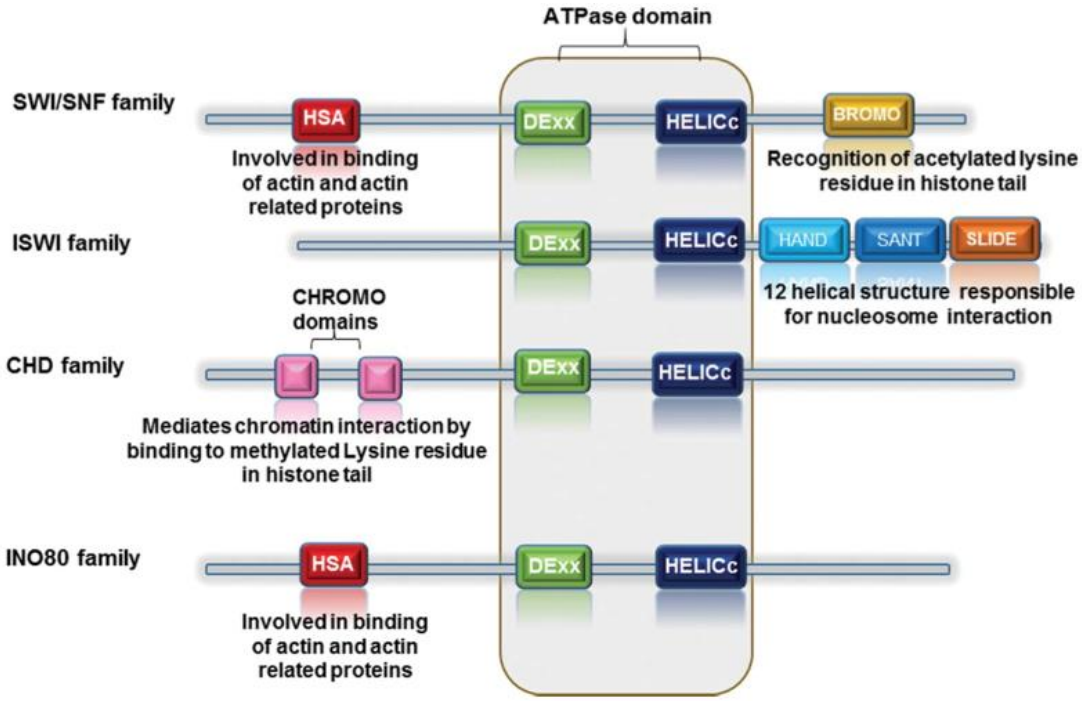

Figure 4. Domain structure of four chromatin remodelling families.

Diagrammatic representations of four families of chromatin remodelling complexes. ATPase domain of chromatin-remodelling complexes consists of an N-terminal DExx and a C-terminal HELICc subdomain, separated by an insert region. The differences between families are determined by additional domains, such as HAS, HAND, SANT, SLIDE, bromo- and chromodomains.
(Modified from M. Tyagi et al. 2016[123])

There are a number of well-established biological contexts where CRC are required, such as transcription, formation of evenly spaced nucleosome arrays and chromatin assembly facilitaion[114,124].

Transcriptional remodelling is required for activation of regulatory elements of genome[124], such as promoters[125,126]. Regulatory elements of active genes are stably cleared of nucleosomes, to allow quick access of transcription factors required for the regulation of the genes[127]. Experiments on rapidly transcribed HSP70 in Drosophila revealed three-fold decrease of H3 on the body of the gene after heat shock[128]. The dependence of transcription on dynamic and transient chromatin structure change in gene bodies was also demonstrated[129]. During transcription, RNA polymerase complex displaces the nucleosomes what it passes. To recover this disrupted state, new histones are deposited back less than 1 min after passage, which generates a dynamic equilibrium of histone eviction and deposition in sites of transcription[129]. Rapid transcription and more moderate transcription have different requirements[130]. During rapid transcription nucleosome frequently undergo transient octamer

loss or exchange. In case of more moderate transcription either only H2A/H2B dimers undergo frequent loss/exchange or transient octamer loss occurs more rarely[130].

Another important remodelling context is onset of proper spacing and structure of chromatin after DNA-processing events[114]. Optimal density and appropriate spacing of nucleosomes are critical for newly synthesized chromatin after replication[114]. Chromatin remodelling complexes are also required for the conversion of prenucleosomes to nucleosomes during chromatin assembly[131]. There is some overlapping between molecular machinery involved in processes of assembly and remodelling. Some ATP-dependent factors that can slide nucleosomes are also, together with chaperones, can assemble chromatin. Functional synergy between remodelling and assembly by same ATP-dependent factors was demonstrated on CHD1, which can participate in both assembly and remodelling processes[132]. Chromatin remodelling-defective Chd1 can still induce assembly, however the arrays that are created are not spaced in periodic manner. Non-defective CHD1 can remodel those disorderly distributed nucleosomes into periodic arrays. This implicates that while CHD1 assembly function helps to create arrays of nucleosomes, its remodelling function is in charge of proper spacing and organisation of array[132]. ACF was also demonstrated to have both histone depositing and chromatin remodelling functions, with both reaction requiring ATP[133]. These data expose that assembly and remodelling functions of some ATP-dependant chromatin machineries are distinct but synergetic.

To carry out these diverse functions CRCs utilize a number of global mechanisms of action. CRCs have been observed to catalyse the mobilization and re-positioning of nucleosomes, the transfer of a histone octamer from a nucleosome to a separate DNA template, the creation of dinucleosome-like structures from mononucleosomes, and the generation of superhelical torsion in DNA[114,117,132,134].

The regular spacing between nucleosomes is achieved by generating superhelical torsion in DNA, using energy of ATP hydrolysis[135]. This leads to alteration of local DNA topology and disruption of histone contacts, allowing the histone octamer to move along the DNA until regular spacing between nucleosomes is set[135]. There are two general mechanisms of action of nucleosome repositioning – sliding and looping[136]. SWI/SNF enzymes increase chromatin accessibility by DNA looping, whereas ISWI enzymes induce nucleosome sliding. During sliding, local DNA twist or bulge progresses over the histone octamer surface in a wave-like manner[136]. This causes the octamer to be relocated relative to the DNA sequence. Sliding change the location of the exposed DNA, not the amount that is exposed. The looping

mechanism makes nucleosomal DNA globally distorted and more susceptible to restriction nuclease digestion[137]. During looping DNA segment from one edge of the nucleosome is being detached that leads to DNA unwrapping. Together with looping SWI/SNF group is also shown to be able to introduce topological changes in closed circular nucleosomal arrays[138].

For nucleosome exchange promoted by SWR1, a mechanism similar to SWI/SNF activity was proposed[103]. SWR1 catalyses unwrapping of nucleosomal DNA from the entry or exit positions of the nucleosome thus exposing the DNA-binding surface of H2A-H2B dimer[103]. The unwrapping is facilitated by intrinsic tendency of octamer to dissociate to H2A-H2B dimers and the $(H3\text{-}H4)_2$ tetramer and by action of SWR1 complex factors. In the end SWR1 complex deposits Htz1-H2B dimer, which takes vacant place of previously placed H2A-H2B, reassembling a nucleosome particle containing one each of H2A-H2B and Htz1-H2B dimers[103]. The diverse CRCs mechanisms of work mirror their numerous functions in cellular processes. Next chapters are dedicated to overview four main families of chromatin remodelling complexes.

3.3.3.1 ISWI family

ISWI-containing factors are highly conserved and have different roles in chromatin assembly, nucleosomal spacing and repair[139]. ISWI-containing CRC have been reported in many species, including yeast ISW1 and ISW2, Drosophila ACF, NURF and CHRAC, human hACF, hNURF, hCHRAC, RSF, NoCR and ToRC.

Even though ISWI is able to carry out nucleosome remodelling, nucleosome rearrangement and chromatin assembly reactions on its own *in vitro*[140], it is always identified *in vivo* in a complex with other factors [121]. The role of proteins associated with ISWI may be to stimulate, enhance and regulate the activity of the remodelling engine or to define the biological context within which a nucleosome remodelling reaction occurs[121].

Drosophila complex ACF consists of two subunits: Acf1 and the ISWI ATPase. Acf1 enhances and modulates the activity of ISWI and synergistically cooperate with it in the assembly of chromatin and nucleosome spacing[133]. *In vitro* assay revealed that ACF, NAP-1 or CAF-1, core histones, plasmid DNA and ATP are efficient for nucleosome assembly[141,142]. ACF is shown to participate in both setting regular spacing after chromatin assembly and transcription factor-mediated disruption of nucleosome arrays[142]. ACF is capable to assemble

chromatin containing H1 linker histone, which is more repressive than H1-lacking chromatin[143].

CHRAC is a complex similar to ACF, and contains ACF1 and ISWI, but also possess two more subunits – CHRAC14 and CHRAC16 - histone fold containing proteins[144]. CHRAC has a function in the replication regulation by altering the nucleosomal structure at the origin of replication, that allows efficient initiation of replication[145]. CHRAC is able to mobilize nucleosomes and relocate them to a central position on the DNA.

While ACF and CHRAC set regular periodic arrays, another drosophila ISWI-containing CRC – NURF - disrupts nucleosome periodicity[146]. NURF was shown to facilitate transcription factor-mediated disruption of physiologically spaced nucleosomal arrays[147]. This disruption sets accessible chromatin structure at the promoter regions of genes, thus promoting transcriptional activation. NURF is able to rapidly reposition a full histone octamer to adjacent positions on the same DNA fragment, by lowering the activation energy for short-range sliding of a histone octamer[146]. While CHRAC slides nucleosome from a fragment end toward the middle, NURF is able to slide central nucleosome in bidirectional way [146]. NURF perturbs histone–DNA interactions in mononucleosomes when added at a stoichiometry of one NURF per 20 nucleosome core particles[147]. It shares this characteristic with SWI-SNF factors, however they disrupt interaction at higher stoichiometry and unwrap nucleosomal DNA, while NURF only slides octamer along DNA[146].

Human homologues of ISWI containing complexes were identified (Fig. 5). The human ISWI family of remodelling ATPases comprises the Snf2H and Snf2L proteins that form complexes with different non-catalytic subunits. RSF complex consists of ATPase hSNF2H and p325 (Rsf-1)[148]. RSF can induce regular periodic nucleosome spacing and was found to be able to assemble chromatin without histones *in vitro*[149]. hACF, consisting of SNF2h and hACF1 is involved into replication through highly condensed regions of chromatin, such as pericentromeric heterochromatin[150]. hNURF is comprised of SNF2L ATPase and non-catalytic subunits BPTF and pRBAP46/48 and is implicated into facilitation of transcription factor binding[151]. NoRC consists of SNF2h and Tip5 and is shown to specifically repress rDNA transcription in chromatin[122]. The functional specificity of these factors is determined by their non-ATPase subunits composition. For example, TIP5 of NoRC modulates complex affinity to nucleosome, while CtBP subunit of NoRC homologue ToRC mediates entire complex localization[152]. The diverse subunit composition of ISWI family complexes determines their numerous functions in chromatin-related processes.

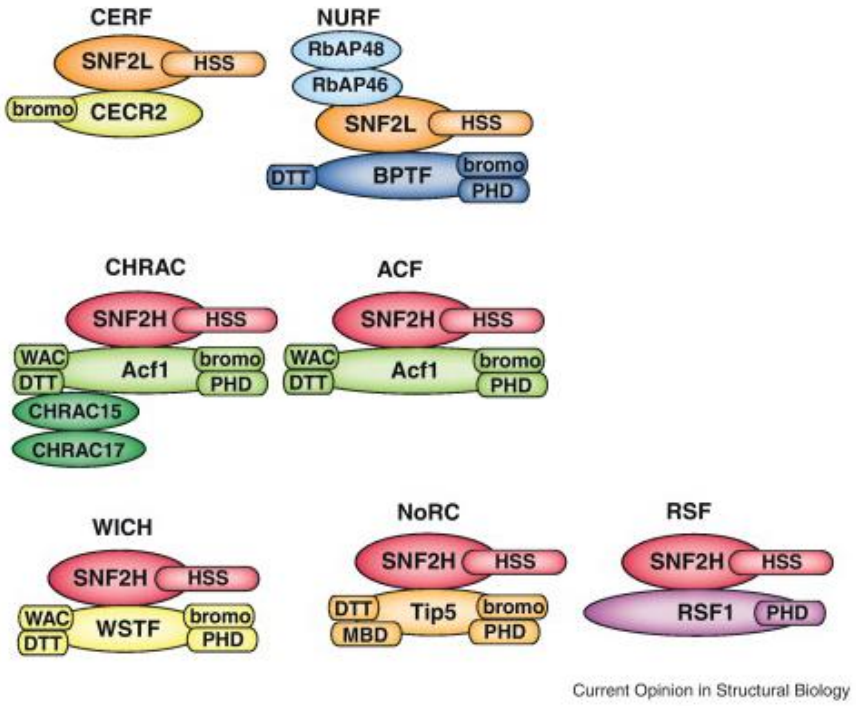

Figure 5. Mammalian chromatin remodelling complexes of ISWI family

Diagrammatic representations of ISWI family complexes. The subunits are represented as ellipses and conserved protein motifs as rectangles. HSS is the HAND, SANT and SLIDE domains.
(Modified from Bartholomew et al., 2014[153])

3.3.3.2 SWI-SNF family

In eukaryotic cells there are two subfamilies of SWI/SNF chromatin remodelling complexes, differing by the presence of the subunits[95]. First is the SWI/SNF group that contains yeast SWI/SNF, drosophila BAP and human BAF. Second is the RSC group, which contains yeast RSC, drosophila PBAP and human PBAF complexes[119,154]. Despite similarities to other organism's complexes, mammalian SWI/SNF complexes feature more diversity of subunits that are combinatorially assembled into functional subcomplexes[154]. This divergence is likely caused by developmentally distinct functions, since a number of mSWI/SNF complexes subunits have an important function in embryonic development[155-157]. SWI-SNF family complexes utilize energy of ATP hydrolysis to mobilize nucleosomes and make the DNA accessible for various nuclear processes[158,159]. They are involved into DNA breaks repair, replication, transcription activation and repression[160-163].

hSWI/SNF complex mediates ATP-dependent disruption of nucleosome core that is accompanied by changes in DNA topology[164]. It was demonstrated *in vitro* that hSWI/SNF can exchange nucleosome between normal and activated state in an ATP-dependent

process[165]. Activated nucleosomes are topologically different and characterized by DNA loops on the nucleosome surface[158]. They are more sensitive to digestion by DNAse, restriction enzymes, and micrococcal nuclease, which implies that they have more open, accessible structure[165]. This structure change helps transcription factors to bind to the site of DNA, as exemplified on activator Gal4-AH[164]. Presence of hSWI/SNF and ATP enhanced Gal4-AH binding to DNA more than 100-fold. Swi/Snf complexes are shown to be recruited to promoters to carry out their remodelling function through direct interactions with DNA-bound activators or repressors[166]. RSC complex was also was demonstrated to facilitate transcription, by the means of disassembling nucleosomes in order to remove them from promoters[134,167].

Together with role in transcriptional activation, SWI-SNF subfamily complexes are also shown to be involved into transcriptional repression. ChIP experiments revealed that subunits of hSWI/SNF complexes are present at repressed promoters[168,169]. Ability to both activate and repress transcription could be attributed to distinct forms of Swi/Snf each carrying out their functions. Some forms of Swi/Snf are shown to possess histone deacetylases that can promote repression[170]. SWI/SNF was also shown to facilitate and increase efficiency of DNA replication. A direct interaction between Ini1/hSNF5 subunit of human SWI/SNF complex and the human papillomavirus E1 replication protein was demonstrated[171]. This interaction is essential for the efficient replication of papilloma-virus DNA. These data establish SWI/SNF-containing complexes as a multi-functional factors, which utilize their chromatin remodeling activity to facilitate diverse chromatin-related processes.

3.3.3.3 CHD/Mi-2 family

CHD/Mi-2 family CRCs are playing important roles in the regulation of transcription, differentiation and developmental processes[172,173]. Some of CHD family factors, i.e. CHD5 and CHD8 are tumour suppressors, implicated in a number of human diseases[172,174,175].

There are three subfamilies within CHD/Mi-2 family differing by additional domains (Fig. 6). Chd1 and Chd2 subfamily contains DNA-binding domain; Chd3-Chd5 subfamily (Mi-2 subfamily) has N-terminal PHD Zn-finger-like domains; Chd6-Chd9 possess paired BRK (Brahma and Kismet) domains, a SANT-like domain, CR domains, and a DNA-binding domain[172].

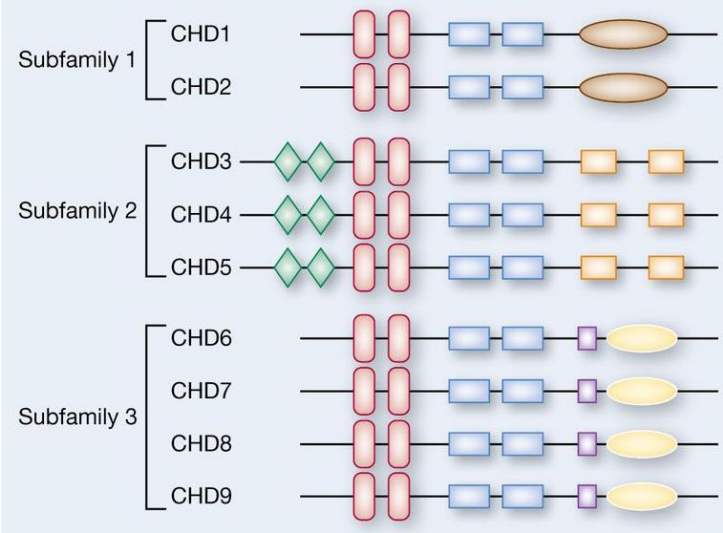

Figure 6. CHD subfamilies domain organisation.

Diagrammatic representations of three CHD subfamilies of chromatin-remodelling factors. Green diamonds, PHD finger domains; red vertical boxes, chromodomains; blue rectangular boxes, split SNF2-like helicase/ATPase domain; brown oval, DNA-binding motif; orange boxes, domains of unknown function (DUF1, DUF2); light blue box, SANT domain; yellow oval, BRK domains.
(Modified from Kolla et al., 2014[176])

Early studies of Drosophila Chd1 using polytene chromosomes established its ability to alter chromatin structure in a way that facilitates gene expression[177]. Chd1 can participate in both chromatin assembly and remodelling processes, first facilitating formation of nucleosome arrays and then remodelling them to be evenly spaced[132]. It was shown that those processes are distinct and carried out by different domains on the Chd1[132]. *In vitro* reaction containing purified Chd1, NAP-1 chaperone, core histones and relaxed DNA was enough to catalyse the ATP-dependent transfer of histones to the DNA by a mechanism that yields regularly spaced nucleosomes[143]. Interestingly Chd1 could only assemble chromatin without linker histone H1, but not H1-containing one, which indicates CHD1 role into assembly of less compact, active chromatin[143]. Drosophila Chd1 together with RI-specific chaperone HIRA is shown to participate in assembly of parental chromatin during early Drosophila development[178]. Yeast Chd1 is shown to be part of two complexes – SAGA (Spt-Ada-Gcn5 acetyltransferase) and SLIK (SAGA-like), two highly homologous and conserved multi-subunit histone acetyltransferase complexes. SAGA acetylates nucleosomes surrounding the promoter, facilitating recruitment of additional transcriptional factors that lead to gene activation[179]. SAGA activity was demonstrated to depend on Chd1[180].

Drosophila Chd3-Chd5 family proteins (Mi2) are DNA-dependent, nucleosome-stimulated ATPase cores of NuRD complexes[181,182], which possesses both nucleosome remodelling and histone deacetylase activities[183]. They can bind and mobilize nucleosomes along a linear DNA fragment. NuRD complexes efficiently disrupts histone–DNA contacts and remodels mono- and polynucleosomes in an ATP-dependent manner[182,184].

3.3.3.4 INO80/SWR1 family

INO80 and SWR1 complexes are evolutionarily conserved from yeast to human and share several subunits[185]. They have been implicated in a number of process, including chromatin assembly, transcription regulation, double strand breaks repair and cell-cycle checkpoint activation[185,186].

INO80 has a numerous functions in chromatin processing that are determined by its diverse catalytic activities. INO80 shows both DNA-dependent ATPase activity and 3′ to 5′ specific helicase activity[124]. It is able to binds free DNA with an apparent binding constant comparable to that of SWI/SNF[187], which is important for its chromatin functions. INO80 complex can mobilize and remodel mononucleosomes in an ATP-dependent manner[187]. INO80 complex utilizes its remodelling function to play an important role in transcription regulation[185]. It was demonstrated that chromatin remodelled by INO80 complex shows a 10-fold increase of transcriptional activation[124]. INO80 complex also has a function in replication, by remodelling, removing and reassembling nucleosomes in the path and behind the replication fork[188]. Finally, INO80 complex remodelling is involved in DNA-repair processes, by facilitating nucleosome exchange from damaged regions[186]. INO80 mutants are hypersensitive to DNA damaging agents and to double-strand breaks (DSBs) induced by the HO endonuclease[189]. It was shown that INO80 and other components of INO80 complex are recruited to an HO-induced DSB, where they directly remodel chromatin in order to facilitate processing of the lesion[189].

The mechanism for some of INO80 complex functions is linked to its regulation of H2A.Z histone distribution[190]. H2A.Z was shown to be mislocalized across the yeast genome in the absence of INO80, with its overall pattern becoming disrupted. A model was proposed in which Ino80 catalyse the ATP-dependent removal of unacetylated H2A.Z from chromatin that surrounds stalled replication forks or double strand breaks, thus contributing to genome

stability[190]. INO80-induced H2A.Z/H2B replacement by canonical H2A/H2B is opposite to the activity of other member of the INO80 family of ATPases - SWR1, which replaces H2A/H2B with H2A.Z/H2B dimers. SWR1 and INO80 perform similar dimer exchange reactions but with opposing specificities, precisely regulating H2A and H2A.Z distribution according to cellular requirements (Fig. 7).

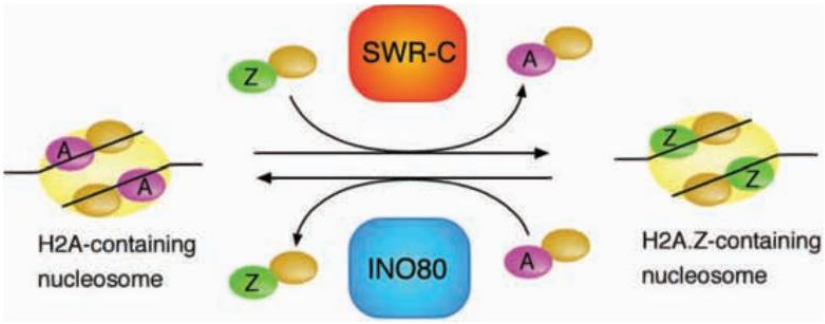

Figure 7. H2A and H2A.Z exchange by INO80 and SWR1

SWR1 replaces H2A/H2B with H2A.Z/H2B, while INO80 replaces H2A.Z/H2B dimers with H2A/H2B ones.
(Modified from S. Watanabe et al., 2010[190])

SWR1 complex have molecular weight of approximately 1 MDa and consists of 14 subunits. SWR1 complex is conserved in eukaryotes, with SRCAP and p400 being its mammals homologues. All SWR1 homologues are able to exchange variant histone H2A.Z/H2B dimer for a canonical H2A/H2B dimer at nucleosomes flanking histone-depleted regions, such as promoters[103-105]. Swc2 unit of SWR1 complex directly binds to and is essential for exchange reaction of H2AZ/H2B dimers for canonical ones, thus being the histone chaperone of this complex[102]. Histone acetylation PTM plays an important role in SWR1-mediated histone exchange. NuA4 complex was shown to acetylate Htz1 *in vivo* after it was deposited by the SWR1 complex[191]. This Htz1 acetylation is required for its transcriptional activation, opposition of gene-silencing, and chromosome stability functions[185]. Mutants of NuA4 and SWR1 complexes share several phenotypes, implicating their functional synergy, possibly mediated by shared subunits[185,191].

SWR1 complex structure containing all subunits was visualized by 3D electron microscopy[192]. It revealed presence of functional modules within SWR1 complex: substrate-handling N- and C-Modules, ATPase module and Rvb1/Rvb2 ring[192] (Fig. 8). Each module is distinct, but highly linked with others. Chemical crosslinking and mass spectrometric analysis confirmed that subunits show numerous interactions between each other, thus being highly

interconnected. Rvb1/Rvb2 ring acts an assembly platform for substrate-interacting N- and C-Modules modules, while Swr1 ATPase bridges N-Module with the Rvb1/Rvb2. Comparison of nucleosome-free and nucleosome-bound SWR1 complex structures revealed conformational changes occurring upon binding[192]. At first, nucleosome binds over a central depression formed between the Swr1 ATPase and the Rvb1/Rvb2 ring. Then SWR1 complex engages the nucleosome core particle via its catalytic ATPase subunit, which makes it assume extended conformation. Interestingly, SWR1 complex and nucleosome has a limited interaction that may reflect unique mechanistic aspects of the dimer-exchange reaction, different from other remodelers[192].

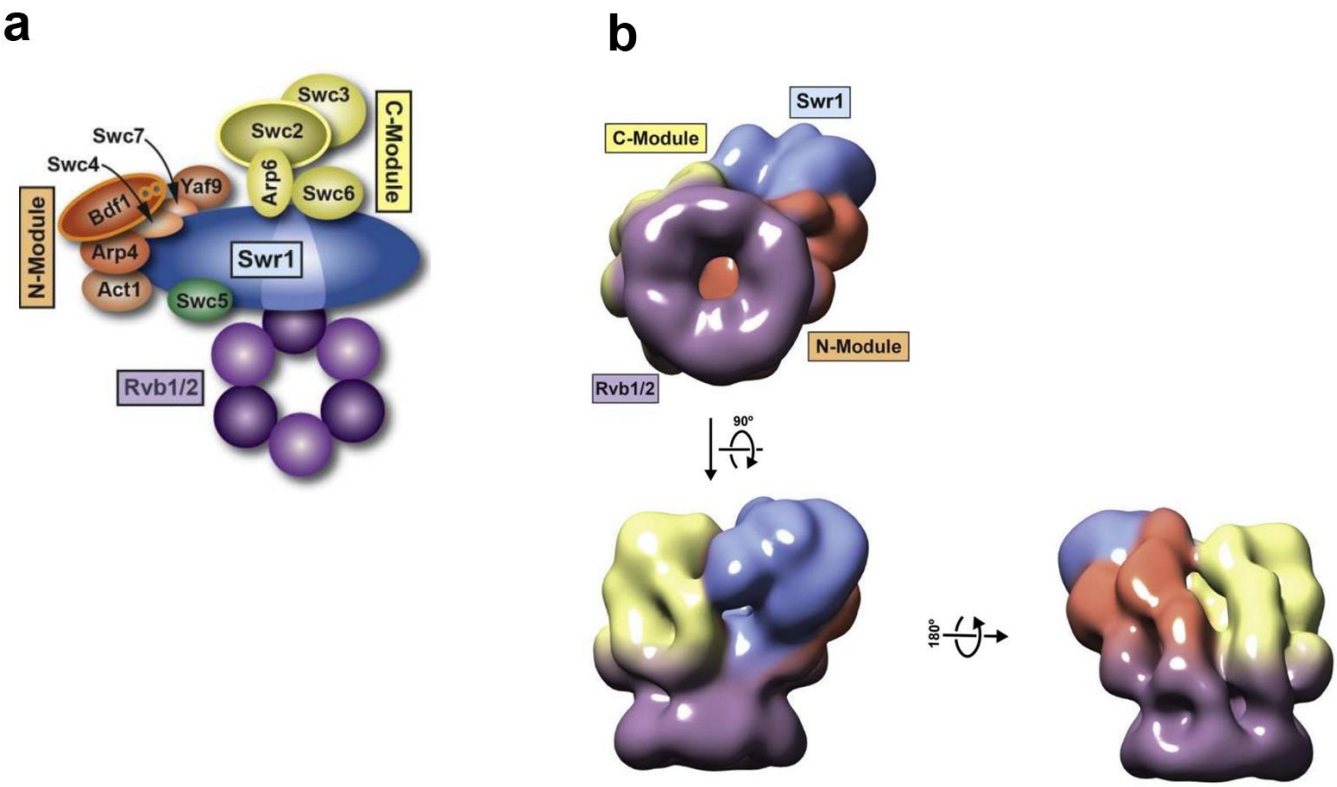

Figure 8. SWR1 complex organisation

(a) Schematic representation of the SWR1 complex subunits.
(b) Cryo-NS structure of SWR1 complex at 28 Å resolution. All subunits are arranged into following regions: Swr1 ATPase (blue), Rvb1/Rvb2 hexamer ring (purple), histone–binding N-Module (orange) and H2.Z/H2B-binding C-Module (yellow).
(Modified from Vu Q. Nguyen et al., 2013[192]).

3.4 Chromatin assembly

Chromatin functions both as a scaffold and a regulator of all DNA metabolism processes, such as replication, repair and transcription. During these processes, chromatin structure is subjected to a temporary disruption followed by a timely reformation, which requires chromatin assembly[193,194]. There are two types of chromatin assembly - replication coupled (RC) and replication independent (RI).

RC assembly is required for *de novo* formation of chromatin. For this purpose canonical histones – H2A, H2B, H3 and H4 are transcribed during S phase[23] and used for packaging the newly replicated genome[79]. RC chromatin assembly is an initial step that creates basis for all DNA-associated processes.

RI chromatin assembly is in charge of histone replacement that occurs on existing nucleosomes – which is requirement of such processes as transcription, DNA damage repair, DNA recombination and histone exchange on telomeres and pericentromeric heterochromatin. RI assembly occurs through whole cell cycle[79] and utilizes variant histones instead of canonical. RI chromatin assembly is a constant process of chromatin maintenance and regulation.

RC and RI assemblies are divided by different histones pools, separated cell cycle times and different histone chaperones, meaning that normally those processes are not overlapping. As an example of such divergence, canonical histone H3.1 is incorporated during RC assembly by the means of CAF-1 chaperone, while variant histone H3.3 is incorporated during RI assembly with HIRA chaperone[81,195,196]. However in cases of abnormal depletion of either canonical or variant histones or their chaperones, compensatory mechanisms are activated, revealing that RC and RI machineries can be partially replaceable. Cells that are depleted of CAF-1 p60 subunit have disruptions in replication-coupled H3.1 incorporation[196]. As an attempt to fill resulted nucleosome gaps, H3.3 starts to get incorporated by HIRA into the sites of replication, meaning that RI-specific machinery and histones start acting as a RC assembly replacement[196]. A complementary mechanism of RC machinery acting as a RI assembly replacement was characterized in Drosophila. Depletion of variant H3.3 histone was shown to lead to incorporation of canonical H3 histone, accompanied by upregulation of endogenous H3 genes[197].

Described nucleosome gap filling processes are few of the many ways how chromatin maintain its integrity by the means of timely chromatin assembly. After DNA damage, reestablishment of the initial chromatin structure is carried out by repair-coupled chromatin

assembly[198,199]. It was demonstrated, that CAF-1 promotes nucleosome assembly during the processing of single-strand breaks[200]. Interaction of CAF-1 and PCNA may be involved in coordination of interplay between DNA damage repair signals and chromatin restoration[200]. Other histone chaperones, FACT and HIRA are shown to be recruited to the UVC-damaged chromatin to facilitate histone exchange there[201,202]. These assembly processes are necessary to restore the functions of chromatin, as exemplified by transcription reactivation after events of damage[202].

Finally, chromatin assembly is setting conditions for maintenance of chromatin states between mitotic cell divisions[203]. During RC assembly, chromatin is generated from a pool of both newly synthesized histones and recycled parental ones. The level of all PTMs is fully restored within one cell cycle. This recycling allows for keeping PTM information between cell generations, propagating stable and specified epigenetic states. To summarise, chromatin assembly is a vital process, that sets chromatin landscape, maintains processes that occurs on it and guards its integrity.

3.5 Chromatin assembly machinery

There are two major factor groups that are involved in chromatin assembly; ATP-dependent assembly factors and histone chaperones[5]. There is an *in vitro* evidence of chromatin assembly that can happen either with chaperones only (NAP-1)[5] or ATP-dependent assembly factors only (RSF)[149]. However, available research shows that for efficient formation of evenly spaced arrays of chromatin observed *in vivo*, both histone chaperones and ATP-utilizing chromatin assembly factors are required[5,178].

3.5.1 Histone chaperones

Histone chaperones are a diverse group of proteins that physically binds histones. Their structure is varied, with acidic stretches, rich in glutamic and aspartic acids being common motif. These stretches are often found near the chaperones C-terminus. Histone chaperones play critical role in all steps of histone cycle. They protect histones from non-specific interactions and modifications and facilitate histone recruitment to chromatin and are involved in nucleosome incorporation, eviction and exchange[10]. *In vitro* studies revealed that at physiological ionic strength, histone chaperones are necessary to shield positive charge of

histones to prevent the formation of disordered insoluble aggregates between histones and DNA[204]. Histones of H2A-group are often interacting with chaperones through their C-terminal alphaC helix domain, that was demonstrated on H2A.Z chaperones YL1[7], Anp32E[11] and Chz1[18]. Many of histone chaperones, like Nap-1, Chz1 and ANP32E are not essential for viability and many seem to have overlapping functions. This suggests that there is a high degree of functional redundancy of histone chaperones, even if each of them have some degree of functional specialization[205,206]. Histone chaperones usually have a preference to either H3–H4 or H2A–H2B histones[80].

3.5.1.1 H3-group/H4 histone chaperones

One of the first identified and characterized histone chaperones was CAF-1. CAF-1 is an evolutionarily conserved H3-H4 chaperone complex of three subunits - p150, p60 and RbAp48. It is an essential factor for cell viability of multi-cellular organisms[207]. CAF-1 was shown to deposit H3-H4 for *de novo* chromatin formation[208] and chromatin restoration after DNA damage[200]. CAF-1 acts as a part of chromatin assembly complex (CAC). CAC contains CAF-1 and histones H3 and H4 that possess unique acetylation pattern, that is an important marker for assembly[80]. CAF-1 is recruited to the sites of replication foci[209] by an interaction with the DNA polymerase through PCNA[210]. At replication foci CAF-1 deposit newly synthesised H3–H4 behind replication forks[208]. Together with functions in replicative assembly, CAF-1 is also shown to participate in the maintenance of heterochromatin[211,212].

Asf1 is H3-H4 chaperone involved in both RC and RI chromatin asembly[213,214]. Asf1 forms heterotrimeric complexes with newly synthesized H3-H4 dimers in cytoplasm and transfer them to the sites of nucleosome assembly in the nucleus[215]. At the replicative fork, Asf1 is shown to form stable complex with putative replicative MCM helicase and H3-H4 histones. Asf1 seems to have a double function during replication, as it binds both *de novo* synthetized histones and parental histones[214]. It's thought that Asf1 coordinates histone supply and replication fork progression[216]. Asf1 is also involved in assembly after DNA damage, by means of interaction with DNA damage checkpoint kinase Rad53[217]. Asf1 is often found in a complex with other histone chaperones, acting as a histone donor or acceptor.

HIRA is a H3.3 variant histone chaperone. It incorporates H3.3 to sites of active transcription in a RI way[14]. In HIRA knockout, ES cells genome-wide enrichment of H3.3 at promoters and in the body of active genes is disrupted, suggesting a critical requirement for

HIRA in H3.3 deposition at these specific regions[218]. HIRA is shown to be associated with and carry out at least some of its functions by cooperating with other factors - UBN1, CABIN1 and ASf1a. Complexes containing these factors are involved in formation of senescence-associated heterochromatin, gene transcription and cell cycle progression[219,220]. HIRA and XNP (X-linked nuclear protein) can recognise chromatin defects and be recruited to the nucleosome-depleted regions, facilitating assembly there[221]. HIRA is essential for assembly of paternal chromatin during early Drosophila development[178]. It utilizes CHD1 to incorporate of H3.3 in the male pronucleus in an ATP-dependant manner[178]. The interaction of HIRA with its functional partners may be facilitated by its conserved WD-repeats domains. Those domains are present in a set of functionally diverse proteins that are part of macromolecular complexes and shown to provide interface for protein interaction[222].

DAXX is another histone chaperone specific for H3.3. It was discovered in H3.3 associated fraction purified from HeLa cells[84]. It physically interacts with H3.3 both *in vitro* and *in vivo* with higher affinity than with canonical H3.1[84]. DAXX was demonstrated to facilitate the deposition of H3.3 *in vitro*[84]. It forms a complex with chromatin remodelling factor ATRX in order to utilize its ATPase activity for its chromatin assembly function[223]. *In vivo,* DAXX and ATRX were shown to deposit H3.3 in pericentric heterochromatin and assist its transcription[84]. ATRX is implicated in H3.3 accumulation at other specific chromosome landmarks, such as telomeres[218]. DAXX is also shown to mediate recruitment of H3.3-H4 dimers to nuclear bodies, thus maintaining pool of H3.3 for further deposition into chromatin[224].

3.5.1.2 H2A-group/H2B histone chaperones

Nap-1 is a highly conserved H2A-group/H2B histone chaperone with several roles in both RC and RI assemblies. Nap-1 histone group is evolutionary conserved and includes Drosophila Nap-1, human Nap-1-like and yeast Vps75. While *in vitro* it has an affinity for both H2A/H2B and H3/H4[225], *in vivo* it associates with H2A-H2B only[226]. Nap-1 is required for H2A-H2B deposition and exchange across the genome[227,228]. Nap-1 and ATP-dependant factor dCAF-1 complex is demonstrated to efficiently assemble of chromatin with repeat length of the chromatin similar to that of native chromatin[226]. Nap-1 can also form regular nucleosomal arrays on its own without the need of ATP-dependant factor *in vitro*[229]. Together with its deposition function, Nap-1 was shown to facilitate assembly by removing restrictive

histone-DNA interactions[230], which may explain its ability to assemble chromatin without help of chromatin remodelling complexes[5]. There is growing data implicating Nap-1 maintenance of various histone pools. NAP-1 is shown to act as a linker histone chaperone in Xenopus eggs and to modulate the pool of linker histones[231]. It was also demonstrated to maintain a soluble pool of H2A.Z in the cytoplasm that may be important for the dynamic exchange of H2A-group/H2B histones within nucleosomes[205]. Finally, NAP-1 associates with Kap114p, a main nuclear importin of histones H2A and H2B[232], that also corroborates its role in the histone pool maintenance.

FACT is a H2A-group/H2B histone chaperone complex, consisting of two core subunits, SPT16 and SSRP1. FACT physically interacts with nucleosomes, with Spt16 subunit is in charge of H2A/H2B interaction, and SSRP1 of H3-H4 one[233]. FACT is shown to be involved in Pol II–driven transcript elongation *in vivo*[234]. *In vitro* it was revealed that FACT can both displace H2A-H2B dimers during transcription and then place them back after transcription has occurred[233]. This implicates that FACT possess both assembly and disassembly activity to effectively regulate H2A-H2B enrichment at the sites of transcription[233]. FACT is also shown to be a chaperone for histone variants H2A.Z[235] and H2A.X[236], depositing and evicting them within nucleosomes.

ANP32E is histone variant H2A.Z chaperone, capable of facilitating H2A.Z removal[11]. ANP32E is a member of the p400/TIP60 chromatin remodelling complex. ANP32E has specificity to H2A.Z/H2B dimers that it achieves through interaction of its ZID domain with αC-helix of H2A.Z[11]. ChIP-seq profile in ANP32E −/− cells revealed that its depletion leads to accumulation of H2A.Z at enhancers and insulators, which are otherwise normally cleared of it[11]. *In vitro* assays of ANP32E incubation with the H2A.Z immobilized nucleosomes resulted in the dissociation of H2A.Z from the nucleosome[11], further confirming its histone eviction function. ANP32E disassembly function is utilized during DNA repair, by removing H2A.Z from DNA double-strand breaks and promoting nucleosome reorganization there[237].

Yeast Chz1 is a conserved H2A.Z chaperone that transport Htz1 to SWR1 for H2A replacement in chromatin[6]. Both Chz1 and Nap-1 can reciprocally substitute for the binding to Htz1-H2B and its delivery to SWR1 complex, implicating overlapping functions between them[6,205]. Chz1 interacts with Htz1 using its CHZ motif – a highly conserved region, that is also located in the C-terminus of human Chz1 homologue HIRIP3[6] (Fig. 9).

Figure 9. CHZ motif is evolutionary conserved from yeast to human

Multiple sequence alignments of CHZ motifs in eukaryotes. Blue, acidic residues; Purple, basic residues; Red, nonpolar residues; Green, polar residues.
(Modified from E. Luk et al, 2007[6])

Crystal structure of CHZ and H2A-H2B fusion confirms Chz1 specific interaction with H2A.Z/H2B dimers with CHZ motif being critical for its stabilization[12]. CHZ motif was shown to possess bipolar charge distribution with three basic residues and five acidic residues located separately. Interestingly, it utilizes this bipolarity to interact with both positively and negatively charged histone residues[12]. This finding implicates that there are more complex requirements of histone chaperones and they are not merely negatively charged molecules that shield positive histone charge[12]. After delivery by NAP-1 or Chz1, another H2A.Z chaperone - Swc2 - binds Htz1-H2B dimers and facilitate their exchange within SWR1 complex[102,192]. Swc2 is conserved in metazoans as an YL1, which is part of a SRCAP chromatin remodelling complex[102].

3.5.2 Chromatin machinery interplay

Chromatin assembly and disassembly are highly regulated processes made possible by cooperation and interplay between components of chromatin machinery and other cellular factors[207].

The factors involved into *de novo* chromatin formation was extensively studied and described[214,238,239] (Fig. 10). *De novo* chromatin formation occurs immediately after DNA replication, with histones from the parental chromosome being randomly distributed to the two daughter DNA strands. Parental histones are shown to be transferred by chaperone Asf1[214]. The rest of nucleosomes is assembled from the newly synthesized histones. They are deposited onto DNA in step-wise manner[80,207] from two non-nucleosomal histone pools: one containing nascent H3 and H4, and another containing H2A and H2B in association with NAP-1 chaperone[240].

As a first step, newly synthesized acetylated H3–H4 dimers are transferred from histone Asf1 to histone CAF-1 or Rtt106 by their direct interaction[241]. CAF-1 or Rtt106 are assembling $(H3–H4)_2$ tetramers from dimers before further deposition[242]. Afterwards, they load $(H3–H4)_2$ onto naked DNA by interacting with proliferating cell nuclear antigen (PCNA)[210]. PCNA acts as a DNA polymerase clamp and thus targets CAF-1 to replication forks. *In vitro* experiments revealed maximum efficiency of assembly when both factors are present[213]. At this point, $(H3–H4)_2$ and DNA forms a stable intermediate[131].

Second step involves Nap-1-facilitated addition of two H2A-H2B dimers to the H3-H4 tetrasomes positioned on the DNA[241]. Those initial histone-DNA structures formed by histone chaperones are called nascent nucleosomes or pre-nucleosomes. They contain all four core histones and look similar to mature chromatin under microscope[239]. However, they are randomly positioned, are unable to supercoil DNA like mature chromatin and has weakened contacts with DNA[239].

The final step is the maturation of nascent chromatin that consist of a few processes. ATP-dependant factors start to convert pre-nucleosomes to the nucleosome arrays. Their remodelling activities arrange nucleosome arrays to make them evenly spaced on the DNA[117,239]. ACF is shown to carry out those functions during *de novo* formation [239]. After formation of regular nucleosome arrays, histone deacetylases remove acetyl groups from them, which leads to DNA-nucleosome wrapping seen in the mature chromatin[238]. Histone deacetylation is shown to be required for the maturation of newly replicated chromatin[243]. Linker histones are incorporated into the nucleosomes after initial formation of mature chromatin[239], possibly by NAP-1[231]. Mature chromatin is characterised by regularly spaced nucleosomes, resistance to DNaseI digestion, deacetylation of H4 and the binding of histone Hl in larger eukaryotes[62].

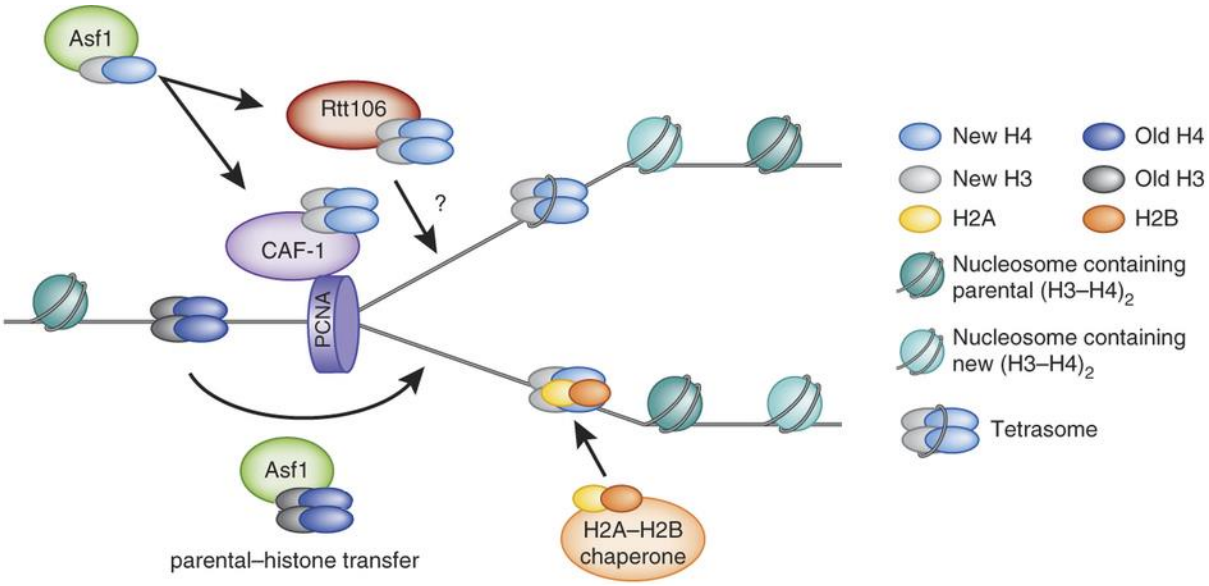

Figure 10. Replication-coupled chromatin assembly machinery interplay.

Newly synthesized histone H3–H4 dimers are imported into the nucleus by Asf1. They are transferred to CAF-1 and Rtt106 for $(H3–H4)_2$ formation and deposition onto newly synthesized DNA, which in part depend on interaction between CAF-1 and PCNA. Rtt106 tethering mark is not yet known. Parental histones are transferred by Asf1. H2A-H2B chaperon involved into RC chromatin assembly is Nap-1. Additional explanations in text.
(Modified from R. J Burgess and Z. Zhang, 2013[242])

Mechanisms of variant histones incorporation during RI-assembly are also dependent on cooperation between different cellular factors and marks[79] (Fig. 11). During transcription, Asf1 transfers H3-H4 dimers to HIRA factor, a three subunits complex consisting of HIRA histone chaperone, UBN1, and Cabin1. HIRA, together with chromatin remodelling factor CHD1, carries out histone exchange reaction at the transcription sites[132,178]. HIRA is recruited to those sites by the means of interaction with double-stranded DNA and RNA polymerase complex. This molecular tethering allows cooperation between H3.3 exchange and gene transcription[242]. Deposition and exchange of H2A-group/H2B during transcription is carried out by Nap-1, FACT and Chz1 histone chaperones.

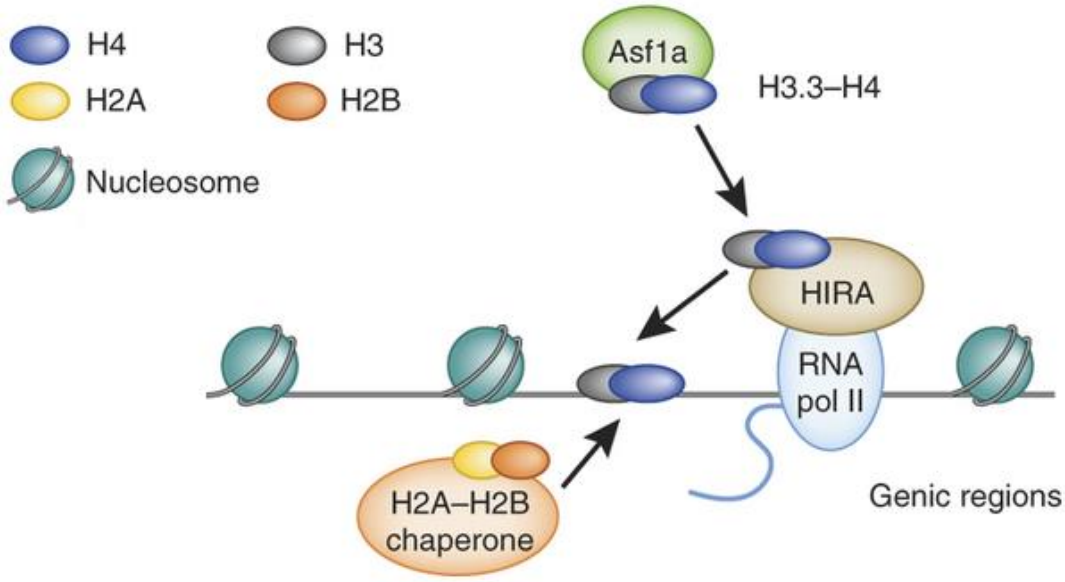

Figure 11. Replication-independent chromatin assembly machinery interplay during transcription.

H3.3–H4 of the Asf1a–H3.3–H4 complex is transferred to HIRA factor for deposition of H3.3–H4 at the sites of RNA polymerase II binding. Histone chaperones like FACT and NAP-1 facilitate H2A-group/H2B dimers exchange. Additional explanations in text.
(Modified from R. J Burgess and Z. Zhang, 2013[242])

Chromatin disassembly also requires interplay and cooperation between factors of chromatin machinery. The chromatin-remodelling factor RSC is cooperating with either Nap-1 or Asf1 chaperones to carry out its chromatin disassembly function[167]. Together with those histone chaperone, it disassembles nucleosome in a stepwise manner. At first, RSC and Nap-1 remove H2A/H2B dimers that leads to tetramer formation[167]. Afterwards by binding with H3/H4 tetramers, it completely disassembles the remainder of nucleosome with the release of naked DNA. FACT chaperone can also be involved in this process, by weakening interactions between H2A-H2B dimers and H3-H4 tetramers[233].

The understanding of interplay between elements of chromatin machinery depends on the studies of individual factors, their interactions, functions and mechanisms of action. Human chromatin machinery is of special interest considering numerous links of chromatin factors to both common and rare diseases[4,172,244]. To contribute to this research, we studied two human chromatin factors - HIRIP3, a histone chaperone candidate and SRCAP, a chromatin remodelling complex. In following chapters available data relevant to those factors will be reviewed, followed by the results achieved in this project.

4 MATERIALS AND METHODS

This work took advantage of three expression systems of proteins, each utilizing either *E.coli*, insect or HeLa cells. *E.coli* pET expression system was used for multiple interaction studies. Insect cells were used for their ability to express high molecular weight proteins. Finally, HeLa cells were used for purification of protein complex in context of human cellular environment.

4.1 Protein expression in *E.coli*

DNA sequences of proteins studied in this work were PCR amplified and sub-cloned into vector constructs of pET system, under the control of T7 promoter[245] (Table 1). PCR-directed mutagenesis was used to generate all mutation sequences. Constructs were introduced into competent BL21-CodonPlus-RIL bacteria (Stratagene) using standard heat-shock transformation procedure[246]. Transformed cells were grown in Luria Bertani Broth at 37 °C, with appropriate antibiotics (Table 1), till an absorbance of 0.5 at 600 nm. Expression was induced by adding a final concentration of 1 mM isopropyl-β-d-thiogalactopyranoside (Euromedex), which activates expression of genes under control of T7 promoter. After induction, cells were further grown for 2 hours at 25 °C. Cell pellets were collected by low speed centrifugation and stored at -80°C.

Sequence	Vector backbone	Cloning strategy	Bacterial resistance	Epitope tag
wt H2A, wt H2B	E. Coli, bicistronic pET28b, T7 promoter	H2A inserted in MCS via XhoI+NotI ; H2B inserted in MCS via NdeI-BamHI	kanamycin	FLAG (H2A), HIS (H2B)
wt H2A.Z, wt H2B	E. Coli, bicistronic pET28b, T7 promoter	H2A.Z inserted in MCS via XhoI+NotI ; H2B inserted in MCS via NdeI-BamHI	kanamycin	FLAG (H2A.Z), HIS (H2B)
S1A H2A, wt H2B	E. Coli, bicistronic pET28b, T7 promoter	S1A H2A inserted in MCS via XhoI+NotI ; H2B inserted in MCS via NdeI-BamHI	kanamycin	FLAG (S1A H2A), HIS (H2B)
S122A H2A, wt H2B	E. Coli, bicistronic pET28b, T7 promoter	S122A H2A inserted in MCS via XhoI+NotI ; H2B inserted in MCS via NdeI-BamHI	kanamycin	FLAG (S122A H2A), HIS (H2B)
HIRIP3	E. Coli, pGEX-5X.1,	inserted in MCS via	ampicillin	GST

1-556	T7 promoter	XhoI+NotI		
HIRIP3 1-370	E. Coli, pGEX-5X.1, T7 promoter	inserted in MCS via XhoI+NotI	ampicillin	GST
HIRIP3 371-556	E. Coli, pGEX-5X.1, T7 promoter	inserted in MCS via XhoI+NotI	ampicillin	GST
HIRIP3 371-556	E. Coli, pGEX-5X.1, T7 promoter	inserted in MCS via XhoI+NotI	ampicillin	GST
HIRIP3 397-556	E. Coli, pET28b, T7 promoter	inserted in MCS via XhoI+NotI	kanamycin	FLAG
HIRIP3 403-527	E. Coli, pGEX-5X.1, T7 promoter	inserted in MCS via XhoI+NotI	ampicillin	GST
HIRIP3 403-514	E. Coli, pGEX-5X.1, T7 promoter	inserted in MCS via XhoI+NotI	ampicillin	GST
HIRIP3 425-527	E. Coli, pGEX-5X.1, T7 promoter	inserted in MCS via XhoI+NotI	ampicillin	GST
HIRIP3 1-553	E. Coli, pGEX-5X.1, T7 promoter	inserted in MCS via XhoI+NotI	ampicillin	GST
wt H2A	E. Coli, pGEX-5X.1, T7 promoter	inserted in MCS via XhoI+NotI	ampicillin	GST
H2A 1-123	E. Coli, pGEX-5X.1, T7 promoter	inserted in MCS via XhoI+NotI	ampicillin	GST
H2A 1-111	E. Coli, pGEX-5X.1, T7 promoter	inserted in MCS via XhoI+NotI	ampicillin	GST
H2A 1-98	E. Coli, pGEX-5X.1, T7 promoter	inserted in MCS via XhoI+NotI	ampicillin	GST
H2A 1-92	E. Coli, pGEX-5X.1, T7 promoter	inserted in MCS via XhoI+NotI	ampicillin	GST
wt TIP49A	E. Coli, bicistronic pET15b, T7 promoter	inserted in MCS via XhoI+NotI	ampicillin	HIS
wt TIP49B	E. Coli, bicistronic pET15b, T7 promoter	inserted in MCS via XhoI+NotI	ampicillin	HIS
wt TIP49A, wt TIP49B	E. Coli, bicistronic pET28b, T7 promoter	TIP49A inserted in MCS via XhoI+NotI ; TIP49B inserted in MCS via NdeI-BamHI	kanamycin	FLAG (TIP49B), HIS (TIP49A)
wt YL1	E. Coli, bicistronic pET28b, T7 promoter	inserted in MCS via SalI+NotI	kanamycin	FLAG
wt YL1	E. Coli, pGEX-5X.1, T7 promoter	inserted in MCS via SalI+NotI	ampicillin	GST
YL1 1-110	E. Coli, pGEX-5X.1, T7 promoter	inserted in MCS via SalI+NotI	ampicillin	GST
YL1 111-230	E. Coli, pGEX-5X.1, T7 promoter	inserted in MCS via SalI+NotI	ampicillin	GST
YL1 231-364	E. Coli, pGEX-5X.1, T7 promoter	inserted in MCS via SalI+NotI	ampicillin	GST

Table 1. pET system constructs used for expression in E. coli.

All tags are N-terminal to protein. All genes are of human origin. wt – full length wild type protein; MCS - multiple cloning site.

4.2 Protein expression in SF9 insect cells

In order to generate proteins in insect cells, we used Invitrogen Bac-to-Bac Baculovirus expression System (Fig. 12). First, we have sub-cloned each gene of interest in the pFastBac donor plasmid, inserted in MCS. Following constructs were used in this studies:

FLAG–SRCAP 1-2270
HIS–H2A.Z/ T7–H2B, bicistronic
HIS–TIP49A
HA–TIP49B
TIP49A/TIP49B (no tags), bicistronic
HIS–YL1
HA–YL1

After amplification, generated pFastBac plasmid was used for transformation of DH10Bac *E.coli* competent cells. Using antibiotic selection coupled with blue-white selection, we identified colonies in which transposition had occurred, thus containing recombinant bacmid. Recombinant bacmid was subsequently amplified and used for SF9 cells transfection using Cellfectin II reagent (Thermo Fisher Scientific). Collected recombinant baculovirus particles (RBPs) were used either for virus stock amplification or infection of Sf9 insect cells. After virus amplification, RBP were collected and filtered through 0.22 μm filter, then stored in a 4°C dark room.

SF9 cells (*Spodoptera frugiperda*) were grown either in T-flasks (adherent cultures) or in spinner flasks (suspension cultures). They were cultured at 27°C in medium consisting of 10 % fetal heat-inactivated bovine serum, 5 mL/L penicillin-streptomycin and 1X Grace's insect cell culture supplemented medium (Gibco). When cells reach a density of 2×10^6 to 4×10^6 cells/ mL, they were passaged to a seeding density of 3×10^5 to 5×10^5cells/ mL. For protein expression, cells were infected at 2×10^6. Cells concentrations were evaluated using Malassez hemocytometer. To produce protein, Sf9 insect cells were infected with the recombinant baculoviruses, harvested after 48 to 72 hours, washed once with PBS and stored in pellet form at -80°C. Optimal virus concentrations and infection time were determined by test infections.

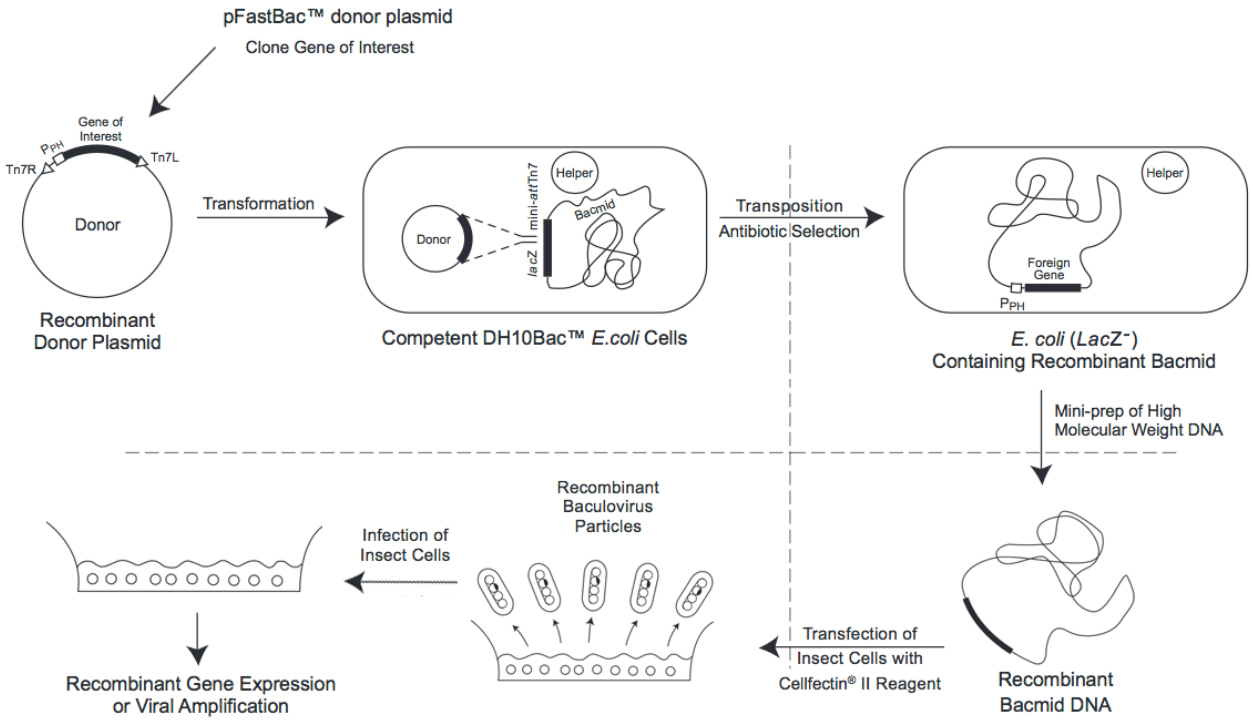

Figure 12. Work-flow of baculovirus expression system.

(Modified from Invitrogen Bac-to-Bac Baculovirus Expression System User guide, publication number MAN0000414)

4.3 Protein expression in HeLa cells

The coding sequence of HIRIP3 was PCR-amplified and sub-cloned into the XhoI-NotI sites of the pREV-HTF retroviral vector in frame with an N-terminal FLAG and HA tags. Retroviruses were produced in Phoenix retrovirus packaging cells and used to infect target HeLa cells, as described previously[247]. Briefly, Phoenix cells were transfected using pREV-HTF and viral particles were used to transduce HeLa cells. Stably transduced HeLa cell populations were established by triple immunomagnetic selection using Dynabeads cd25 (Invitrogen). Cell line distribution of positive cells was checked by immunofluorescence of cells using standard procedures[248]. Rat anti-HA antibody (Roche) was used at 1/200 dilution; the secondary antibody goat anti-Rat IgG coupled to Alexa Fluor 488 (Molecular Probes) was used at 1/400 dilution. Selected cell line expressing HIRIP3 protein fused to N-terminal FLAG- and HA-epitope tags (eHIRIP3) was grown in suspension culture to achieve four litres. Cells were maintained in incubator equipped with HEPA (High-efficiency particulate arrestance) filter, at 37°C and 5% CO2. Cells were grown in Dulbecco's Modified Eagle Medium (Thermo Fisher Scientific), supplemented with 10% FBS and 0.1 mg/ml

penicillin/streptomycin solution. Cell pellets were collected by low speed centrifugation and stored at -80°C.

4.4 Protein methods

4.4.1 Protein purification

In order to evaluate interaction between proteins, we used TAP (Tandem affinity purification) - TAG approach[84]. After generation of cellular extracts from either *E.Coli*, insect or HeLa cells, we subjected them to batch purification by the epitope tags (Table 2).

To generate soluble extracts from *E.Coli* and insect cells, pellets were re-suspended in buffer TGEN (20 mM Tris-HCl pH 7.65; 300 mM NaCl, 3mM MgCl2, O.1mM EDTA, 10% glycerol, 0.01% NP40, 1mM PMSF, 1x Roche cOmplete Protease Inhibitor Cocktail) and lysed by Wheaton glass dounce homogenizer (insect) or freeze–defreeze cycles (E. *coli*), followed by sonication in both cases. The soluble fraction was recovered by high-speed centrifugation. HeLa cells palettes we used to produce soluble cellular extract, soluble nuclear extract and insoluble extract as described previously[249].

For batch purification assay, extracts were mixed with appropriate agarose resin and incubated at 4 °C (Table 2). After the binding, extract-resin solution was centrifuged, supernatant was removed and the resin washed extensively with TGEN buffer. Afterword, the resin-bound proteins were eluted from the resin by adding appropriate eluent agent (Table 2) and incubating at 4 °C. Eluates were collected, and where applicable, were subjected to dialysis against TGEN buffer and second step of purification with other agarose resin. For protein pull-down assays, equal stoichiometric volumes of dialysed purified proteins were mixed, incubated for two hours at 4 °C and subjected to batch purification, as described above. After final step of purification eluates were flash frozen for storage at -80°C.

Tag	Name	Binding time	Eluent agent	Elution time	Company
FLAG	Anti-Flag M2 Affinity Gel purified immunoglobulin beads	5 hours	5 mg/ml Flag peptides	12 hours	Sigma
GST	Glutathione Sepharose 4B	1 hour	20mM gluthathione	1 hour	GE Healthcare Life Sciences
HA	Pierce Anti-HA Agarose	5 hours	5 mg/ml HA peptides	12 hours	Thermo Fisher Scientific
HIS	cOmplete His-Tag Purification Resin	1 hours	300mM imidazol	1 hour	Roche

Table 2. Resin used in purification assays

In order to evaluate specificity of resin beads binding, we have made cross-reaction tests with GST and FLAG tags fused proteins. Constructs of GST-tagged HIRIP3 and FLAG-H2A/HIS-H2B were expressed separately and were subjected to GST and FLAG purification assays (Fig. 13). We have confirmed that GST beads doesn't cross-react with FLAG tagged proteins and FLAG beads doesn't cross-react with GST tagged proteins in our experimental conditions.

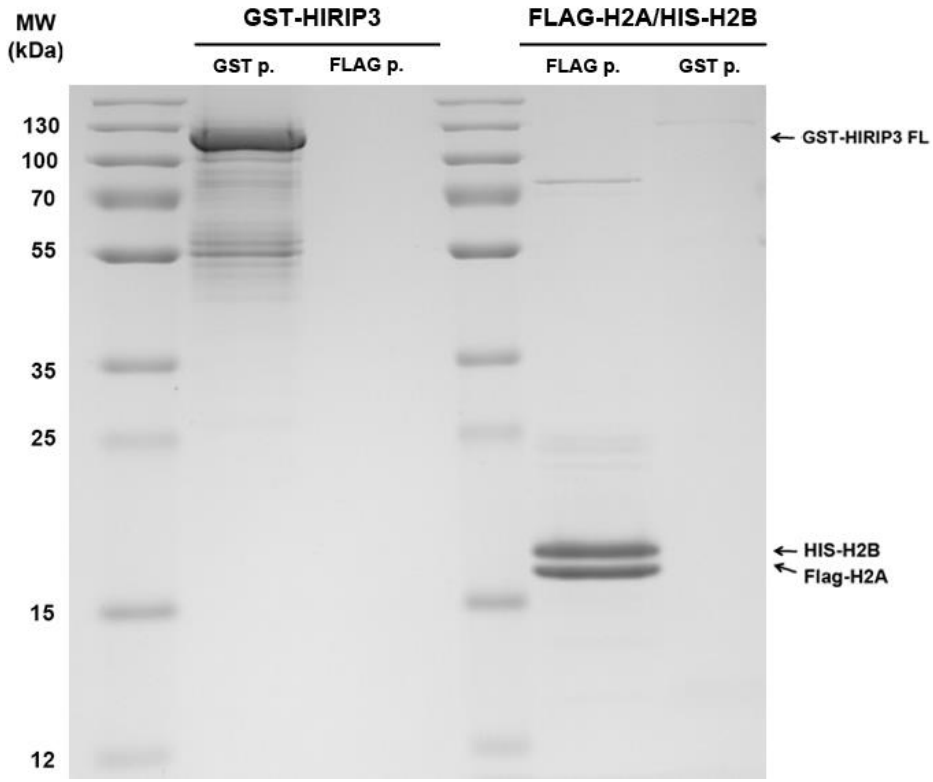

Figure 13. Resin binding specificity control

HIRIP3 FL - full length (1-556) of HIRIP3; MW - molecular weight. GST p. – purification by GST tag; FLAG p. – purification by FLAG tag.
GST-HIRIP3 and FLAG-H2A/HIS-H2B constructs were expressed in *E.Coli*. Generated soluble cellular extracts were subjected to either GST or FLAG tags purification.

4.4.2 SDS-polyacrylamide gel electrophoresis (SDS-PAGE)

Protein eluates were mixed with SDS-PAGE sample buffer, heated for 5 min at 95°C and loaded onto the 12% Tris-Glycine or 4-12% Bis-Tris polyacrylamide gel. Proteins were separated at 180 V until the dye front had reached the bottom of the gel. The molecular weight of proteins was estimated by running unstained (Mark12 Unstained Standard, ThermoFisher Scientific) and pre-stained (PageRuler Plus, ThermoFisher Scientific) marker proteins. Following electrophoresis, proteins were stained with either Coomassie Brilliant Blue, silver or subjected to Western blotting.

4.4.3 Staining of protein gels

For Coomassie staining, polyacrylamide gels were fixed for at least 30 min in fixation solution (30% ethanol / 10% acetic acid). Afterword they were incubated in Coomassie staining solution (0.025% Coomassie Blue R-250 in 10% acetic acid) for 20 min on a slowly rocking platform. To enhance visualization of proteins, gels were destained by boiling in tap water and further incubation on the rocking platform.

The staining of protein gels with silver nitrate solution was carried out using SilverQuest Kit (Thermo Fisher Scientific).

4.4.4 Western blotting

Western blotting was carried out using standard procedures[250]. Proteins were separated by SDS-PAGE and transferred to nitrocellulose or PVDF membranes using the Bio-Rad blotting system. The gel was placed onto a membrane and sandwiched between gel-sized Whatman papers soaked in transfer buffer (25 mM Tris, 192 mM glycine, 20% methanol). The proteins were then transferred onto the membrane for 1 h (120 V constant) at 4°C. The transfer reaction was cooled by the addition of an ice block into the transfer chamber. After transfer, nitrocellulose filters were incubated for 1 h in blocking solution (1x PBS, 5% dried milk and 0.1% Tween-20) in order to reduce the non-specific background. After blocking, membrane were washed three times in PBS-Tween (10 min each) and incubated overnight at 4°C with primary antibodies (Table 3). After 3 washes (10 min each, in PBS-Tween), secondary antibodies were added to membranes for 1 hour incubation. After last 3 washes in

PBS-Tween, antigen-antibody complexes were detected using Enhanced Chemi-Luminescence substrate.

Name	Clone	Company/source
anti-HA	3F10, monoclonal	000000011867423001, ROAHAHA Roche
anti-H3 CT, pan	A3S, monoclonal	05-928, Upstate Biotechnologies
anti-H2B	polyclonal	07-371, Upstate Biotechnologies
anti-H2A.Z	polyclonal	kind gift by Stefan Dimitrov
anti-H2A	polyclonal	kind gift by Stefan Dimitrov
anti-CK2 alpha	polyclonal	A300-197A-M, Bethyl Laboratories
anti-FLAG	M2, Monoclonal	Sigma Aldrich, A8592
anti-YL1	EXM10001, Monoclonal	Epigex
anti-TIP49A	Monoclonal	Abcam
anti-TIP49B	42, Monoclonal	BD Transduction Laboratories- BD Biosciences

Table 3. Antibodies used in this work

4.4.5 Mass spectrometry

Preparation of proteins for mass spectrometry was carried out using using an ion-trap mass spectrometer (ThermoFinnigan LTQ-Orbitrap Velos), as described previously[11].

4.5 Structural modelling

Chz1 and H2A.Z/H2B fusion structures were used from 2JSS[12], the structure of budding yeast chaperone Chz1 complexed with histones fusion H2A.Z-H2B. H2A/H2B dimer structure were used from 1ID3[251], the yeast nucleosome particle. Figures have been made using PyMOL program (The PyMOL Molecular Graphics System, Version 1.3 Schrödinger, LLC.), http://www.pymol.org/

The structures were superimposed using align action for H2B region identical for both structures.

4.6 Phosphorylation assay

Recombinant histone complexes were generated by expressing bicistonic pET28b vector in *E.coli*, followed by double step affinity purification of cell's soluble fraction carried out as described[252]. Phosphorylation assay of H2A/H2B, S1A H2A/H2B and S122A

H2A/H2B was carried out as described previously[253] with minor modifications. 0.75 mg of each of the protein complexes were incubated for 30 minutes at 30°C in a buffer containing 70mM Tris-HCl, 10mM MgCl2, 5mM DTT, 0.5m Ci P32 ATP and 100 ng of each of recombinant CK2α1/β and CK2α2/β. Recombinant CK2α1/β (CSNK2A1/B) 05-184 and CK2α2/β (CSNK2A2/B) 05-185 were purchased from Carna Biosciences. Reactions were stopped by Laemmli sample buffer, boiled for 10 minutes, migrated through a 14% SDS-polyacrylamide gel, dried on paper and revealed by exposure to radiography film.

5 RESULTS AND DISCUSSION

5.1 PROJECT I. Identification and characterization of HIRIP3 as a novel histone H2A chaperone

HIRIP3 (HIRA-interacting protein 3) is a 556 amino acid mammalian protein. Its gene is located on the short arm of chromosome 16 and consists of seven exons. HIRIP3 protein is highly charged, with 20.1% and 21.1% acidic and basic residues respectively. HIRIP3 mRNAs of fetal and adult origins consist of two low-level transcripts of approximately 2.0 and 2.9 kb[13]. Both transcripts are similarly expressed in fetal kidney, with a predominance of the larger transcript in adult skeletal muscle and smaller one in adult heart. HIRIP3 is a mainly nuclear protein and was shown to be extensively scattered throughout the nucleus, with nucleoli devoid in interphase cells[253]. During mitosis, HIRIP3 is excluded from condensed chromatin, but is concentrated in mitotic spindles at metaphase and in midbody junctions at the end of telophase[253].

HIRIP3 domain structure features glutamic acid-rich and polyserine regions in its N-terminal and central position respectively and CHZ motif located in C-terminus. CHZ motif is a conserved from yeast to human and is shown mediate histone chaperone Chz1 interaction with H2A.Z[6]. CHZ motif of HIRIP3 may also be involved into the histones processing. While roles of other regions within HIRIP3 are unknown, based on available data, serine region may

act as the phosphorylation sites of HIRIP3[253] and glutamic acid-rich region may mediate its DNA-related functions[254].

HIRIP3 was shown to be a HIRA interacting partner in the yeast protein interaction trap studies[13]. HIRA is a H3.3 variant histone chaperone which incorporates H3.3 in replication independent during active transcription[14] and chromatin structure recovery after DNA damage[201]. The HIRA-HIRIP3 interaction was confirmed by *in vitro* pull-down experiments[13]. HIRA interacting partners - UBN1, CABIN1 and ASf1a are shown to be involved into the chromatin processing, by the means of enhancing and modulating HIRA activity[219,220]. While the HIRA-HIRIP3 complex function is unknown, it is possible that it is associated with chromatin metabolism, similar to other HIRA containing complexes.

HIRIP3 is shown to both interact with and be phosphorylated by CK2 kinase[253]. Two-hybrid interaction studies revealed both CK2 alpha and beta subunits as interacting partner of HIRIP3[253]. HIRIP3 protein is heavily phosphorylated *in vivo* and were shown to be affected by phosphatase treatment, which results in its faster migration on SDS-PAGE gel[253]. The minimal consensus site for phosphorylation by CK2 occurs several times in HIRIP3. Consequently HIRIP3 was shown to be phosphorylated by CK2 both *in vitro* and *in vivo*[253], establishing itself as a CK2 kinase substrate. CK2 is an evolutionary conserved ubiquitous serine/threonine kinase that forms a tetrameric complex consisting of two catalytic and two regulatory subunits[15]. CK2 participates in a complex series of cellular events, including gene regulation, cell cycle progression and maintenance of cell viability that it may achieve by facilitating protection of cellular proteins from caspase action. CK2 phosphorylation is known to regulate histone chaperones localization and functions as shown for the histone chaperones Nap-1[19] and FACT[255]**.** A number of other downstream targets of CK2 also have a role in chromatin metabolism[16].

Taking those data together, HIRIP3 is highly implicated to participate into chromatin dynamics. First, it is directly interacting with H3.3 specific chaperone HIRA, which interacting partners are often involved in chromatin associated processes. Second, HIRIP3 is interacting with and getting phosphorylated by CK2 kinase, which downstream targets have roles into the chromatin processing. Finally, HIRIP3 is homologous to Chz1 yeast protein, which is a histone chaperone specific to H2A.Z.

Despite available data about HIRIP3, its function is not yet discovered. In this project, we aimed to identify HIRIP3 role in the context of chromatin dynamics and to study whenever it has characteristics of a histone chaperone. We have found that HIRIP3 is stably associated with H2A histone *in vivo*. Using *in vitro* interaction studies we have identified

minimal domain sufficient for HIRIP3 interaction with H2A/H2B dimers. Finally, we have shown that interaction with HIRIP3 is dependent on the alphaC helix of H2A. Taken together, our data establish HIRIP3 as a novel histone chaperone specific to canonical H2A histone.

5.1.1 Results

5.1.1.1 H2A/H2B dimers *are co-purified with HIRIP3 in vivo*

In order to evaluate HIRIP3 as a histone chaperone, we started with the purification of HIRIP3 complex *in vivo*. We aimed to test whether HIRIP3 is directly associated with histones, since physical interaction with histones is an important indicator of histone chaperone activity[10]. Towards this goal, we established a stable HeLa cell line expressing N-terminally FLAG-HA epitope-tagged human HIRIP3 (e-HIRIP3). Cell line was verified to be positive by Western blotting and immunofluorescence with anti-HA antibodies. We generated cellular and nuclear extracts from said cell line and subjected them to tandem FLAG and HA immunopurification, which allowed us to identify proteins that are forming complex with eHIRIP3 (Fig. 14a). In the soluble nuclear extract (SNE) and insoluble nuclear extract (INE), we detected 3 bands between 10-17 kDa, which is the usual observed molecular weight of histones. Mass spectrometry and western blotting analysis of the purified eHIRIP3 complex identified that the complex indeed contained histones, and among them H2A and H2B (Fig. 14b, table 4). H2A.Z was revealed to be excluded from eHIRIP3 complex (Fig. 14b). Our data show that, unlike Chz1 which interacts with H2A.Z, HIRIP3 forms complex with H2A *in vivo*. eHIRIP3 complex was also shown to contain H3 histones, implicating that HIRIP3 may interact with H2A/H2B dimers within entire H2A-containing nucleosome (Fig. 14b). These findings reveal that HIRIP3 is stably associated with histones *in vivo* and may have function related to their metabolism.

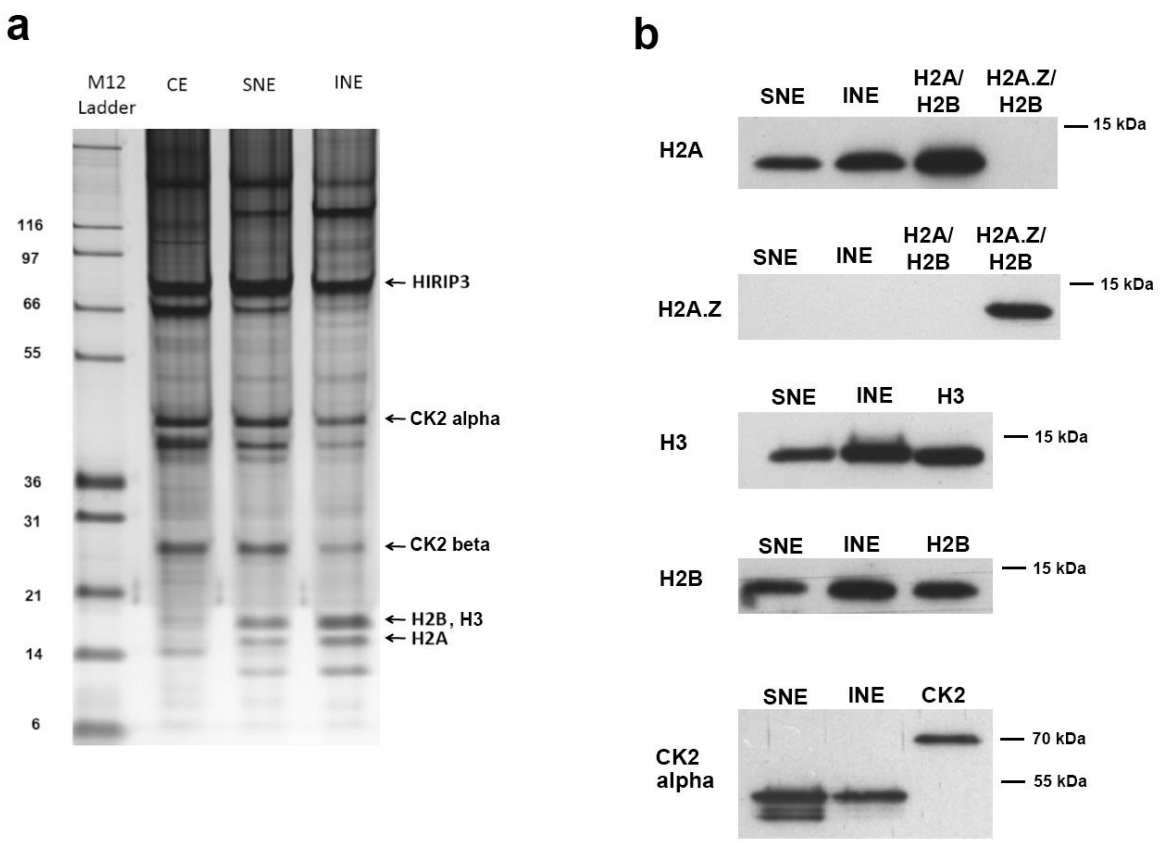

Figure 14. H2A/H2B dimers are co-purified with HIRIP3 *in vivo*

(A) Silver staining of e-HIRIP3 complex purified from HeLa cells stably expressing e-HIRIP3, separated by fractionation (CE - cellular extract, SNE - soluble nuclear extract, INE - insoluble nuclear extract).
(**B**) Western blotting analysis of the SNE and INE fractions of e-HIRIP3 complex. Fractions were probed with anti-H2A, anti-H2A.Z, anti-H2B, anti-H3 and anti-CK2 antibodies. The last slot in each experiment is an independently purified protein used as an antibody control. The control used for CK2 alpha subunit is GST-CK2 alpha, which is 26 kDa larger than endogenous CK2 alpha because of GST fusion protein.

Protein	Peptides
PRKDC	88
HIRIP3	41
SPT16	34
KU86	20
SSRP1	19
KU70	19
AMPD2	17
ANM5	14
CSNK2A1	8
KIF11	6
RFC5	5
NPM	4
UBP7	4
CK2 alpha	2
RFC4	2
HSP7C	2
HS90A	2
TBA2	2
UBE1	1
H2B type 1-B	1
DNL4	1
PWP2	1
HNRPK	1
PP2CG	1
PARP1	1
EF2	1
XPO5	1
IPO7	1
DHX15	1
Q5JP53	1
RFC3	1
Q7Z6Y5	1
MSH2	1

Table 4. Mass spectrometry data of the SNE fraction of e-HIRIP3 complex.

5.1.1.2 HIRIP3 interacts with H2A/H2B and H2A.Z/H2B dimers in vitro

To characterize HIRIP3 interaction with histones, we moved to the *in vitro* expression systems. Using pET expression system in *E. coli*, we co-expressed GST-HIRIP3 with either H2A/H2B or H2.Z/H2B histone dimers. Generated *E.coli* suspension cultures were subjected to soluble fraction isolation with consecutive double affinity purification experiments by GST and FLAG tags. SDS-PAGE analysis of eluates revealed that HIRIP3 binds to both H2A/H2B and H2A.Z/H2B dimers with the similar affinity (Fig. 15). This result rises the possibility that HIRIP3 can interact with both H2A and H2A.Z, similar to histone chaperones Nap-1[205] and FACT[235]. However, in *in vivo* complexes, H2A.Z was not detected within the eHIRIP3 complex, meaning that HIRIP3 either doesn't interact with it *in vivo* or interaction is too transient to be detected. Taken together, our data show that HIRIP3 stably interacts with H2A/H2B dimers in *vivo*, even though HIRIP3 has affinity to and can bind both H2A/H2B and H2A.Z/H2B dimers *in vitro*.

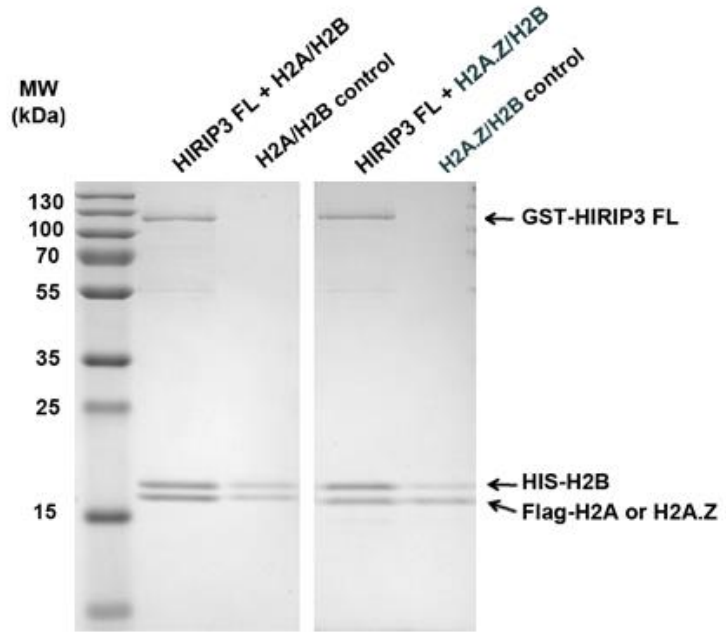

Figure 15. HIRIP3 interacts with H2A/H2B and H2A.Z/H2B *in vitro*

Construct coding GST-tagged full-length HIRIP3 was co-expressed with either FLAG-H2A/HIS-H2B or FLAG-H2A.Z/HIS-H2B dimers constructs. Soluble cellular extracts were isolated and subjected to double GST and FLAG immunopurification assay.
HIRIP3 FL - full length (1-556) HIRIP3; MW - molecular weight. H2A(Z)/H2B control - purified FLAG-H2A(Z)/HIS-H2B used as marker of observed molecular weight of histone dimers.

5.1.1.3 HIRIP3 CHZ motif is critical for H2A/H2B interaction

Next step was to further characterize HIRIP3 and H2A/H2B interaction by mapping the HIRIP3 domain involved in histone recognition and binding. To achieve this aim, we used a structure-based mutational analysis of HIRIP3. To start with histone binding domain identification, first we generated two mutants, each consisting roughly of a half of the protein. First one is comprised of 1-370 residues and the second of 371-556 residues of HIRIP3 (Fig. 16). 1-370 mutant contained N-terminal regions specific to HIRIP3, while 371-556 mutant contained CHZ motif (484-507) and its surrounding regions. We have co-expressed each of those mutants with H2A/H2B dimers and generated soluble extracts. GST purification assay revealed that 371-556 mutant interacts with dimers with similar affinity as full-length protein, while 1-370 showed no interaction (Fig. 17a). In order to determine the HIRIP3 minimal domain required for interaction with H2A, we further truncated 371-556 region from both N and C-terminal sides (Fig. 17b, c). N-terminally truncated 403-527 mutant was interacting with H2A/H2B dimers with full affinity, while interaction of 425-527 one was severely decreased (Fig. 17b). C-terminally truncated mutant 403-527 showed full affinity, while 403-514 one showed decreased affinity and also was subjected to degradation, indicating that protein became destabilized (Fig. 17c). These experiments let us to identify 403-527 HIRIP3 region as a minimal domain, sufficient for the full affinity interaction with H2A/H2B dimers.

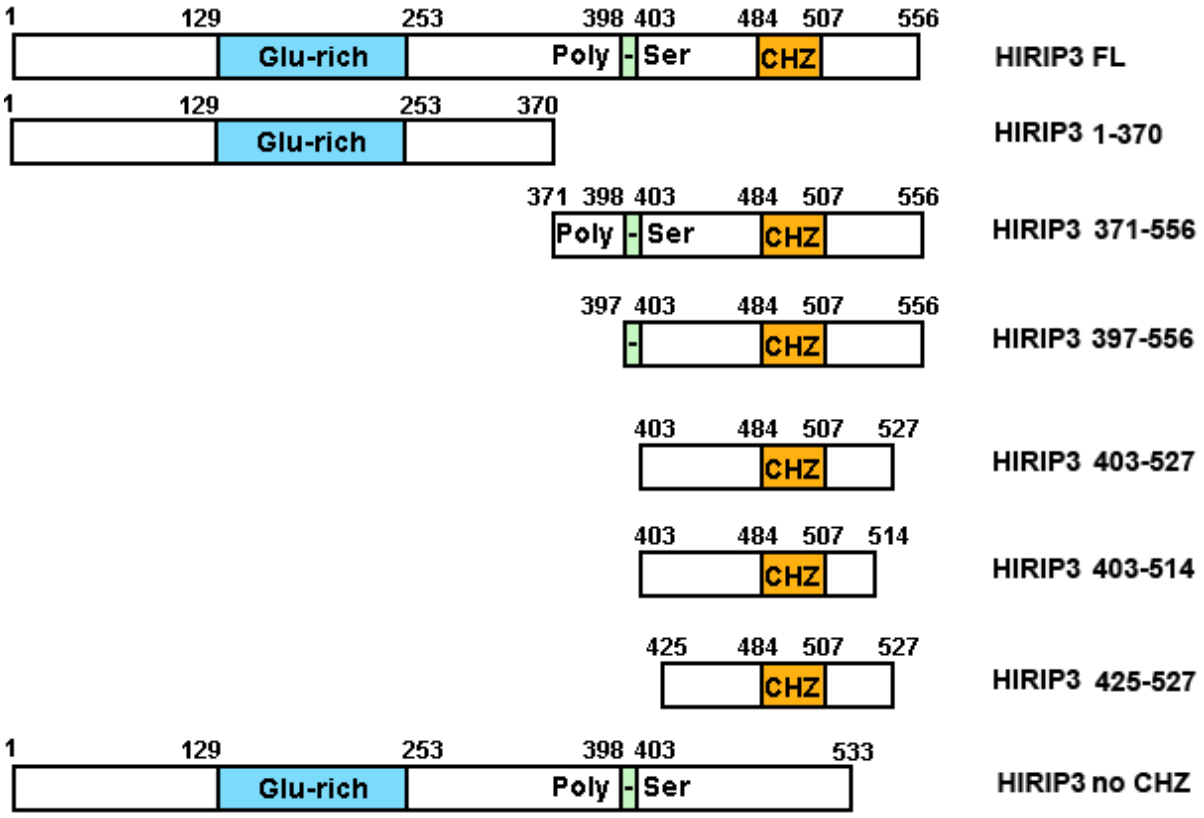

Figure 16. HIRIP3 full-length and mutants' domain composition

Schematic representation of full-length HIRIP3 and HIRIP3 mutants, used in this work: HIRIP3 1-370, HIRIP3 371-556, HIRIP3 397-556, HIRIP3 403-527, HIRIP3 403-514, HIRIP3 425-527 and HIRIP3 without CHZ domain (1-484 fused to 507-556).
Glutamic acid-rich region (blue), polyserine region (green), CHZ motif (orange).

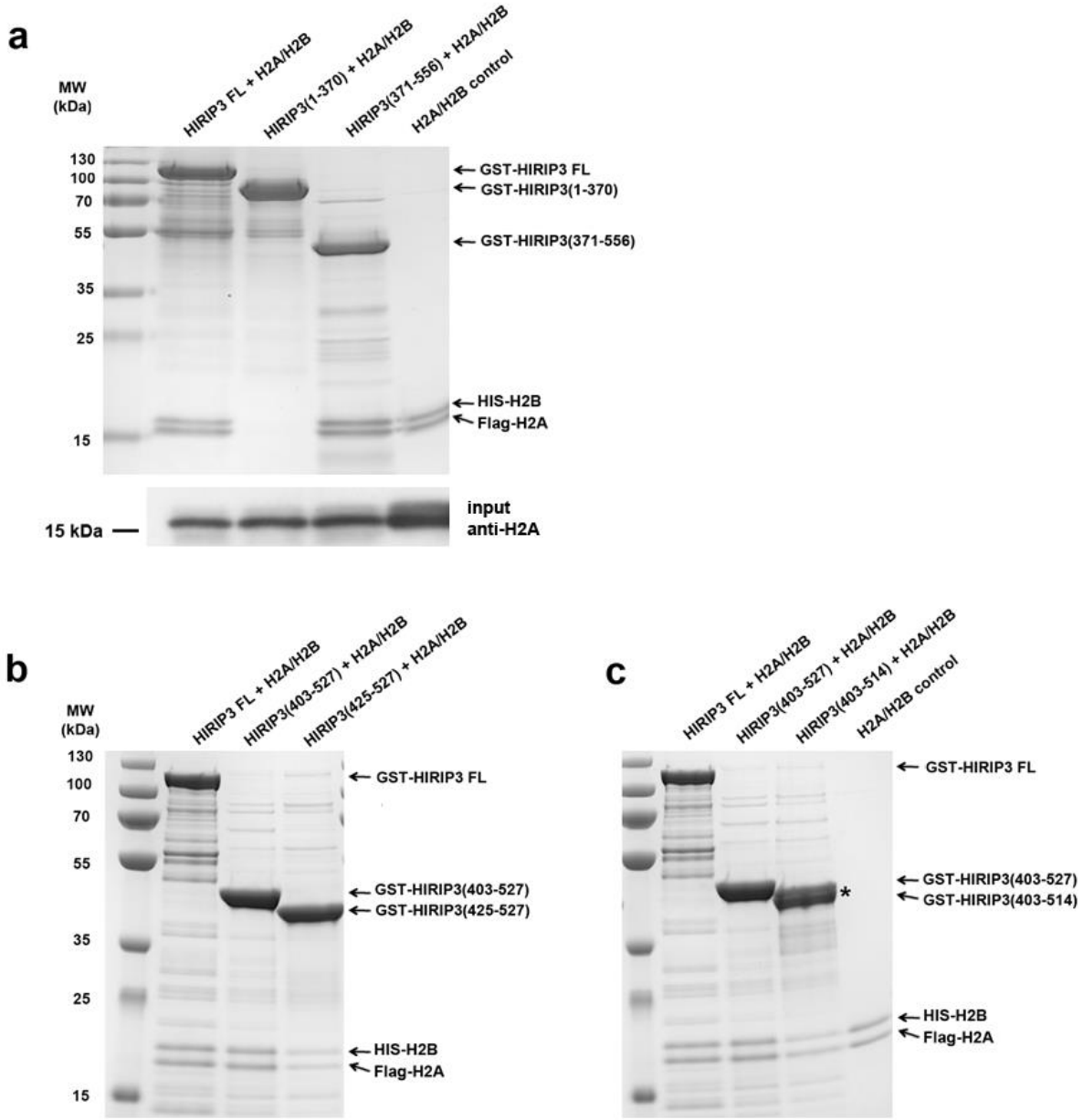

Figure 17. HIRIP3 utilizes CHZ-containing 403-527 region to interact with H2A/H2B dimers

All figures: HIRIP3 FL - full length (1-556) of HIRIP3; MW - molecular weight. H2A/H2B control - purified FLAG-H2A/HIS-H2B used as marker of observed molecular weight of histone dimers.
(a) GST purification assay of GST-HIRIP3 FL, GST-HIRIP3 (1-370) and GST-HIRIP3 (371-556) co-expressed with FLAG-H2A/HIS-H2B dimers. 371-556 region of HIRIP3 is revealed to interact with histones. This region contains CHZ motif (484-507). Top, Coomassie staining; Bottom, anti-H2A western blotting of soluble cellular extracts (inputs). All samples show similar H2A expression level.
(b) N-terminal truncations of GST-HIRIP3 (403-527 and 425-527) were used in GST purification assay with FLAG-H2A/HIS-H2 dimers. 403-527 shows the same affinity to dimers as HIRIP3 FL, while 425-527 revealed decreased affinity.
(c) Same as (b), but with truncations from C-terminal end (403-527 and 403-514). 403-527 shows same affinity to dimers as HIRIP3 FL, while 403-514 revealed decreased affinity and were also degraded (degraded product marked by asterisk).

Our next step was to test whether CHZ motif was essential for HIRIP3 interaction with H2A/H2B or whether this interaction could be attributed to non-CHZ motif regions only. Towards this goal, we constructed deletion mutant of HIRIP3, which lacked CHZ domain (Fig. 16). Interaction with this mutant was abolished (Fig. 18), indicating that CHZ motif of HIRIP3 is indispensable for interaction with H2A/H2B. In conclusion, our data revealed that HIRIP3 interacted with H2A/H2B dimers through extended 403-527 region, with 484-507 CHZ motif being critical for this interaction.

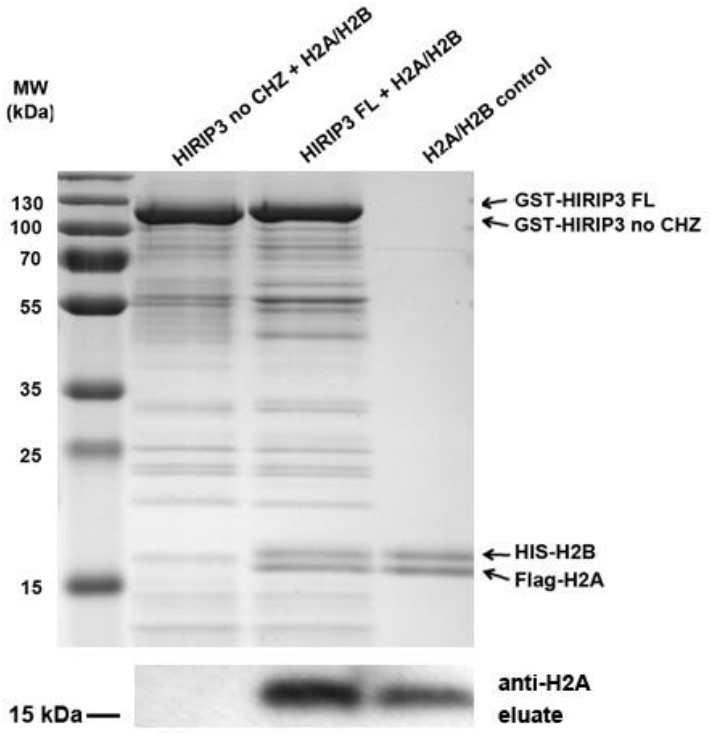

Figure 18. CHZ motif of HIRIP3 is necessary for interaction with H2A/H2B dimers

HIRIP3 FL - full length (1-556) of HIRIP3; MW - molecular weight. H2A/H2B control - purified FLAG-H2A/HIS-H2B used as marker of observed molecular weight of histone dimers.
Either GST-HIRIP3 FL or GST-HIRIP3 with no CHZ motif were co-expressed with FLAG-H2A/HIS-H2B and were subjected to GST purification assay. HIRIP3 lacking CHZ motif had its interaction with H2A/H2B abolished. Top, Coomassie staining; bottom, anti-H2A western blotting of GST eluates.

5.1.1.4 H2A interacts with HIRIP3 through its alphaC domain

After identifying HIRIP3 minimal interaction region, we aimed to identify the H2A domain involved in this interaction. Toward this goal, we generated truncations of H2A starting from C-terminus: 1-123, 1-111, 1-98 and 1-92 (Fig. 19a). Truncations were selected based on available data in the literature showing the importance of H2A alphaC helix for interaction with several histone chaperones[7,11,18]. We co-expressed the GST-H2A truncation mutants with 397-556 region of FLAG-HIRIP3, which contains minimal domain, and carried out FLAG purification assays to test their interaction. Residues 98-111 of H2A were revealed to be critical for interaction with HIRIP3 (Fig. 19b). This region contains the alphaC helix, that was shown to be in charge of interaction with several H2A-group chaperones, such as Chz1[18], YL1[7] and Anp32E[11]. This result indicates that HIRIP3 interacts with H2A via the help of its alphaC helix, which is characteristic of H2A-group histone chaperones.

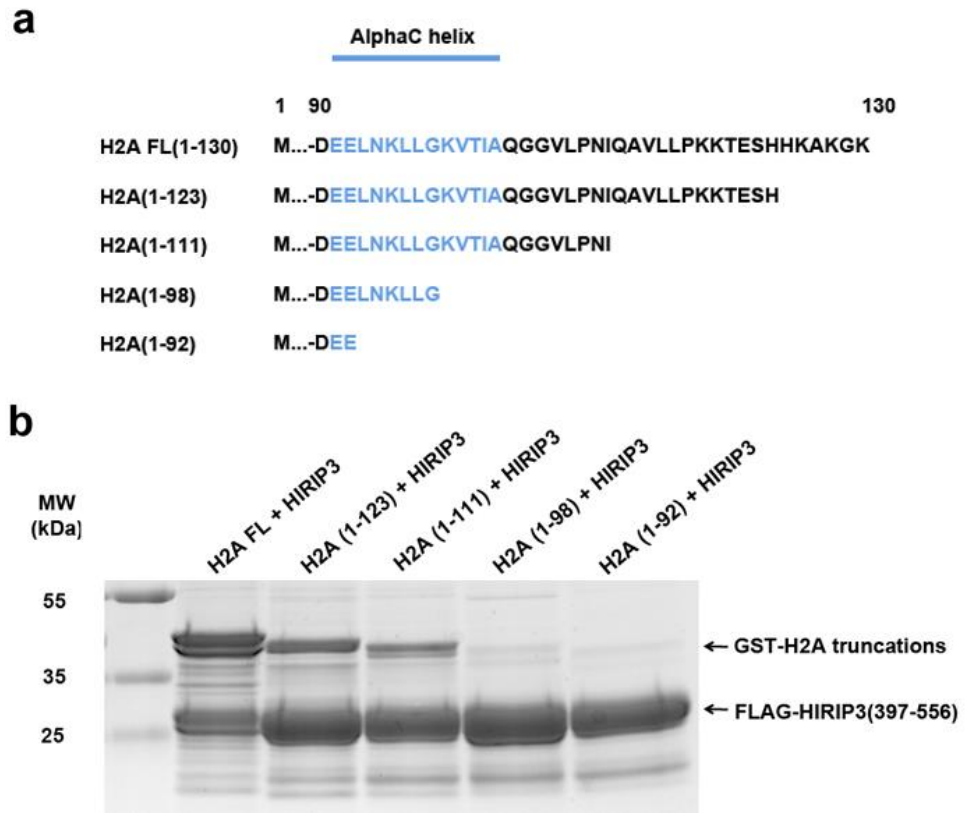

Figure 19. HIRIP3 interacts with H2A through its alphaC helix

(A) Schematic representation of full-length H2A and H2A truncations, used in this work: H2A 1-130 (FL, full-length), H2A 1-123, H2A 1-111, H2A 1-98 and H2A 1-92.
AlphaC helix region is indicated in blue.

(B) FLAG purification assay of H2A-GST truncations with 397-556 FLAG-HIRIP3. Interaction is gradually decreased from full-length to 1-111 truncation and is lost for 1-98 mutant. MW- molecular weight

5.1.1.5 Structural considerations of HIRIP3 and H2A/H2B interaction

In order to visualize HIRIP3 and H2A/H2B interaction, we took advantage of available structural data. We superimposed Chz1 and H2A.Z-H2B fusion structure (2JSS)[12] with H2A/H2B dimer from yeast nucleosome particle structure (1ID3)[251] (Fig. 20). We aimed to determine whether CHZ motif can be modelled to interact with H2A/H2B dimers. We found that CHZ motif + H2A/H2B alignment is very close to that of CHZ motif + H2A.Z-H2B. CHZ motif lies on top of H2B alphaC and bends around it to have its ends reaching H2A alpha2. Interestingly, alphaC helix of H2A doesn't participate in the interaction with CHZ motif, implicating that HIRIP3 utilizes other residues from 403-527 minimal domain for this interaction.

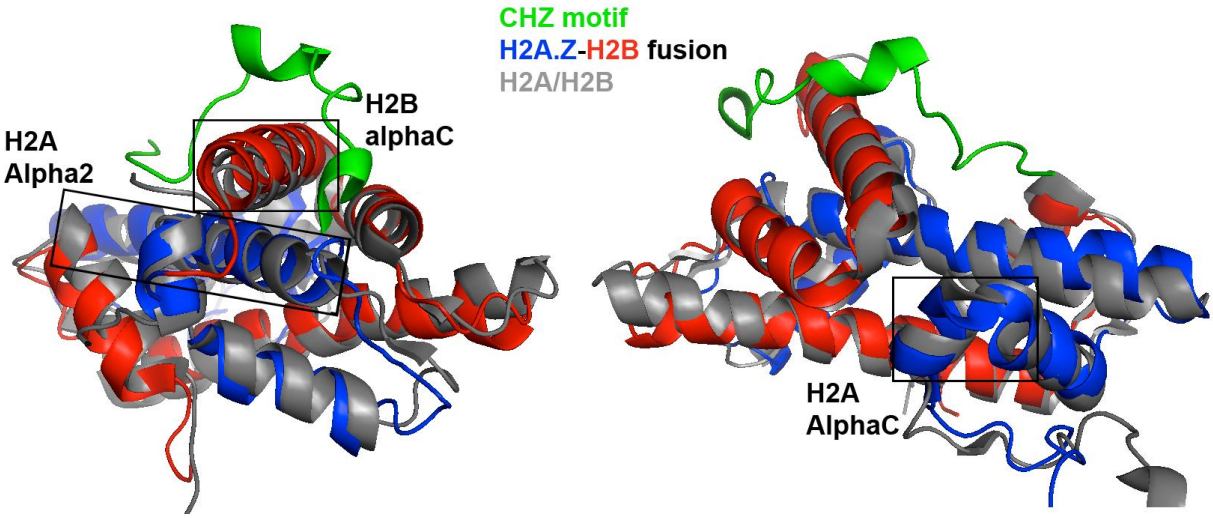

Figure 20. Simulated interaction between CHZ motif and H2A/H2B dimers

Green - CHZ motif from 2JSS, Blue - H2A.Z region of H2A.Z-H2B fusion from 2JSS, Red - H2B region of H2A.Z-H2B fusion from 2JSS, Grey - H2A/H2B dimer from 1ID3. Boxed - alphaC helix of H2A.Z and H2A; alpha2 helix of H2A.Z and H2A; alphaC helix of H2B.

5.1.1.6 CK2 phosphorylates H2A within eHIRIP3 complex

Mass spectrometry analysis of the HIRIP3 complex also revealed the presence of the CK2 kinase within the complex (Table 4). Western blotting against alpha subunit of CK2 confirmed CK2 being part of the HIRIP3 complex (Fig. 14b). The presence of CK2 in the HIRIP3 complex could either play a role in HIRIP3 phosphorylation or have other unknown functions in the context of HIRIP3 complex. To test the latter possibility, we used a phosphorylation assay to evaluate whether CK2 can phosphorylate the H2A/H2B dimers. Toward this goal, we generated two H2A non-phosphorylable mutants (S1A and S122A). Phosphorylation assay revealed that CK2 can phosphorylate full length H2A histone and S122A mutant but not the S1A mutant (Fig. 21). The S1A mutation completely abolished phosphorylation of H2A, indicating that Serine 1 site is critical for H2A phosphorylation. This S1 site is not present in H2A.Z histone. The presence of HIRIP3, CK2 and H2A/H2B in one stable complex implicates a functional connection between those factors that may be regulated through phosphorylation.

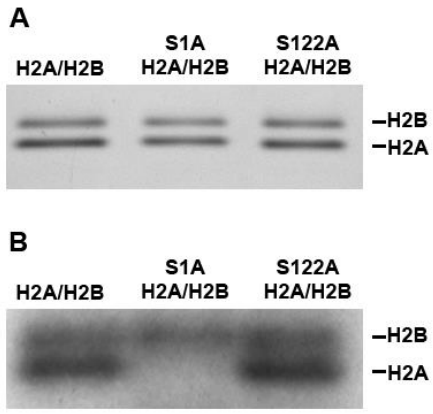

Figure 21. S1 H2A is critical for H2A phosphorylation by CK2

(A) H2A/H2B, S1A H2A/H2B and S122A H2A/H2B recombinant proteins were generated using pET expression system in *E. coli*. 1 mg of each dimer were subjected to electrophoresis on 12% SDS-polyacrylamide gel and visualized by Coomassie Blue staining.
(B) 0.75 mg of each H2A/H2B, S1A H2A/H2B and S122A H2A/H2B recombinant protein was incubated at 30°C for 30 min in the presence of CK2 kinase and [γ -^{32}P] ATP. Reactions were subjected to electrophoresis on 14% SDS-polyacrylamide gel and revealed by exposure to radiography film.

5.1.2 Discussion

5.1.2.1 HIRIP3 interaction with H2A/H2B dimers in vivo and in vitro

The first step of this work was identification of HIRIP3 interaction with histones both *in vivo* and *in vitro*. At first, we have purified eHIRIP3 complex from HeLa cells *in vivo.* This complex contained H2A and H2B histones, but no H2A.Z ones. Since H2A and H2B have a high affinity for each other and carry out their functions as dimers[242], we suggest that HIRIP3 associates with them as a H2A/H2B dimer complex. HIRIP3 and H2A/H2B association *in vivo* supports the notion of their functional connection, since complex formation is often a hallmark of functional cooperation. For example, other H2A-group/H2B histone chaperones, such as YL1[7] and ANP32e[11] were shown to co-purify with the histones *in vivo*. Along with H2A and H2B, H3 histone was also identified within eHIRIP3 complex. The presence of H3 may indicate HIRIP3 association with $(H3–H4)_2$ tetramers or entire nucleosome particle.

Secondly, using *in vitro* purification assays, we further confirmed HIRIP3 interaction with H2A/H2B dimers. HIRIP3 were found to not discern between H2A/H2B and H2A.Z/H2B dimers *in vitro* and to bind them with similar affinity. The fact that HIRIP3 was found to associate *in vivo* with H2A/H2B and not with H2A.Z/H2B dimers, like Chz1, raised the question of evolutionary divergence of CHZ motif-containing proteins. It may be attributed to an evolutionary changes in the chromatin machinery and to the different cellular requirements between yeast and mammals. The regions of HIRIP3 that are not present in Chz1 may be involved in mediating this specificity. They may serve as a scaffold for interaction with other proteins, such as HIRA, which was shown to interact with HIRIP3[13]. Those additional regions may, as well, contain motifs that could be targeted by post-translational modifications, and hence could contribute to unique HIRIP3 interactions and functions. CK2 phosphorylation may be involved in HIRIP3 histone specificity, since it is known to regulate histone chaperone localization and functions as shown for the H2A histone chaperones Nap1[19] and FACT[255]. It is important to note that Chz1, while characterized as H2A.Z chaperone *in vivo*, is also able to interact with H2A *in vitro*[6]. This fact supports the notion that *in vitro* Chz1 and HIRIP3 are both unable to discriminate among H2A-group histones. Those interactions are modulated by other cellular factors, leading to the histone specificity we observe *in vivo*. Taken together, our data established HIRIP3 as a novel interaction partner of H2A/H2B canonical histone dimer *in vivo* and *in vitro*.

5.1.2.2 Structural basis of HIRIP3 interaction with H2A/H2B dimer

This work have demonstrated that mammalian HIRIP3 interacts with H2A in a similar fashion as yeast Chz1 interacts with H2A.Z, with the help of its conserved CHZ motif. Structural simulation corroborates similarities of those two interactions, with CHZ motif closely aligning with both H2A.Z/H2B and H2A/H2B dimers. In comparison with Chz1 and H2A.Z interaction, that is mediated by 55 residue region of Chz1[6], we showed that HIRIP3 interacts with H2A using more extensive 124-residues region. This 403–527 region contains additional residues both to N-and C-terminal sides of CHZ motif. Those regions may contribute to larger interaction interface between HIRIP3 and H2A and additional non-CHZ-motif mediated connections. Despite involvement of other regions, we show that CHZ motif is indispensable for HIRIP3 interaction with H2A/H2B. We propose that identified CHZ-motif containing domain of HIRIP3 utilize it entire surface to interact with H2A/H2B dimers.

Structural simulation of CHZ motif and H2A/H2B interaction revealed that both H2A and H2B histones are likely to be directly involved into interaction with HIRIP3. AlphaC region of H2B was found to provide extensive binding surface for CHZ motif, while alpha2 of H2A was shown to have multiple contacts with it. H2A-group of histones is highly divergent and often determine specificity to the chaperones[89], as exemplified on the YL1 chaperone[7]. While H2B histones doesn't contribute to specific recognition by chaperones in the same way as H2A-group chaperones do, they may act as scaffold for chaperone-histone binding or have other functions. It was shown that highly basic domain of the H2B N-terminal tail plays an important role during nucleosome assembly by FACT histone chaperone, that it may achieve by stabilization of the nascent nucleosome[256]. CHZ motif also possesses a specific charge distribution that facilitates its interaction with both H2A.Z and H2B histones residues[12]. As a Chz1 homologue, HIRIP3 may have similar interaction dynamic with H2A and H2B, utilizing charged CHZ motif and other 403–527 regions to extensively interact with both histones.

Finally, we have shown that HIRIP3 interacts with H2A C-terminal alphaC helix region, which is a hallmark of a several other chaperones, including Chz1[18]. According to the structural simulation, CHZ motif doesn't directly bind to either H2A.Z or H2A alphaC helix, corroborating the importance of other regions aside from CHZ motif for the interaction. Taken together, our data establish 403 – 527 region of HIRIP3 as minimal domain necessary for interaction with alphaC of H2A and other regions of H2A/H2B dimer.

5.1.2.3 CK2 kinase function within HIRIP3 complex

This work indicates a possible functional connection between HIRIP3, histones and CK2 kinase. eHIRIP3 complex was revealed to contain both CK2 alpha subunit and H2A/H2B dimers. While their presence within complex could be explained only by interactions with HIRIP3, we have demonstrated that there is also a functional connection between CK2 and H2A. We have shown that CK2 kinase phosphorylates H2A in S1 position. This position is not conserved in H2A.Z, which may be the reason of observed phosphorylation specificity to H2A. The presence of CK2 kinase and its phosphorylation of both HIRIP3 and H2A rises the possibility of close interplay within HIRIP3 complex that is mediated by phosphorylation. Post-translational modifications are shown to act as molecular switches for histones functions. For example, phosphorylation of H2A.X is an essential step for its functionality during DNA repair[64] and acetylation/deacetylation processing of H3-H4 tetramers is indispensable for its incorporation during *de novo* chromatin assembly[243]. Based on the data of HIRIP3 interaction with H2A/H2B dimers (present work) and the fact that CK2 was shown to associate with H2A[257], we suggest that HIRIP3, H2A/H2B and CK2 may act as a cross-interacting cooperating complex.

5.1.2.4 HIRIP3 as a novel H2A/H2B histone chaperon

On the basis of our data, we propose HIRIP3 as a histone chaperone specific for H2A. First, it associates with H2A/H2B dimers both *in vitro* and *in vivo*. Second, HIRIP3 interacts with histones using CHZ motif, a region conserved with other histone chaperone Chz1. Finally, HIRIP3 interaction with H2A is dependent on alphaC helix, which is hallmark of histone chaperones interaction with H2A-group histones. Taken together, our study establishes mammalian HIRIP3 protein as a novel histone chaperon specific to H2A, that utilizes its CHZ motif-containing 403-527 region to interact with the H2A C-terminal alphaC helix.

5.2 PROJECT II. Reconstitution of SRCAP complex functional complex

SRCAP (SNF2-related-CBP activator protein) is a 350-kDa mammalian protein homologous to the Swi2/Snf2 family of ATPases. SRCAP was originally identified in a yeast two-hybrid screen for proteins that interact with the histone acetyltransferase CBP (*C*REB-*b*inding *p*rotein). Subsequently, SRCAP was found to function as a co-activator for nuclear receptors and to synergize with CBP in this process[258]. SRCAP domain structure mirrors its diverse cellular functions. SRCAP contains SNF2-like split ATPase domains, an N-terminal HSA (Helicase-SANT-associated) domain, central CBP-binding domain and three C-terminal AT-hook DNA-binding motifs (Table 5).

Domain	Residues	Function within the SRCAP complex
HSA	127 - 196	Binding site for nuclear actin and actin-related proteins[259]
ATPase domains	626 - 907(N-term) 2043 - 2156(C-term)	Catalysis of chromatin remodelling[105]
CBP-binding	1380-1670	Interaction with CBP and modulation of its ability to activate transcription[258]
DNA hooks	2813-2824 2936-2948 3004-3016	DNA-binding and facilitation of changes in the structure of the DNA[260]

Table 5. SRCAP domain's functions

SRCAP is closely related to *Drosophila* Domino and yeast SWR1 ATPases. Domino is shown to have gene expression regulatory effects[103], while SWR1 complex is directly involved into exchange of variant H2A.Z histones, thus regulating chromatin landscape[102]. SRCAP also shares sequence similarity with the p400 helicase subunit of the TRRAP/TIP60, a histone acetyltransferase that has roles in transcriptional activation, double strand DNA break repair, and apoptosis. Alike its homologues, SRCAP forms a multi-subunit complex with chromatin modifying and gene regulatory functions. SRCAP acts as a catalytic core of the entire complex and was shown to directly catalyse H2A.Z/H2B histone exchange reaction[261].

SRCAP complex consists of 10 proteins, including ATPases TIP49A and TIP49B, actin-related proteins ARP6 and BAF53a, histone chaperone YL1, histones and Gas41, ZnFhit1, DMAP1[262]. Along with SRCAP, another subunit of SRCAP complex, YL1, was shown to be directly involved into H2A.Z/H2B histone metabolism[7]. *YL1* is a 364 amino acid protein evolutionarily conserved from human to yeast, *and is* homologous to *S. cerevisiae*

Swc2/Vps72. YL1 is a shared subunit of the TRRAP/TIP60 HAT and SRCAP complexes and has multiple roles in chromatin modification and remodelling in cells[262]. YL1 acts as a histone chaperone of SRCAP complex, physically binding alphaC of H2A.Z using its ZID region[7]. YL1 is a functional core of SRCAP complex responsible for histones binding and deposition. *In vitro* assay revealed that YL1 is sufficient for deposition of H2A.Z/H2B dimers for nucleosome formation. The crystal structure of the human YL1-H2A.Z/H2B complex confirmed their specific interaction, with both H2A.Z alphaC helix extension and entire DNA-binding surface of H2A.Z-H2B playing roles into its mediation[7].

TIP49A and TIP49B subunits of SRCAP complex were also extensively studied in context of chromatin metabolism. They are conserved AAA+ (ATPases associated with various cellular activities) class ATPases that are universally present in chromatin-remodelling multi-protein complexes[185,263]. TIP49A and TIP49B have functions as both monomers and oligomers. In chromatin remodelling complexes they are always identified as either homohexamers or heterohexamers[264]. Upon nucleotide binding, TIP49A and TIP49B are shown to undergo conformational changes that facilitate their activity[265]. They operate by promoting conformational changes or remodelling, and are mainly involved in the disassembly of protein aggregates[265]. AAA+ group proteins were shown to be essential for the chromatin remodelling activity of INO80 complex[266]. While exact role of TIP49A and TIP49B within SRCAP complex is not known, they may play similar role in enhancing entire complex remodelling activity.

ARPs (actin related proteins) were found as subunits in many chromatin modifying complexes. In SRCAP complex two factors of this group – ARP6 and BAF53a – are present. ARPs function as the conformational switches that control either the activity or the assembly of complexes[267]. ARPs are demonstrated to couple ATP hydrolysis to protein conformational changes[267]. Despite the presence of a number of actin factors within chromatin remodelling complexes, their functions are not redundant, and both ARP6[268,269] and BAF53a[157] were shown to be essential for transcription of flowering genes and regulation of hemopoiesis. ARP proteins present within SRCAP complex may also be involved into complex formation mediation.

Another subunit of SRCAP complex, GAS41 of YEATS family of proteins, is mainly acting as transcriptional co-activator. All of the YEATS family proteins are components of multi-subunit complexes involved in chromatin modification and transcription[270]. GAS41 is essential for RNA transcription, since its depletion leads to significant decrease in RNA synthesis and subsequently cell death[271]. GAS41 functions are likely mediated by its

interaction with transcriptional factors (TF) and modulation of their activity. Gas41 was shown to directly interact with TFIIF, utilizing its YEATS domain for this interaction[272]. GAS41 is also an interaction partner of TF AP-2beta that regulates transcription of a number of genes involved in mammalian development, differentiation and carcinogenesis[273]. GAS41 both stimulates the transcriptional activity of AP-2beta over the reporters and enhances its DNA-binding activity[273]. GAS41 possible role, within SRCAP complex, may be tethering entire complex to the transcription loci, mediated by its intrinsic ability to be a transcriptional co-activator. It may share this function with DMAP1, which is also shown to modulate transcription factors functions[274].

It is not known how subunits of SRCAP complex cooperate with each other to carry out the entire complex functions. To answer this question it is important to elucidate interaction network among them. This can reveal the presence of sub-complexes, an interconnected group of proteins that are mediating specific tasks within the complex. Characterization of functional modules is an essential step for understanding how SCRAP complex carry out its functions mechanistically. It could also provide insight for its cooperation with other complexes, biological context dependence and regulation. In this project, we aimed to identify and reconstitute minimal functional sub-complex of SCRAP. Using YL1 histone chaperone as a functional core, we found TIP49A and TIP49B as its interaction partners among SRCAP complex subunits. Further interaction studies revealed connections between SRCAP, TIP49A/B, YL1 and H2A.Z/H2B factors, which were subsequently reconstituted as a stable complex *in vitro*. This complex contained all factors sufficient for chromatin remodelling activity of SRCAP complex, thus being its functional module. Our project have set up a basis for further studies of functional sub-complex of SRCAP complex, e.g. using cryo-electron microscopy.

5.2.1 Results

5.2.1.1 YL1 interacts with TIP49A and TIP49B ATPases

The first step of SRCAP complex interaction network study was screening for subunits that binds YL1 protein. Previously, we have characterized YL1 as a histone chaperone of SRCAP complex[7]. Considering histone chaperones central role in chromatin remodelling, YL1 was chosen as possible core of a SRCAP complex functional sub-complex. We have screened for proteins directly interacting with YL1 among the SRCAP complex subunits. For this purpose pET constructs containing tagged YL1 and other subunits of SRCAP complex were co-expressed using E. coli expression system. The generated cellular extracts were subjected to affinity purification using HIS tag. HIS eluate from each extract was analysed by SDS-PAGE and western blotting. YL1 was found to interact with TIP49A and Tip49B (Fig. 22). These proteins are AAA+ class ATPases that are universally present in chromatin-remodelling multi-protein complexes as hexamers. The presence of YL1 in HIS eluate was checked by western blotting with antibodies against YL1 (Fig. 22, bottom). TIP49A appears to have a higher affinity for YL1 than for TIP49B. These data demonstrate that YL1 interacts with both TIP49A and TIP49B, albeit with different affinity.

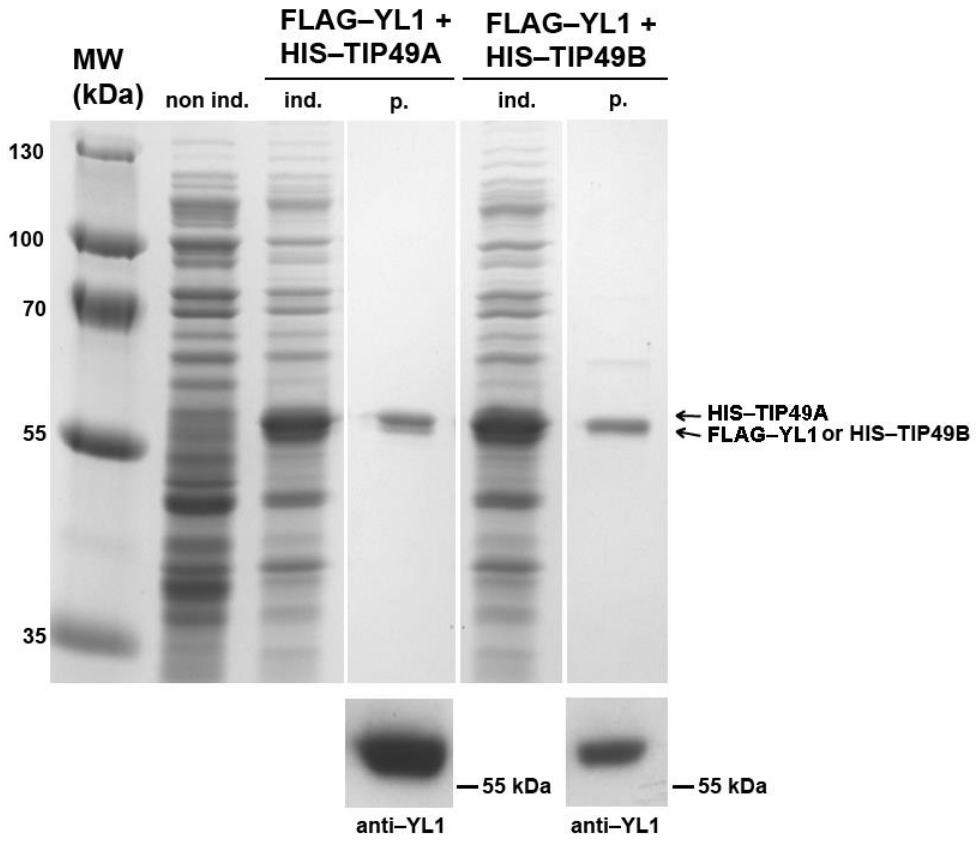

Figure 22. YL1 interacts with TIP49A and TIP49B

The YL1-FLAG construct was co-expressed with either HIS-TIP49A or HIS-TIP49B constructs. Cellular soluble extracts were subjected to affinity purification. Generated HIS eluates were used for SDS-PAGE followed by Coomassie staining (top) or western blotting with anti-YL1 antibodies (bottom). YL1-FLAG and HIS-TIP49B complex appears as one band on Coomasie stained gel, since they run at approximately the same molecular weight.
Non ind. - non IPTG induced cell culture; Ind. - IPTG induced cell culture; P. - HIS purification from soluble cell extract; MW - molecular weight

To further visualize the interaction between TIP49A and YL1, we have generated construct of YL1 tagged with 26 kDa GST tag. We have co-expressed GST-YL1 and FLAG-TIP49A constructs and did two step FLAG then GST purification from generated cellular extract. These two proteins have maintained interaction even after double purification (Fig. 23A). Our next step was to find out which domain of YL1 is in charge of its interaction with TIP49A. We have co-expressed three mutants of GST-YL1 - 1-110, 111-230 and 231- 364 with FLAG-TIP49A and subjected cellular extract to two steps GST-FLAG purification. Only the 111-230 central region of YL1 region maintained interaction with TIP49A after double purification (Fig. 23B). Previously we have shown that YL1 1-69 N-terminal region mediate its interaction with H2A.Z/H2B histone dimers[7]. Taken together these data demonstrate that

YL1 uses different regions for interaction with histones and TIP49A and is putatively capable of interaction with both within complex.

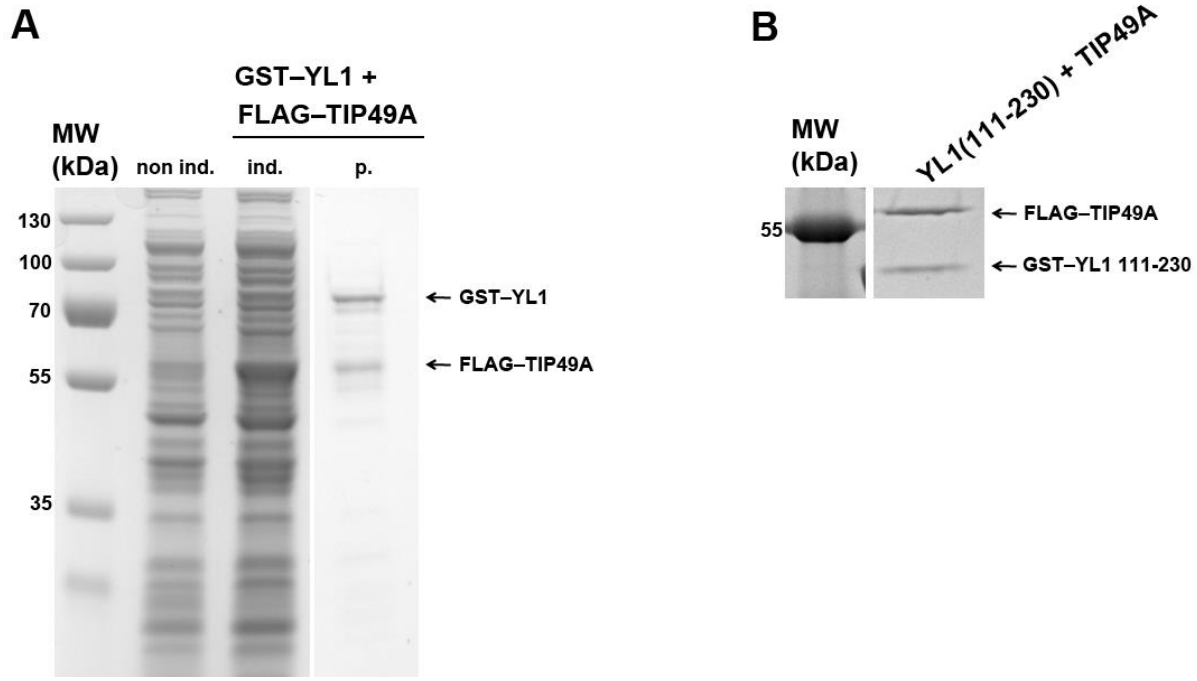

Figure 23. YL1 interacts with TIP49A using its 111-230 region

(A) Co-expression and of GST-YL1 and FLAG-TIP49A, followed by double purification by FLAG and GST tags.
Non ind. - non IPTG induced cell culture; Ind. - IPTG induced cell culture; p. - FLAG and GST double purification assay, MW - molecular weight
(B) Co-expression of GST-YL1 111-230 and FLAG-TIP49A, followed by FLAG and GST double purification assay.

5.2.1.2 TIP49A/B, YL1 and H2A.Z/H2B form a complex in vitro

Identified interaction of YL1 and TIP49A/B exposes a link between two complexes existing within SRCAP complex. First is TIP49A and TIP49B, two ATPases usually forming a hexamer ring with each other; and another is YL1 and H2A.Z/H2B, histone chaperone and histone dimer substrate of SRCAP complex[7]. These two sub-complexes might be connected with each other by means of YL1 and TIP49A/B interaction. To test this idea,

we aimed to reconstitute complex that contained both of those sub-complexes, i.e., YL1, TIP49A/B and H2A.Z/H2B histone dimers.

First, we separately co-expressed and purified TIP49A/Tip49B and YL1/H2A.Z/H2B complexes. Afterwards, we subjected them to dialysis in order to remove reagents that may interfere with further application. We mixed stoichiometric equal amount of both generated complexes and subjected this mix to FLAG pull-down. After this treatment, we were able to reconstitute a complex, which consisted of all five subunits: TIP49A/TIP49B/YL1/H2A.Z/H2B (Fig. 24). This result indicates that these subunits are capable of formation of stable highly inter-connected complex. Considering functional importance of histone chaperones and ATPases of TIP family, the identified five subunits may act as the functional sub-complex of SRCAP complex, with TIP49A/B and YL1 acting as its core.

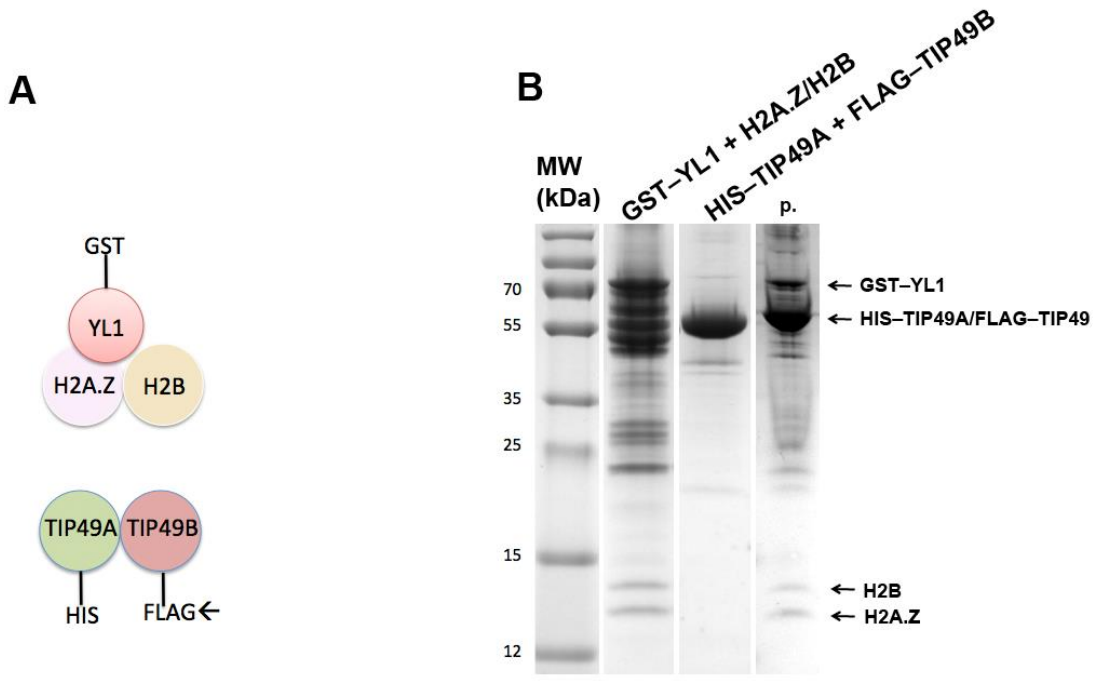

Figure 24. Reconstitution of TIP49A/TIP49B/YL1/H2A.Z/H2B complex

(A) Graphical representation of constructs used for purification in B (slot 3). Arrow indicates tag used for purification.
(B) Two separate purification were carried out using GST-YL1 and H2A.Z/H2B (without tags) constructs (slot 2) and HIS-TIP49A and FLAG-TIP49B construct (slot 3). After mixing stoichiometric equal amount of each, protein mix were subjected to FLAG purification (slot 4).
P. - FLAG purification, MW - molecular weight

5.2.1.3 SRCAP, TIPA49/TIP49B, YL1 and H2A.Z/H2B is a functional sub-complex within SRCAP complex

In order to finalise reconstitution of functional sub-complex within SRCAP complex, we aimed to add SRCAP ATPase to the already identified five subunits. SRCAP is a catalytic core of SRCAP complex, necessary for H2A.Z exchange function of the entire complex. Since histone chaperones and Swi2/Snf2 family ATPases are two essential subunits for the chromatin remodelling, the complex containing both of them and subunits they directly bound to, could be functionally sufficient for the histone exchange.

In order to express 350 kDa SRCAP protein, we moved to the baculovirus system of expression, since *E. coli* system doesn't support expression of proteins of such high molecular weight. Expression in baculovirus also has the benefit of setting post-translational modifications that may be unavailable in *E.coli* system. We have started with generating and expressing recombinant bacmids containing full-length FLAG-SRCAP sequence (1-3230). The expression were checked by western blot with antibodies specific to FLAG tag. The full-length SRCAP product was detected mostly in the insoluble fraction and was severely degraded, deeming it unsuitable for interaction studies. In order to stabilize SRCAP protein we have made SRCAP truncation mutant 1-2270, that contains HSA and ATPase domains located at N-terminal and central regions, and lacks three DNA hooks in C-terminal region (Fig. 25). This construct was detected mostly in soluble fraction and wasn't subjected to degradation. The DNA hook domains were shown to mediate connections with nucleosomal DNA, and may act as an enhancer of the SRCAP complex binding to the nucleosome. Since they are not known to mediate interaction with proteins, they putatively may be dispensable for non-nucleosomal interactions of SRCAP. The following interaction studies were carried out using SRCAP truncation mutant 1-2270.

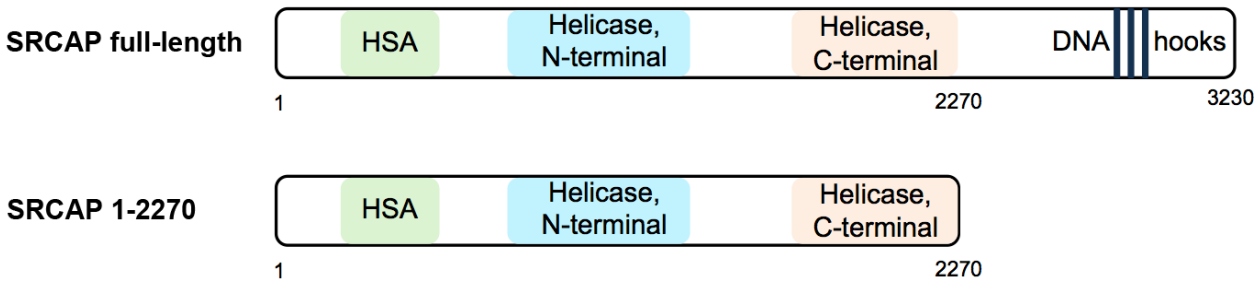

Figure 25. SRCAP constructs used in this study

SRCAP 1-3230, full-length; SRCAP 1-2270, mutant without C-terminal region containing DNA hooks.

Together with FLAG-SRCAP, we have generated bacmids for baculovirus system expression of HIS-TIP49A, HA-TIP49B HA-YL1 and H2A.Z-HIS/T7-H2B proteins, in order to co-express and reconstitute all subunits in one system. We were co-infecting SF9 insect cells with those bacmids, collecting cells with recombinant proteins and carrying out affinity purification by FLAG tag. We were gradually checking complex formation after each step (Fig 26, A-C). Based on available data of yeast Rvb and SWR1 interaction, which are yeast homologues of TIPs and SRCAP, we have co-infected SF9 cell with FLAG-SRCAP 1-2270, TIP49A-HIS and TIP49B-HA constructs. After purification by FLAG tag, eluates were subjected to SDS-PAGE for visualization. 1-2270 SRCAP and TIP49A/B run close to the expected molecular weight sizes, approximately 252 and 51 kDa, respectively (Fig 26. A, top). In order to confirm the presence of TIP49A/B, we subjected eluates to western blot using antibodies specific to HIS (for detection of TIP49A) and HA (for detection of TIP49B). Both were shown to be present in the FLAG eluate (Fig 26. A, bottom), confirming that SRCAP is forming a complex with TIP49A/B. The next step was the addition of YL1, by means of co-infection of 4 baculovirus constructs, encoding SRCAP, TIP49A, TIP49B and YL1. The presence of YL1 was checked by WB using antibodies specific to it (Fig 26. B). Finally, we have made a co-infection of all subunits involved identified in interaction studies i.e. SRCAP, TIPA49/TIP49B, YL1 and H2A.Z/H2B (Fig 26. D). So far, we have used monocistronic constructs to produce each protein. Increasing number of constructs could have led to difficulties in adjusting amount of each virus used to infect the insect cells. In order to lessen amount of separate constructs, we have generated and used two bicistronic constructs - H2A.Z-HIS/H2B-T7 and TIP49A/TIP49B (no tags). Using them together with SRCAP and YL1 constructs, we were able to form and purify complex consisting of all six subunits, with presence of factors confirmed by western blot, using antibodies specific to each protein (Fig. 26, C, left and bottom). We were able to get rid of most contaminating cellular proteins by doing two-step purification by HA and FLAG tags (Fig. 26, C, right). Taken together, our data demonstrate formation of stable sub-complex that contains all subunits sufficient for SRCAP function as chromatin remodelling factor. The reconstituted sub-complex is suitable for further studies, e.g. using cryo-electron microscopy.

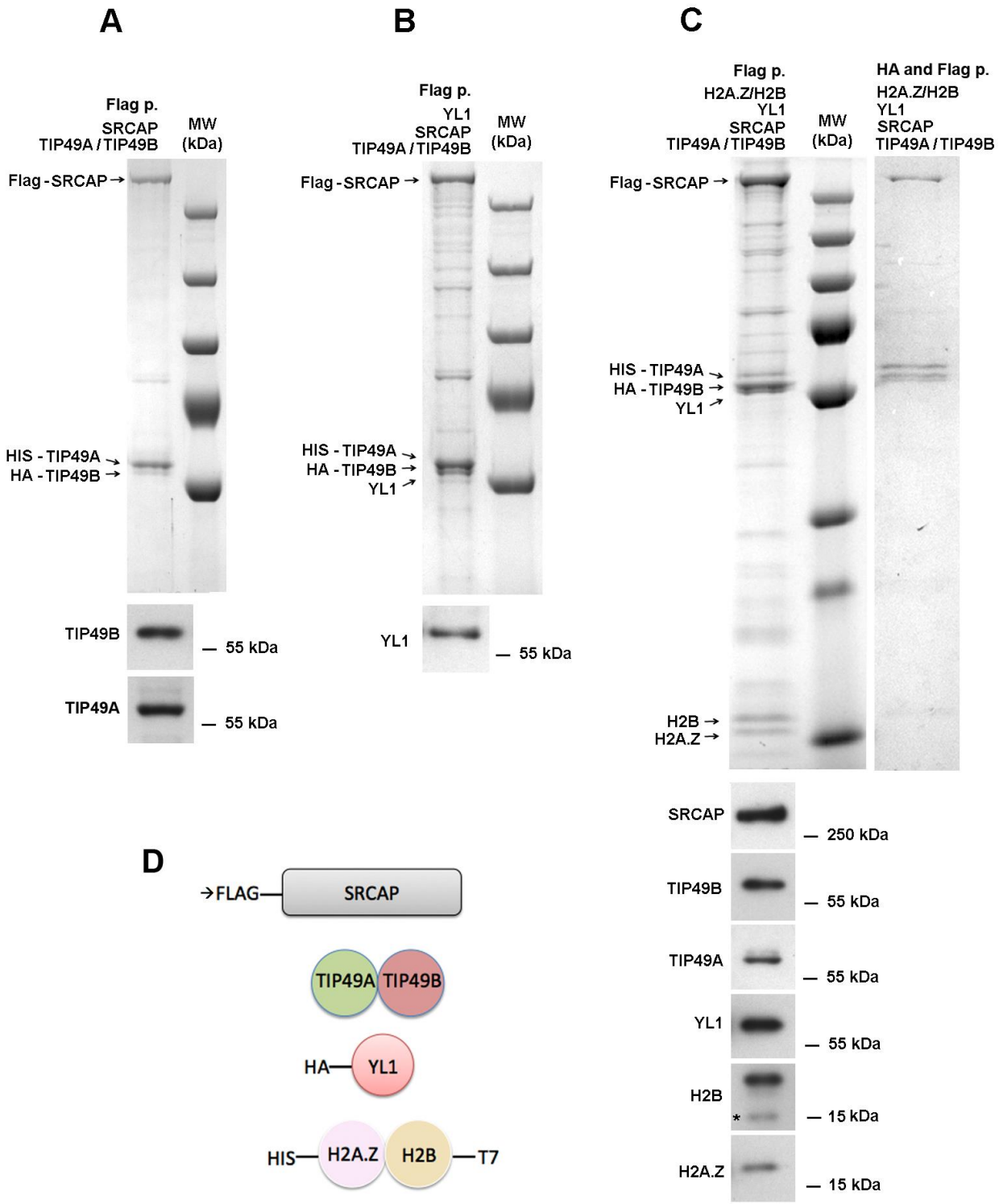

Figure 26. Purification of SRCAP core complex from SF9 cells

(A-C) – FLAG p. - FLAG tag purification from infected SF9 cells extracts. FLAG eluate was used for SDS-PAGE followed by Coomassie staining (top) and western blotting (bottom).
(A)- Co-infection with FLAG-SRCAP 1-2270, HIS –TIP49A and HA—TIP49B constructs
(B) - Co-infection with FLAG-SRCAP 1-2270, HIS -TIP49A and HA-TIP49B and HA-YL1 constructs
(C) - Co-infection with FLAG-SRCAP 1-2270, TIPA49-TIPB49 bicistronic, HA-YL1, and HIS-H2A.Z / T7-H2B bicistronic constructs. Asterisk indicate degradation product. Flag purification (left) and consecutive HA and FLAG purifications (right) were carried out.

(D) - Graphical representation of constructs used for co-infection from C. Arrow indicates tag used for one step purification

5.2.2 Discussion

This study was dedicated to reconstitution of a functional sub-complex within SRCAP complex using *E. coli* and baculovirus expression systems. Step by step, we were identifying subunits within complex that were interacting with each other. This approach allowed us to reconstitute highly interconnected sub-complex that contained all subunits of SRCAP complex, which were shown to be directly involved into chromatin remodelling.

5.2.2.1 YL1 interaction with TIP49A and TIP49B

Our first step was the identification of interaction between chaperone YL1 and TIP49A and TIP49B ATPases. YL1 is a histone chaperone of SRCAP complex, thus its interaction partners are likely to be also involved into histone processing. Even though, YL1 has affinity for both TIP49A and TIP49B, it may not necessarily bind both of them in SRCAP complex. Previous studies of TIP49A/B interaction with nucleosome demonstrated that TIP49A competes with TIP49B for nucleosome binding[275]. The same interaction dynamic might be true in case of TIP49A/B interaction with YL1, where only one protein of TIP group binds to YL1 *in vivo*. The lesser affinity of YL1 for TIP49B, than for TIP49A identified in this work may be indicative of it. Our further interaction studies demonstrated the formation of a complex that contained both YL1+H2A.Z/H2B and TIP49A/TIP49B sub-complexes *in vitro*. Interaction between these two sub-complexes may be necessary for enhancing and modulation of histone processing within entire SRCAP complex.

5.2.2.2 TIP49A/B ATPases functions within SRCAP complex

The interaction of TIP49A/B ATPases with YL1 raised the question of TIP's function within the sub-complex. It was shown that TIP49A and TIP49B are capable of catalysing H2A.Z exchange reaction on their own[275]. This reaction requires both proteins and could use H2A.Z, but not H2A or H2A.X as a substrate, indicating its H2A.Z-specific action. TIP49A knockdown was demonstrated to cause impairment of H2A.Z exchange at specific

chromatin regions, which further corroborates its critical targeted action on H2A.Z exchange[275]. H2A K5 acetylation, mediated by Tip60 histone acetyltransferase complex (HAT), was shown to be a requirement for H2A.Z exchange process mediated by TIP49A/B[275,276]. This acetylation-facilitated exchange of H2A.Z by TIP49A/B indicates interplay between TIPs proteins and HATs to carry out its function. Proposed mechanism involves two steps, with initial TIP60 acetylation of nucleosomal H2A localized in target promoters followed by TIP49A/B-induced deposition of H2A.Z into promoter regions[275,276]. Considering that YL1 and TIP49A/B are shared subunits of both TRRAP/TIP60 histone acetyltransferase and SRCAP complexes[262], their function in H2A.Z exchange reaction may in part depend on interplay between those complexes, facilitated by acetylation.

5.2.2.3 SRCAP ATPase functions within SRCAP complex

Experiments using baculovirus expression system allowed us to identify interaction between TIP49A/B and SRCAP ATPase. It is in agreement with other data showing interaction of Rvb1 with SWR1, a TIP49A and SRCAP yeast homologues, respectively[192].

SRCAP has double function within the SRCAP complex. First is to catalyse the chromatin remodelling process[5]. SRCAP ATPase activity is shown to be a key process necessary for H2A.Z/H2B histones exchange[261]. SRCAP complex purified from HeLa cells was shown to facilitate exchange of H2A.Z/H2B dimers into nucleosomes *in vitro*[105]. Complementary study showed that SRCAP is critical for the deposition of H2A.Z *in vivo*[261]. ChIP assays revealed presence of SRCAP on both inactive and active genes promoters, which occurs adjacent to the sites of H2A.Z deposition. Depletion of SRCAP levels leads to decreased deposition of H2A.Z and to a decrease in mRNA levels of a subset of actively transcribed genes. Taken together, these results suggest a critical role for SRCAP in transcription, achieved by its chromatin remodelling activity. Second role of SRCAP is to act as a scaffold for complex functional modules, similar to SWR1 complex[9]. Domains present is SRCAP, such as HSA and CBP-binding, were shown to mediate interaction with other proteins. TIP49A/B may use extensive SRCAP region as a platform for their hexamer ring assembly. Together, our results support SRCAP as a main catalytic subunit of the entire complex, involved into both its formation and chromatin processing functions.

5.2.2.4 Interaction network within SRCAP sub-complex

As a final step, we have reconstituted sub-complex of all six subunits studied in this work - SRCAP, YL1, TIP49A, TIP49B and H2A.Z/H2B, using a baculovirus expression system. In this sub-complex, The SRCAP subunit is likely acting as a bridge for other subunits, in same manner as SWR1 acts for SWR1 complex[192]. TIP49 A/B are shown to have chaperone-like activity for building chromatin remodelling complexes[277] and may contribute to connection of other subunits to SRCAP. The interaction studies carried out in this work demonstrate that SRCAP complex subunits are highly interconnected with each other. So far, interactions between YL1 and TIP49A/TIP49B (this study), YL1 and H2A.Z/H2B[7], TIP49A and TIP49B[263], SRCAP and TIP49A/TIP49B (this study), TIP49A/B and nucleosome[275] have been discovered. The exact manner and sequence of these interaction may correspond to cellular requirements of chromatin remodelling complexes. The possible scheme of interactions within identified minimal complex may be SRCAP acting as a platform for TIP49A/B binding, while YL1 complexed with H2A.Z/H2B is being bridged to the SRCAP by means of its TIP49A interaction.

5.2.2.5 Identified sub-complex is a functional module of SRCAP complex

The reconstituted six subunits sub-complex contains histone chaperone YL1, Swi2/Snf2 family ATPase SRCAP and AAA+ family ATPases TIP49A/B. These factors were shown to be essential for processes of chromatin remodelling and assembly, with SRCAP[261] and TIPs[275] catalysing H2A.Z exchange reaction, while YL1 directly binding and depositing histones for the exchange[7]. TIP49A/B and SRCAP activities have different chromatin contexts, e.g. unlike TIPs, SRCAP is not dependent on histone acetylation. Co-existence of differently regulated ATPases within one complex, implicates presence of two H2A.Z incorporation pathways, each utilizing either SCRAP or TIPs ATPases. The necessity of those multiple pathways may correspond to different contexts of H2A.Z incorporation, which is shown to occur in active[96,97], repressive chromatin[100] and at euchromatin/heterochromatin boundary[99]. SRCAP and TIP49A/B both possess intrinsic ability to exchange H2A.Z, which may be further modulated regarding cellular requirements *in vivo*. Taking together available functional data of these factors, we propose the six identified subunits as a minimal functional sub-complex of the SRCAP complex.

6 OUTLOOK

The principal result of this work was the characterization of HIRIP3 as a histone chaperone. We have shown HIRIP3 to be specific to canonical histone H2A. Other H2A histone chaperones, such as NAP1 and FACT have established functions in chromatin assembly and DNA repair facilitating. Future studies of HIRIP3 would need to evaluate its precise function as a histone chaperone and place it into context of chromatin dynamics. ChIP-sequencing could reveal the sites of HIRIP3 genome localization. Based on HIRIP3 distribution and overlapping with other genomic features, such as promoters, it would be possible to decipher its functions. Genomic landscape comparison of wild types cells and knockdown of HIRIP3 could demonstrate either accumulation or depletion of H2A distribution, further evaluating HIRIP3 role in chromatin metabolism.

This work have established structural specificity of HIRIP3 interaction with H2A histone. These data would be enhanced by structural assessing of this interaction using X-ray crystallography. We have shown that HIRIP3 interacts with H2A with an extensive 124-residues region. While we could already simulate how CHZ motif of this region would interact with H2A/H2B dimer, the exact non-CHZ region interactions are still not visualized. Considering that alphaC of H2A doesn't directly interact with CHZ motif, the identification of non-CHZ regions involved in this interaction, would greatly enhance our understanding of HIRIP3/H2A complex formation.

The second result of this work was the identification and reconstitution of functional module within SCRAP complex. The total molecular weight of this sub-complex is 400-600 kDa, depending whether TIP49A/B are in dimer or hexamer form. This module is suitable for structure solving using cryo-electron microscopy approach. In order to generate the amount of sub-complex suitable for those studies, we have established a protocol for purification that takes advantage of baculovirus expression system.

The structure of minimal SRCAP sub-complex would reveal exact interaction of its subunits and their spatial organisation relative to each other. This would give new insights into the complex formation and its intrinsic characteristics, such as flexibility/rigidity. Comparison of sub-complex structure with and without histones could reveal conformational changes that occurs in SRCAP complex during histone dimer binding. Comparing functional module structure coupled with dimers vs entire nucleosome could demonstrate the mechanism of SRCAP nucleosome engaging, possibly in a step-wise manner. The discovery of SRCAP

sub-complex conformational changes would enhance our understanding of entire complex functions as a chromatin remodelling factor.

7 BIBLIOGRAPHY

1 Polo, S. E. & Almouzni, G. Histone metabolic pathways and chromatin assembly factors as proliferation markers. *Cancer letters* **220**, 1-9, doi:10.1016/j.canlet.2004.08.024 (2005).

2 Filipescu, D., Szenker, E. & Almouzni, G. Developmental roles of histone H3 variants and their chaperones. *Trends in genetics : TIG* **29**, 630-640, doi:10.1016/j.tig.2013.06.002 (2013).

3 Rakyan, V. K., Preis, J., Morgan, H. D. & Whitelaw, E. The marks, mechanisms and memory of epigenetic states in mammals. *Biochem J* **356**, 1-10 (2001).

4 Skene, P. J. & Henikoff, S. Histone variants in pluripotency and disease. *Development* **140**, 2513-2524, doi:10.1242/dev.091439 (2013).

5 Polo, S. E. & Almouzni, G. Chromatin assembly: a basic recipe with various flavours. *Current opinion in genetics & development* **16**, 104-111, doi:10.1016/j.gde.2006.02.011 (2006).

6 Luk, E. *et al.* Chz1, a nuclear chaperone for histone H2AZ. *Molecular cell* **25**, 357-368, doi:10.1016/j.molcel.2006.12.015 (2007).

7 Latrick, C. M. *et al.* Molecular basis and specificity of H2A.Z-H2B recognition and deposition by the histone chaperone YL1. *Nature structural & molecular biology* **23**, 309-316, doi:10.1038/nsmb.3189 (2016).

8 Kornberg, R. D. Chromatin structure: a repeating unit of histones and DNA. *Science* **184**, 868-871 (1974).

9 Luger, K., Mader, A. W., Richmond, R. K., Sargent, D. F. & Richmond, T. J. Crystal structure of the nucleosome core particle at 2.8 A resolution. *Nature* **389**, 251-260, doi:10.1038/38444 (1997).

10 Elsasser, S. J. & D'arcy, S. Towards a mechanism for histone chaperones. *Bba-Gene Regul Mech* **1819**, 211-221, doi:10.1016/j.bbagrm.2011.07.007 (2012).

11 Obri, A. *et al.* ANP32E is a histone chaperone that removes H2A.Z from chromatin. *Nature* **505**, 648-653, doi:10.1038/nature12922 (2014).

12 Zhou, Z. *et al.* NMR structure of chaperone Chz1 complexed with histones H2A.Z-H2B. *Nature structural & molecular biology* **15**, 868-869, doi:10.1038/nsmb.1465 (2008).

13 Lorain, S. *et al.* Core histones and HIRIP3, a novel histone-binding protein, directly interact with WD repeat protein HIRA. *Molecular and cellular biology* **18**, 5546-5556 (1998).

14 Ray-Gallet, D. *et al.* HIRA is critical for a nucleosome assembly pathway independent of DNA synthesis. *Molecular cell* **9**, 1091-1100 (2002).

15 Litchfield, D. W. Protein kinase CK2: structure, regulation and role in cellular decisions of life and death. *Biochem J* **369**, 1-15, doi:10.1042/BJ20021469 (2003).
16 Barz, T., Ackermann, K., Dubois, G., Eils, R. & Pyerin, W. Genome-wide expression screens indicate a global role for protein kinase CK2 in chromatin remodeling. *J Cell Sci* **116**, 1563-1577, doi:10.1242/jcs.00352 (2003).
17 Assrir, N., Filhol, O., Galisson, F. & Lipinski, M. HIRIP3 is a nuclear phosphoprotein interacting with and phosphorylated by the serine-threonine kinase CK2. *Biological chemistry* **388**, 391-398, doi:10.1515/BC.2007.045 (2007).
18 Wang, A. Y., Aristizabal, M. J., Ryan, C., Krogan, N. J. & Kobor, M. S. Key functional regions in the histone variant H2A.Z C-terminal docking domain. *Molecular and cellular biology* **31**, 3871-3884, doi:10.1128/MCB.05182-11 (2011).
19 Calvert, M. E. *et al.* Phosphorylation by casein kinase 2 regulates Nap1 localization and function. *Molecular and cellular biology* **28**, 1313-1325, doi:10.1128/MCB.01035-07 (2008).
20 Kornberg, R. D. & Lorch, Y. Twenty-five years of the nucleosome, fundamental particle of the eukaryote chromosome. *Cell* **98**, 285-294 (1999).
21 Arents, G., Burlingame, R. W., Wang, B. C., Love, W. E. & Moudrianakis, E. N. The nucleosomal core histone octamer at 3.1 A resolution: a tripartite protein assembly and a left-handed superhelix. *Proceedings of the National Academy of Sciences of the United States of America* **88**, 10148-10152 (1991).
22 Woodcock, C. L., Skoultchi, A. I. & Fan, Y. Role of linker histone in chromatin structure and function: H1 stoichiometry and nucleosome repeat length. *Chromosome research : an international journal on the molecular, supramolecular and evolutionary aspects of chromosome biology* **14**, 17-25, doi:10.1007/s10577-005-1024-3 (2006).
23 Marzluff, W. F. & Duronio, R. J. Histone mRNA expression: multiple levels of cell cycle regulation and important developmental consequences. *Current opinion in cell biology* **14**, 692-699 (2002).
24 Whitfield, M. L. *et al.* Stem-loop binding protein, the protein that binds the 3' end of histone mRNA, is cell cycle regulated by both translational and posttranslational mechanisms. *Molecular and cellular biology* **20**, 4188-4198 (2000).
25 Gaspar-Maia, A. *et al.* MacroH2A histone variants act as a barrier upon reprogramming towards pluripotency. *Nature communications* **4**, 1565, doi:10.1038/ncomms2582 (2013).
26 Nakanishi, S. *et al.* A comprehensive library of histone mutants identifies nucleosomal residues required for H3K4 methylation. *Nature structural & molecular biology* **15**, 881-888, doi:10.1038/nsmb.1454 (2008).
27 Finch, J. T. *et al.* Structure of nucleosome core particles of chromatin. *Nature* **269**, 29-36 (1977).
28 Davey, C. A., Sargent, D. F., Luger, K., Maeder, A. W. & Richmond, T. J. Solvent mediated interactions in the structure of the nucleosome core particle at 1.9 a resolution. *Journal of molecular biology* **319**, 1097-1113, doi:10.1016/S0022-2836(02)00386-8 (2002).
29 Angelov, D. *et al.* The histone variant macroH2A interferes with transcription factor binding and SWI/SNF nucleosome remodeling. *Molecular cell* **11**, 1033-1041 (2003).
30 Gautier, T. *et al.* Histone variant H2ABbd confers lower stability to the nucleosome. *EMBO reports* **5**, 715-720, doi:10.1038/sj.embor.7400182 (2004).
31 Finch, J. T. & Klug, A. Solenoidal model for superstructure in chromatin. *Proceedings of the National Academy of Sciences of the United States of America* **73**, 1897-1901 (1976).

32 Olins, A. L. & Olins, D. E. Spheroid chromatin units (v bodies). *Science* **183**, 330-332 (1974).
33 Robinson, P. J. & Rhodes, D. Structure of the '30 nm' chromatin fibre: a key role for the linker histone. *Current opinion in structural biology* **16**, 336-343, doi:10.1016/j.sbi.2006.05.007 (2006).
34 Routh, A., Sandin, S. & Rhodes, D. Nucleosome repeat length and linker histone stoichiometry determine chromatin fiber structure. *Proceedings of the National Academy of Sciences of the United States of America* **105**, 8872-8877, doi:10.1073/pnas.0802336105 (2008).
35 Grigoryev, S. A., Arya, G., Correll, S., Woodcock, C. L. & Schlick, T. Evidence for heteromorphic chromatin fibers from analysis of nucleosome interactions. *Proceedings of the National Academy of Sciences of the United States of America* **106**, 13317-13322, doi:10.1073/pnas.0903280106 (2009).
36 Shogren-Knaak, M. *et al.* Histone H4-K16 acetylation controls chromatin structure and protein interactions. *Science* **311**, 844-847, doi:10.1126/science.1124000 (2006).
37 Hamiche, A., Schultz, P., Ramakrishnan, V., Oudet, P. & Prunell, A. Linker histone-dependent DNA structure in linear mononucleosomes. *Journal of molecular biology* **257**, 30-42, doi:10.1006/jmbi.1996.0144 (1996).
38 Woodcock, C. L., Frado, L. L. & Rattner, J. B. The higher-order structure of chromatin: evidence for a helical ribbon arrangement. *The Journal of cell biology* **99**, 42-52 (1984).
39 Cremer, T. & Cremer, C. Chromosome territories, nuclear architecture and gene regulation in mammalian cells. *Nature reviews. Genetics* **2**, 292-301, doi:10.1038/35066075 (2001).
40 Sexton, T. *et al.* Three-dimensional folding and functional organization principles of the Drosophila genome. *Cell* **148**, 458-472, doi:10.1016/j.cell.2012.01.010 (2012).
41 Felsenfeld, G. & Groudine, M. Controlling the double helix. *Nature* **421**, 448-453, doi:10.1038/nature01411 (2003).
42 Horowitz, R. A., Agard, D. A., Sedat, J. W. & Woodcock, C. L. The three-dimensional architecture of chromatin in situ: electron tomography reveals fibers composed of a continuously variable zig-zag nucleosomal ribbon. *The Journal of cell biology* **125**, 1-10 (1994).
43 Horowitz, R. A., Koster, A. J., Walz, J. & Woodcock, C. L. Automated electron microscope tomography of frozen-hydrated chromatin: the irregular three-dimensional zigzag architecture persists in compact, isolated fibers. *Journal of structural biology* **120**, 353-362, doi:10.1006/jsbi.1997.3921 (1997).
44 Maeshima, K., Ide, S., Hibino, K. & Sasai, M. Liquid-like behavior of chromatin. *Current opinion in genetics & development* **37**, 36-45, doi:10.1016/j.gde.2015.11.006 (2016).
45 Ricci, M. A., Manzo, C., Garcia-Parajo, M. F., Lakadamyali, M. & Cosma, M. P. Chromatin fibers are formed by heterogeneous groups of nucleosomes in vivo. *Cell* **160**, 1145-1158, doi:10.1016/j.cell.2015.01.054 (2015).
46 Maeshima, K., Imai, R., Tamura, S. & Nozaki, T. Chromatin as dynamic 10-nm fibers. *Chromosoma* **123**, 225-237, doi:10.1007/s00412-014-0460-2 (2014).
47 Kizilyaprak, C., Spehner, D., Devys, D. & Schultz, P. In vivo chromatin organization of mouse rod photoreceptors correlates with histone modifications. *PloS one* **5**, e11039, doi:10.1371/journal.pone.0011039 (2010).
48 Dixon, J. R. *et al.* Topological domains in mammalian genomes identified by analysis of chromatin interactions. *Nature* **485**, 376-380, doi:10.1038/nature11082 (2012).

49 Ciabrelli, F. & Cavalli, G. Chromatin-driven behavior of topologically associating domains. *Journal of molecular biology* **427**, 608-625, doi:10.1016/j.jmb.2014.09.013 (2015).
50 Cremer, M. *et al.* Non-random radial higher-order chromatin arrangements in nuclei of diploid human cells. *Chromosome research : an international journal on the molecular, supramolecular and evolutionary aspects of chromosome biology* **9**, 541-567 (2001).
51 Bickmore, W. A. & van Steensel, B. Genome architecture: domain organization of interphase chromosomes. *Cell* **152**, 1270-1284, doi:10.1016/j.cell.2013.02.001 (2013).
52 McBryant, S. J., Adams, V. H. & Hansen, J. C. Chromatin architectural proteins. *Chromosome research : an international journal on the molecular, supramolecular and evolutionary aspects of chromosome biology* **14**, 39-51, doi:10.1007/s10577-006-1025-x (2006).
53 Bulut-Karslioglu, A. *et al.* A transcription factor-based mechanism for mouse heterochromatin formation. *Nature structural & molecular biology* **19**, 1023-1030, doi:10.1038/nsmb.2382 (2012).
54 Filion, G. J. *et al.* Systematic protein location mapping reveals five principal chromatin types in Drosophila cells. *Cell* **143**, 212-224, doi:10.1016/j.cell.2010.09.009 (2010).
55 Peterson, C. L. & Laniel, M. A. Histones and histone modifications. *Current biology : CB* **14**, R546-551, doi:10.1016/j.cub.2004.07.007 (2004).
56 Bannister, A. J. & Kouzarides, T. Regulation of chromatin by histone modifications. *Cell research* **21**, 381-395, doi:10.1038/cr.2011.22 (2011).
57 Eberharter, A. & Becker, P. B. Histone acetylation: a switch between repressive and permissive chromatin. Second in review series on chromatin dynamics. *EMBO reports* **3**, 224-229, doi:10.1093/embo-reports/kvf053 (2002).
58 Protacio, R. U., Li, G., Lowary, P. T. & Widom, J. Effects of histone tail domains on the rate of transcriptional elongation through a nucleosome. *Molecular and cellular biology* **20**, 8866-8878 (2000).
59 Mujtaba, S., Zeng, L. & Zhou, M. M. Structure and acetyl-lysine recognition of the bromodomain. *Oncogene* **26**, 5521-5527, doi:10.1038/sj.onc.1210618 (2007).
60 Lee, J. S., Smith, E. & Shilatifard, A. The language of histone crosstalk. *Cell* **142**, 682-685, doi:10.1016/j.cell.2010.08.011 (2010).
61 Ling, X., Harkness, T. A., Schultz, M. C., Fisher-Adams, G. & Grunstein, M. Yeast histone H3 and H4 amino termini are important for nucleosome assembly in vivo and in vitro: redundant and position-independent functions in assembly but not in gene regulation. *Genes & development* **10**, 686-699 (1996).
62 Adams, C. R. & Kamakaka, R. T. Chromatin assembly: biochemical identities and genetic redundancy. *Current opinion in genetics & development* **9**, 185-190, doi:10.1016/S0959-437X(99)80028-8 (1999).
63 Rossetto, D., Avvakumov, N. & Cote, J. Histone phosphorylation: a chromatin modification involved in diverse nuclear events. *Epigenetics* **7**, 1098-1108, doi:10.4161/epi.21975 (2012).
64 Rogakou, E. P., Pilch, D. R., Orr, A. H., Ivanova, V. S. & Bonner, W. M. DNA double-stranded breaks induce histone H2AX phosphorylation on serine 139. *J Biol Chem* **273**, 5858-5868 (1998).
65 Cheung, W. L. *et al.* Apoptotic phosphorylation of histone H2B is mediated by mammalian sterile twenty kinase. *Cell* **113**, 507-517 (2003).

66 Banerjee, T. & Chakravarti, D. A peek into the complex realm of histone phosphorylation. *Molecular and cellular biology* **31**, 4858-4873, doi:10.1128/MCB.05631-11 (2011).
67 Sawicka, A. & Seiser, C. Histone H3 phosphorylation - a versatile chromatin modification for different occasions. *Biochimie* **94**, 2193-2201, doi:10.1016/j.biochi.2012.04.018 (2012).
68 Patel, D. J. & Wang, Z. Readout of epigenetic modifications. *Annual review of biochemistry* **82**, 81-118, doi:10.1146/annurev-biochem-072711-165700 (2013).
69 Cowell, I. G. *et al.* Heterochromatin, HP1 and methylation at lysine 9 of histone H3 in animals. *Chromosoma* **111**, 22-36 (2002).
70 Bannister, A. J., Schneider, R. & Kouzarides, T. Histone methylation: dynamic or static? *Cell* **109**, 801-806 (2002).
71 Shi, Y. *et al.* Histone demethylation mediated by the nuclear amine oxidase homolog LSD1. *Cell* **119**, 941-953, doi:10.1016/j.cell.2004.12.012 (2004).
72 Seeler, J. S. & Dejean, A. Nuclear and unclear functions of SUMO. *Nature reviews. Molecular cell biology* **4**, 690-699, doi:10.1038/nrm1200 (2003).
73 Strahl, B. D. & Allis, C. D. The language of covalent histone modifications. *Nature* **403**, 41-45, doi:10.1038/47412 (2000).
74 Pande, V. Understanding the Complexity of Epigenetic Target Space. *Journal of medicinal chemistry* **59**, 1299-1307, doi:10.1021/acs.jmedchem.5b01507 (2016).
75 Falkenberg, K. J. & Johnstone, R. W. Histone deacetylases and their inhibitors in cancer, neurological diseases and immune disorders. *Nature reviews. Drug discovery* **13**, 673-691, doi:10.1038/nrd4360 (2014).
76 Zhang, K., Siino, J. S., Jones, P. R., Yau, P. M. & Bradbury, E. M. A mass spectrometric "Western blot" to evaluate the correlations between histone methylation and histone acetylation. *Proteomics* **4**, 3765-3775, doi:10.1002/pmic.200400819 (2004).
77 Taverna, S. D. *et al.* Yng1 PHD finger binding to H3 trimethylated at K4 promotes NuA3 HAT activity at K14 of H3 and transcription at a subset of targeted ORFs. *Molecular cell* **24**, 785-796, doi:10.1016/j.molcel.2006.10.026 (2006).
78 Hyllus, D. *et al.* PRMT6-mediated methylation of R2 in histone H3 antagonizes H3 K4 trimethylation. *Genes & development* **21**, 3369-3380, doi:10.1101/gad.447007 (2007).
79 Weber, C. M. & Henikoff, S. Histone variants: dynamic punctuation in transcription. *Genes & development* **28**, 672-682, doi:10.1101/gad.238873.114 (2014).
80 Haushalter, K. A. & Kadonaga, J. T. Chromatin assembly by DNA-translocating motors. *Nature reviews. Molecular cell biology* **4**, 613-620, doi:10.1038/nrm1177 (2003).
81 Ahmad, K. & Henikoff, S. The histone variant H3.3 marks active chromatin by replication-independent nucleosome assembly. *Molecular cell* **9**, 1191-1200 (2002).
82 Mito, Y., Henikoff, J. G. & Henikoff, S. Genome-scale profiling of histone H3.3 replacement patterns. *Nature genetics* **37**, 1090-1097, doi:10.1038/ng1637 (2005).
83 Chen, P. *et al.* H3.3 actively marks enhancers and primes gene transcription via opening higher-ordered chromatin. *Genes & development* **27**, 2109-2124, doi:10.1101/gad.222174.113 (2013).
84 Drane, P., Ouararhni, K., Depaux, A., Shuaib, M. & Hamiche, A. The death-associated protein DAXX is a novel histone chaperone involved in the replication-independent deposition of H3.3. *Genes & development* **24**, 1253-1265, doi:10.1101/gad.566910 (2010).

85 Voon, H. P. & Wong, L. H. New players in heterochromatin silencing: histone variant H3.3 and the ATRX/DAXX chaperone. *Nucleic acids research* **44**, 1496-1501, doi:10.1093/nar/gkw012 (2016).
86 Talbert, P. B. & Henikoff, S. Histone variants--ancient wrap artists of the epigenome. *Nature reviews. Molecular cell biology* **11**, 264-275, doi:10.1038/nrm2861 (2010).
87 Malik, H. S. & Henikoff, S. Phylogenomics of the nucleosome. *Nature structural biology* **10**, 882-891, doi:10.1038/nsb996 (2003).
88 Ismail, I. H. & Hendzel, M. J. The gamma-H2A.X: is it just a surrogate marker of double-strand breaks or much more? *Environmental and molecular mutagenesis* **49**, 73-82, doi:10.1002/em.20358 (2008).
89 Bonisch, C. & Hake, S. B. Histone H2A variants in nucleosomes and chromatin: more or less stable? *Nucleic acids research* **40**, 10719-10741, doi:10.1093/nar/gks865 (2012).
90 Maze, I., Noh, K. M., Soshnev, A. A. & Allis, C. D. Every amino acid matters: essential contributions of histone variants to mammalian development and disease. *Nature reviews. Genetics* **15**, 259-271, doi:10.1038/nrg3673 (2014).
91 Suto, R. K., Clarkson, M. J., Tremethick, D. J. & Luger, K. Crystal structure of a nucleosome core particle containing the variant histone H2A.Z. *Nature structural biology* **7**, 1121-1124, doi:10.1038/81971 (2000).
92 Abbott, D. W., Ivanova, V. S., Wang, X., Bonner, W. M. & Ausio, J. Characterization of the stability and folding of H2A.Z chromatin particles: implications for transcriptional activation. *J Biol Chem* **276**, 41945-41949, doi:10.1074/jbc.M108217200 (2001).
93 Kumar, S. V. & Wigge, P. A. H2A.Z-containing nucleosomes mediate the thermosensory response in Arabidopsis. *Cell* **140**, 136-147, doi:10.1016/j.cell.2009.11.006 (2010).
94 Park, Y. J., Dyer, P. N., Tremethick, D. J. & Luger, K. A new fluorescence resonance energy transfer approach demonstrates that the histone variant H2AZ stabilizes the histone octamer within the nucleosome. *J Biol Chem* **279**, 24274-24282, doi:10.1074/jbc.M313152200 (2004).
95 Biterge, B. & Schneider, R. Histone variants: key players of chromatin. *Cell and tissue research* **356**, 457-466, doi:10.1007/s00441-014-1862-4 (2014).
96 Raisner, R. M. *et al.* Histone variant H2A.Z marks the 5' ends of both active and inactive genes in euchromatin. *Cell* **123**, 233-248, doi:10.1016/j.cell.2005.10.002 (2005).
97 Jin, C. *et al.* H3.3/H2A.Z double variant-containing nucleosomes mark 'nucleosome-free regions' of active promoters and other regulatory regions. *Nature genetics* **41**, 941-945, doi:10.1038/ng.409 (2009).
98 Nekrasov, M. *et al.* Histone H2A.Z inheritance during the cell cycle and its impact on promoter organization and dynamics. *Nature structural & molecular biology* **19**, 1076-1083, doi:10.1038/nsmb.2424 (2012).
99 Meneghini, M. D., Wu, M. & Madhani, H. D. Conserved histone variant H2A.Z protects euchromatin from the ectopic spread of silent heterochromatin. *Cell* **112**, 725-736 (2003).
100 Creyghton, M. P. *et al.* H2AZ is enriched at polycomb complex target genes in ES cells and is necessary for lineage commitment. *Cell* **135**, 649-661, doi:10.1016/j.cell.2008.09.056 (2008).
101 Rangasamy, D., Berven, L., Ridgway, P. & Tremethick, D. J. Pericentric heterochromatin becomes enriched with H2A.Z during early mammalian development. *EMBO J* **22**, 1599-1607, doi:10.1093/emboj/cdg160 (2003).

102 Wu, W. H. *et al.* Swc2 is a widely conserved H2AZ-binding module essential for ATP-dependent histone exchange. *Nature structural & molecular biology* **12**, 1064-1071, doi:10.1038/nsmb1023 (2005).
103 Mizuguchi, G. *et al.* ATP-driven exchange of histone H2AZ variant catalyzed by SWR1 chromatin remodeling complex. *Science* **303**, 343-348, doi:10.1126/science.1090701 (2004).
104 Kusch, T. *et al.* Acetylation by Tip60 is required for selective histone variant exchange at DNA lesions. *Science* **306**, 2084-2087, doi:10.1126/science.1103455 (2004).
105 Ruhl, D. D. *et al.* Purification of a human SRCAP complex that remodels chromatin by incorporating the histone variant H2A.Z into nucleosomes. *Biochemistry* **45**, 5671-5677, doi:10.1021/bi060043d (2006).
106 Papamichos-Chronakis, M., Watanabe, S., Rando, O. J. & Peterson, C. L. Global regulation of H2A.Z localization by the INO80 chromatin-remodeling enzyme is essential for genome integrity. *Cell* **144**, 200-213, doi:10.1016/j.cell.2010.12.021 (2011).
107 Mahadevaiah, S. K. *et al.* Recombinational DNA double-strand breaks in mice precede synapsis. *Nature genetics* **27**, 271-276, doi:10.1038/85830 (2001).
108 Celeste, A. *et al.* H2AX haploinsufficiency modifies genomic stability and tumor susceptibility. *Cell* **114**, 371-383 (2003).
109 Celeste, A. *et al.* Genomic instability in mice lacking histone H2AX. *Science* **296**, 922-927, doi:10.1126/science.1069398 (2002).
110 Gonzalez-Romero, R., Mendez, J., Ausio, J. & Eirin-Lopez, J. M. Quickly evolving histones, nucleosome stability and chromatin folding: all about histone H2A.Bbd. *Gene* **413**, 1-7, doi:10.1016/j.gene.2008.02.003 (2008).
111 Chadwick, B. P. & Willard, H. F. A novel chromatin protein, distantly related to histone H2A, is largely excluded from the inactive X chromosome. *The Journal of cell biology* **152**, 375-384 (2001).
112 Costanzi, C. & Pehrson, J. R. Histone macroH2A1 is concentrated in the inactive X chromosome of female mammals. *Nature* **393**, 599-601, doi:10.1038/31275 (1998).
113 Richler, C., Dhara, S. K. & Wahrman, J. Histone macroH2A1.2 is concentrated in the XY compartment of mammalian male meiotic nuclei. *Cytogenetics and cell genetics* **89**, 118-120, doi:15589 (2000).
114 Mueller-Planitz, F., Klinker, H. & Becker, P. B. Nucleosome sliding mechanisms: new twists in a looped history. *Nature structural & molecular biology* **20**, 1026-1032, doi:10.1038/nsmb.2648 (2013).
115 Flaus, A. & Owen-Hughes, T. Mechanisms for ATP-dependent chromatin remodelling: the means to the end. *The FEBS journal* **278**, 3579-3595, doi:10.1111/j.1742-4658.2011.08281.x (2011).
116 Eisen, J. A., Sweder, K. S. & Hanawalt, P. C. Evolution of the SNF2 family of proteins: subfamilies with distinct sequences and functions. *Nucleic acids research* **23**, 2715-2723 (1995).
117 Bouazoune, K. & Kingston, R. E. Assembly, remodelled. *eLife* **2**, e01270, doi:10.7554/eLife.01270 (2013).
118 Flaus, A. & Owen-Hughes, T. Mechanisms for ATP-dependent chromatin remodelling. *Current opinion in genetics & development* **11**, 148-154 (2001).
119 Tang, L., Nogales, E. & Ciferri, C. Structure and function of SWI/SNF chromatin remodeling complexes and mechanistic implications for transcription. *Progress in biophysics and molecular biology* **102**, 122-128, doi:10.1016/j.pbiomolbio.2010.05.001 (2010).

120 Vignali, M., Hassan, A. H., Neely, K. E. & Workman, J. L. ATP-dependent chromatin-remodeling complexes. *Molecular and cellular biology* **20**, 1899-1910 (2000).
121 Langst, G. & Becker, P. B. Nucleosome mobilization and positioning by ISWI-containing chromatin-remodeling factors. *J Cell Sci* **114**, 2561-2568 (2001).
122 Strohner, R. *et al.* NoRC--a novel member of mammalian ISWI-containing chromatin remodeling machines. *EMBO J* **20**, 4892-4900, doi:10.1093/emboj/20.17.4892 (2001).
123 Tyagi, M., Imam, N., Verma, K. & Patel, A. K. Chromatin remodelers: We are the drivers!! *Nucleus* **7**, 388-404, doi:10.1080/19491034.2016.1211217 (2016).
124 Shen, X., Mizuguchi, G., Hamiche, A. & Wu, C. A chromatin remodelling complex involved in transcription and DNA processing. *Nature* **406**, 541-544, doi:10.1038/35020123 (2000).
125 Boeger, H., Griesenbeck, J., Strattan, J. S. & Kornberg, R. D. Removal of promoter nucleosomes by disassembly rather than sliding in vivo. *Molecular cell* **14**, 667-673, doi:10.1016/j.molcel.2004.05.013 (2004).
126 Brown, C. R., Mao, C., Falkovskaia, E., Law, J. K. & Boeger, H. In vivo role for the chromatin-remodeling enzyme SWI/SNF in the removal of promoter nucleosomes by disassembly rather than sliding. *J Biol Chem* **286**, 40556-40565, doi:10.1074/jbc.M111.289918 (2011).
127 Radman-Livaja, M. & Rando, O. J. Nucleosome positioning: how is it established, and why does it matter? *Developmental biology* **339**, 258-266, doi:10.1016/j.ydbio.2009.06.012 (2010).
128 Petesch, S. J. & Lis, J. T. Rapid, transcription-independent loss of nucleosomes over a large chromatin domain at Hsp70 loci. *Cell* **134**, 74-84, doi:10.1016/j.cell.2008.05.029 (2008).
129 Schwabish, M. A. & Struhl, K. Evidence for eviction and rapid deposition of histones upon transcriptional elongation by RNA polymerase II. *Molecular and cellular biology* **24**, 10111-10117, doi:10.1128/MCB.24.23.10111-10117.2004 (2004).
130 Kulaeva, O. I., Gaykalova, D. A. & Studitsky, V. M. Transcription through chromatin by RNA polymerase II: histone displacement and exchange. *Mutation research* **618**, 116-129, doi:10.1016/j.mrfmmm.2006.05.040 (2007).
131 Khuong, M. T., Fei, J., Ishii, H. & Kadonaga, J. T. Prenucleosomes and Active Chromatin. *Cold Spring Harbor symposia on quantitative biology* **80**, 65-72, doi:10.1101/sqb.2015.80.027300 (2015).
132 Torigoe, S. E., Patel, A., Khuong, M. T., Bowman, G. D. & Kadonaga, J. T. ATP-dependent chromatin assembly is functionally distinct from chromatin remodeling. *eLife* **2**, e00863, doi:10.7554/eLife.00863 (2013).
133 Ito, T. *et al.* ACF consists of two subunits, Acf1 and ISWI, that function cooperatively in the ATP-dependent catalysis of chromatin assembly. *Genes & development* **13**, 1529-1539 (1999).
134 Lusser, A. & Kadonaga, J. T. Chromatin remodeling by ATP-dependent molecular machines. *BioEssays : news and reviews in molecular, cellular and developmental biology* **25**, 1192-1200, doi:10.1002/bies.10359 (2003).
135 Fyodorov, D. V. & Kadonaga, J. T. The many faces of chromatin remodeling: SWItching beyond transcription. *Cell* **106**, 523-525 (2001).
136 Narlikar, G. J., Fan, H. Y. & Kingston, R. E. Cooperation between complexes that regulate chromatin structure and transcription. *Cell* **108**, 475-487 (2002).
137 Kingston, R. E. & Narlikar, G. J. ATP-dependent remodeling and acetylation as regulators of chromatin fluidity. *Genes & development* **13**, 2339-2352 (1999).

138 Guyon, J. R., Narlikar, G. J., Sullivan, E. K. & Kingston, R. E. Stability of a human SWI-SNF remodeled nucleosomal array. *Molecular and cellular biology* **21**, 1132-1144, doi:10.1128/MCB.21.4.1132-1144.2001 (2001).
139 Narlikar, G. J., Sundaramoorthy, R. & Owen-Hughes, T. Mechanisms and functions of ATP-dependent chromatin-remodeling enzymes. *Cell* **154**, 490-503, doi:10.1016/j.cell.2013.07.011 (2013).
140 Corona, D. F. *et al.* ISWI is an ATP-dependent nucleosome remodeling factor. *Molecular cell* **3**, 239-245 (1999).
141 Fyodorov, D. V. & Kadonaga, J. T. Dynamics of ATP-dependent chromatin assembly by ACF. *Nature* **418**, 897-900, doi:10.1038/nature00929 (2002).
142 Ito, T., Bulger, M., Pazin, M. J., Kobayashi, R. & Kadonaga, J. T. ACF, an ISWI-containing and ATP-utilizing chromatin assembly and remodeling factor. *Cell* **90**, 145-155 (1997).
143 Lusser, A., Urwin, D. L. & Kadonaga, J. T. Distinct activities of CHD1 and ACF in ATP-dependent chromatin assembly. *Nature structural & molecular biology* **12**, 160-166, doi:10.1038/nsmb884 (2005).
144 Eberharter, A. *et al.* Acf1, the largest subunit of CHRAC, regulates ISWI-induced nucleosome remodelling. *EMBO J* **20**, 3781-3788, doi:10.1093/emboj/20.14.3781 (2001).
145 Alexiadis, V., Varga-Weisz, P. D., Bonte, E., Becker, P. B. & Gruss, C. In vitro chromatin remodelling by chromatin accessibility complex (CHRAC) at the SV40 origin of DNA replication. *EMBO J* **17**, 3428-3438, doi:10.1093/emboj/17.12.3428 (1998).
146 Hamiche, A., Sandaltzopoulos, R., Gdula, D. A. & Wu, C. ATP-dependent histone octamer sliding mediated by the chromatin remodeling complex NURF. *Cell* **97**, 833-842 (1999).
147 Tsukiyama, T. & Wu, C. Purification and properties of an ATP-dependent nucleosome remodeling factor. *Cell* **83**, 1011-1020 (1995).
148 Loyola, A. *et al.* Functional analysis of the subunits of the chromatin assembly factor RSF. *Molecular and cellular biology* **23**, 6759-6768 (2003).
149 Loyola, A., LeRoy, G., Wang, Y. H. & Reinberg, D. Reconstitution of recombinant chromatin establishes a requirement for histone-tail modifications during chromatin assembly and transcription. *Genes & development* **15**, 2837-2851, doi:10.1101/gad.937401 (2001).
150 Collins, N. *et al.* An ACF1-ISWI chromatin-remodeling complex is required for DNA replication through heterochromatin. *Nature genetics* **32**, 627-632, doi:10.1038/ng1046 (2002).
151 Landry, J. W. *et al.* Chromatin remodeling complex NURF regulates thymocyte maturation. *Genes & development* **25**, 275-286, doi:10.1101/gad.2007311 (2011).
152 Emelyanov, A. V. *et al.* Identification and characterization of ToRC, a novel ISWI-containing ATP-dependent chromatin assembly complex. *Genes & development* **26**, 603-614, doi:10.1101/gad.180604.111 (2012).
153 Bartholomew, B. ISWI chromatin remodeling: one primary actor or a coordinated effort? *Current opinion in structural biology* **24**, 150-155, doi:10.1016/j.sbi.2014.01.010 (2014).
154 Wang, W. *et al.* Diversity and specialization of mammalian SWI/SNF complexes. *Genes & development* **10**, 2117-2130 (1996).
155 Nguyen, H. *et al.* Epigenetic regulation by BAF (mSWI/SNF) chromatin remodeling complexes is indispensable for embryonic development. *Cell cycle* **15**, 1317-1324, doi:10.1080/15384101.2016.1160984 (2016).

156 Krosl, J. *et al.* A mutant allele of the Swi/Snf member BAF250a determines the pool size of fetal liver hemopoietic stem cell populations. *Blood* **116**, 1678-1684, doi:10.1182/blood-2010-03-273862 (2010).
157 Krasteva, V. *et al.* The BAF53a subunit of SWI/SNF-like BAF complexes is essential for hemopoietic stem cell function. *Blood* **120**, 4720-4732, doi:10.1182/blood-2012-04-427047 (2012).
158 Liu, N., Peterson, C. L. & Hayes, J. J. SWI/SNF- and RSC-catalyzed nucleosome mobilization requires internal DNA loop translocation within nucleosomes. *Molecular and cellular biology* **31**, 4165-4175, doi:10.1128/MCB.05605-11 (2011).
159 Lorch, Y., Zhang, M. & Kornberg, R. D. Histone octamer transfer by a chromatin-remodeling complex. *Cell* **96**, 389-392 (1999).
160 Chai, B., Huang, J., Cairns, B. R. & Laurent, B. C. Distinct roles for the RSC and Swi/Snf ATP-dependent chromatin remodelers in DNA double-strand break repair. *Genes & development* **19**, 1656-1661, doi:10.1101/gad.1273105 (2005).
161 Martens, J. A. & Winston, F. Recent advances in understanding chromatin remodeling by Swi/Snf complexes. *Current opinion in genetics & development* **13**, 136-142 (2003).
162 Huang, J., Hsu, J. M. & Laurent, B. C. The RSC nucleosome-remodeling complex is required for Cohesin's association with chromosome arms. *Molecular cell* **13**, 739-750 (2004).
163 Angus-Hill, M. L. *et al.* A Rsc3/Rsc30 zinc cluster dimer reveals novel roles for the chromatin remodeler RSC in gene expression and cell cycle control. *Molecular cell* **7**, 741-751 (2001).
164 Kwon, H., Imbalzano, A. N., Khavari, P. A., Kingston, R. E. & Green, M. R. Nucleosome disruption and enhancement of activator binding by a human SW1/SNF complex. *Nature* **370**, 477-481, doi:10.1038/370477a0 (1994).
165 Schnitzler, G., Sif, S. & Kingston, R. E. Human SWI/SNF interconverts a nucleosome between its base state and a stable remodeled state. *Cell* **94**, 17-27 (1998).
166 Peterson, C. L. & Workman, J. L. Promoter targeting and chromatin remodeling by the SWI/SNF complex. *Current opinion in genetics & development* **10**, 187-192 (2000).
167 Lorch, Y., Maier-Davis, B. & Kornberg, R. D. Chromatin remodeling by nucleosome disassembly in vitro. *Proceedings of the National Academy of Sciences of the United States of America* **103**, 3090-3093, doi:10.1073/pnas.0511050103 (2006).
168 Martens, J. A. & Winston, F. Evidence that Swi/Snf directly represses transcription in S. cerevisiae. *Genes & development* **16**, 2231-2236, doi:10.1101/gad.1009902 (2002).
169 Battaglioli, E. *et al.* REST repression of neuronal genes requires components of the hSWI.SNF complex. *J Biol Chem* **277**, 41038-41045, doi:10.1074/jbc.M205691200 (2002).
170 Sif, S., Saurin, A. J., Imbalzano, A. N. & Kingston, R. E. Purification and characterization of mSin3A-containing Brg1 and hBrm chromatin remodeling complexes. *Genes & development* **15**, 603-618, doi:10.1101/gad.872801 (2001).
171 Lee, D., Sohn, H., Kalpana, G. V. & Choe, J. Interaction of E1 and hSNF5 proteins stimulates replication of human papillomavirus DNA. *Nature* **399**, 487-491, doi:10.1038/20966 (1999).
172 Marfella, C. G. & Imbalzano, A. N. The Chd family of chromatin remodelers. *Mutation research* **618**, 30-40, doi:10.1016/j.mrfmmm.2006.07.012 (2007).
173 Ho, L. & Crabtree, G. R. Chromatin remodelling during development. *Nature* **463**, 474-484, doi:10.1038/nature08911 (2010).

174 Kim, M. S., Chung, N. G., Kang, M. R., Yoo, N. J. & Lee, S. H. Genetic and expressional alterations of CHD genes in gastric and colorectal cancers. *Histopathology* **58**, 660-668, doi:10.1111/j.1365-2559.2011.03819.x (2011).
175 Shingleton, J. R. & Hemann, M. T. The Chromatin Regulator CHD8 Is a Context-Dependent Mediator of Cell Survival in Murine Hematopoietic Malignancies. *PloS one* **10**, e0143275, doi:10.1371/journal.pone.0143275 (2015).
176 Kolla, V., Zhuang, T., Higashi, M., Naraparaju, K. & Brodeur, G. M. Role of CHD5 in human cancers: 10 years later. *Cancer research* **74**, 652-658, doi:10.1158/0008-5472.CAN-13-3056 (2014).
177 Stokes, D. G., Tartof, K. D. & Perry, R. P. CHD1 is concentrated in interbands and puffed regions of Drosophila polytene chromosomes. *Proceedings of the National Academy of Sciences of the United States of America* **93**, 7137-7142 (1996).
178 Konev, A. Y. *et al.* CHD1 motor protein is required for deposition of histone variant H3.3 into chromatin in vivo. *Science* **317**, 1087-1090, doi:10.1126/science.1145339 (2007).
179 Roberts, S. M. & Winston, F. Essential functional interactions of SAGA, a Saccharomyces cerevisiae complex of Spt, Ada, and Gcn5 proteins, with the Snf/Swi and Srb/mediator complexes. *Genetics* **147**, 451-465 (1997).
180 Pray-Grant, M. G., Daniel, J. A., Schieltz, D., Yates, J. R., 3rd & Grant, P. A. Chd1 chromodomain links histone H3 methylation with SAGA- and SLIK-dependent acetylation. *Nature* **433**, 434-438, doi:10.1038/nature03242 (2005).
181 Kolla, V. *et al.* The tumour suppressor CHD5 forms a NuRD-type chromatin remodelling complex. *Biochem J* **468**, 345-352, doi:10.1042/BJ20150030 (2015).
182 Wang, H. B. & Zhang, Y. Mi2, an auto-antigen for dermatomyositis, is an ATP-dependent nucleosome remodeling factor. *Nucleic acids research* **29**, 2517-2521 (2001).
183 Zhang, Y., LeRoy, G., Seelig, H. P., Lane, W. S. & Reinberg, D. The dermatomyositis-specific autoantigen Mi2 is a component of a complex containing histone deacetylase and nucleosome remodeling activities. *Cell* **95**, 279-289 (1998).
184 Murawska, M. *et al.* dCHD3, a novel ATP-dependent chromatin remodeler associated with sites of active transcription. *Molecular and cellular biology* **28**, 2745-2757, doi:10.1128/MCB.01839-07 (2008).
185 Bao, Y. & Shen, X. INO80 subfamily of chromatin remodeling complexes. *Mutation research* **618**, 18-29, doi:10.1016/j.mrfmmm.2006.10.006 (2007).
186 van Attikum, H., Fritsch, O. & Gasser, S. M. Distinct roles for SWR1 and INO80 chromatin remodeling complexes at chromosomal double-strand breaks. *EMBO J* **26**, 4113-4125, doi:10.1038/sj.emboj.7601835 (2007).
187 Shen, X., Ranallo, R., Choi, E. & Wu, C. Involvement of actin-related proteins in ATP-dependent chromatin remodeling. *Molecular cell* **12**, 147-155 (2003).
188 Conaway, R. C. & Conaway, J. W. The INO80 chromatin remodeling complex in transcription, replication and repair. *Trends in biochemical sciences* **34**, 71-77, doi:10.1016/j.tibs.2008.10.010 (2009).
189 van Attikum, H., Fritsch, O., Hohn, B. & Gasser, S. M. Recruitment of the INO80 complex by H2A phosphorylation links ATP-dependent chromatin remodeling with DNA double-strand break repair. *Cell* **119**, 777-788, doi:10.1016/j.cell.2004.11.033 (2004).
190 Watanabe, S. & Peterson, C. L. The INO80 family of chromatin-remodeling enzymes: regulators of histone variant dynamics. *Cold Spring Harbor symposia on quantitative biology* **75**, 35-42, doi:10.1101/sqb.2010.75.063 (2010).

191 Keogh, M. C. *et al.* The Saccharomyces cerevisiae histone H2A variant Htz1 is acetylated by NuA4. *Genes & development* **20**, 660-665, doi:10.1101/gad.1388106 (2006).
192 Nguyen, V. Q. *et al.* Molecular architecture of the ATP-dependent chromatin-remodeling complex SWR1. *Cell* **154**, 1220-1231, doi:10.1016/j.cell.2013.08.018 (2013).
193 Li, B., Carey, M. & Workman, J. L. The role of chromatin during transcription. *Cell* **128**, 707-719, doi:10.1016/j.cell.2007.01.015 (2007).
194 Green, C. M. & Almouzni, G. When repair meets chromatin. First in series on chromatin dynamics. *EMBO reports* **3**, 28-33, doi:10.1093/embo-reports/kvf005 (2002).
195 Tagami, H., Ray-Gallet, D., Almouzni, G. & Nakatani, Y. Histone H3.1 and H3.3 complexes mediate nucleosome assembly pathways dependent or independent of DNA synthesis. *Cell* **116**, 51-61 (2004).
196 Ray-Gallet, D. *et al.* Dynamics of histone H3 deposition in vivo reveal a nucleosome gap-filling mechanism for H3.3 to maintain chromatin integrity. *Molecular cell* **44**, 928-941, doi:10.1016/j.molcel.2011.12.006 (2011).
197 Sakai, A., Schwartz, B. E., Goldstein, S. & Ahmad, K. Transcriptional and developmental functions of the H3.3 histone variant in Drosophila. *Current biology : CB* **19**, 1816-1820, doi:10.1016/j.cub.2009.09.021 (2009).
198 Gaillard, P. H. *et al.* Chromatin assembly coupled to DNA repair: a new role for chromatin assembly factor I. *Cell* **86**, 887-896 (1996).
199 Polo, S. E. & Almouzni, G. Chromatin dynamics after DNA damage: The legacy of the access-repair-restore model. *DNA repair* **36**, 114-121, doi:10.1016/j.dnarep.2015.09.014 (2015).
200 Moggs, J. G. *et al.* A CAF-1-PCNA-mediated chromatin assembly pathway triggered by sensing DNA damage. *Molecular and cellular biology* **20**, 1206-1218 (2000).
201 Adam, S., Polo, S. E. & Almouzni, G. Transcription recovery after DNA damage requires chromatin priming by the H3.3 histone chaperone HIRA. *Cell* **155**, 94-106, doi:10.1016/j.cell.2013.08.029 (2013).
202 Dinant, C. *et al.* Enhanced chromatin dynamics by FACT promotes transcriptional restart after UV-induced DNA damage. *Molecular cell* **51**, 469-479, doi:10.1016/j.molcel.2013.08.007 (2013).
203 Alabert, C. *et al.* Two distinct modes for propagation of histone PTMs across the cell cycle. *Genes & development* **29**, 585-590, doi:10.1101/gad.256354.114 (2015).
204 Ito, T., Tyler, J. K. & Kadonaga, J. T. Chromatin assembly factors: a dual function in nucleosome formation and mobilization? *Genes to cells : devoted to molecular & cellular mechanisms* **2**, 593-600 (1997).
205 Straube, K., Blackwell, J. S., Jr. & Pemberton, L. F. Nap1 and Chz1 have separate Htz1 nuclear import and assembly functions. *Traffic* **11**, 185-197, doi:10.1111/j.1600-0854.2009.01010.x (2010).
206 Reilly, P. T. *et al.* Generation and characterization of the Anp32e-deficient mouse. *PloS one* **5**, e13597, doi:10.1371/journal.pone.0013597 (2010).
207 Yu, Z., Liu, J., Deng, W. M. & Jiao, R. Histone chaperone CAF-1: essential roles in multi-cellular organism development. *Cellular and molecular life sciences : CMLS* **72**, 327-337, doi:10.1007/s00018-014-1748-3 (2015).
208 Smith, S. & Stillman, B. Purification and characterization of CAF-I, a human cell factor required for chromatin assembly during DNA replication in vitro. *Cell* **58**, 15-25 (1989).

209 Krude, T. Chromatin assembly factor 1 (CAF-1) colocalizes with replication foci in HeLa cell nuclei. *Experimental cell research* **220**, 304-311, doi:10.1006/excr.1995.1320 (1995).
210 Shibahara, K. & Stillman, B. Replication-dependent marking of DNA by PCNA facilitates CAF-1-coupled inheritance of chromatin. *Cell* **96**, 575-585 (1999).
211 Huang, H. *et al.* Drosophila CAF-1 regulates HP1-mediated epigenetic silencing and pericentric heterochromatin stability. *J Cell Sci* **123**, 2853-2861, doi:10.1242/jcs.063610 (2010).
212 Quivy, J. P. *et al.* A CAF-1 dependent pool of HP1 during heterochromatin duplication. *EMBO J* **23**, 3516-3526, doi:10.1038/sj.emboj.7600362 (2004).
213 Tyler, J. K. *et al.* The RCAF complex mediates chromatin assembly during DNA replication and repair. *Nature* **402**, 555-560, doi:10.1038/990147 (1999).
214 Rocha, W. & Verreault, A. Clothing up DNA for all seasons: Histone chaperones and nucleosome assembly pathways. *FEBS letters* **582**, 1938-1949, doi:10.1016/j.febslet.2008.03.006 (2008).
215 Kadyrova, L. Y., Rodriges Blanko, E. & Kadyrov, F. A. Human CAF-1-dependent nucleosome assembly in a defined system. *Cell cycle* **12**, 3286-3297, doi:10.4161/cc.26310 (2013).
216 Groth, A. *et al.* Regulation of replication fork progression through histone supply and demand. *Science* **318**, 1928-1931, doi:10.1126/science.1148992 (2007).
217 Emili, A., Schieltz, D. M., Yates, J. R., 3rd & Hartwell, L. H. Dynamic interaction of DNA damage checkpoint protein Rad53 with chromatin assembly factor Asf1. *Molecular cell* **7**, 13-20 (2001).
218 Goldberg, A. D. *et al.* Distinct factors control histone variant H3.3 localization at specific genomic regions. *Cell* **140**, 678-691, doi:10.1016/j.cell.2010.01.003 (2010).
219 Zhang, R. *et al.* Formation of MacroH2A-containing senescence-associated heterochromatin foci and senescence driven by ASF1a and HIRA. *Developmental cell* **8**, 19-30, doi:10.1016/j.devcel.2004.10.019 (2005).
220 Rai, T. S. *et al.* Human CABIN1 is a functional member of the human HIRA/UBN1/ASF1a histone H3.3 chaperone complex. *Molecular and cellular biology* **31**, 4107-4118, doi:10.1128/MCB.05546-11 (2011).
221 Schneiderman, J. I., Orsi, G. A., Hughes, K. T., Loppin, B. & Ahmad, K. Nucleosome-depleted chromatin gaps recruit assembly factors for the H3.3 histone variant. *Proceedings of the National Academy of Sciences of the United States of America* **109**, 19721-19726, doi:10.1073/pnas.1206629109 (2012).
222 Neer, E. J., Schmidt, C. J., Nambudripad, R. & Smith, T. F. The Ancient Regulatory-Protein Family of Wd-Repeat Proteins (Vol 371, Pg 297, 1994). *Nature* **371**, 812-812 (1994).
223 Xue, Y. *et al.* The ATRX syndrome protein forms a chromatin-remodeling complex with Daxx and localizes in promyelocytic leukemia nuclear bodies. *Proceedings of the National Academy of Sciences of the United States of America* **100**, 10635-10640, doi:10.1073/pnas.1937626100 (2003).
224 Delbarre, E., Ivanauskiene, K., Kuntziger, T. & Collas, P. DAXX-dependent supply of soluble (H3.3-H4) dimers to PML bodies pending deposition into chromatin. *Genome research* **23**, 440-451, doi:10.1101/gr.142703.112 (2013).
225 Zlatanova, J., Seebart, C. & Tomschik, M. Nap1: taking a closer look at a juggler protein of extraordinary skills. *FASEB journal : official publication of the Federation of American Societies for Experimental Biology* **21**, 1294-1310, doi:10.1096/fj.06-7199rev (2007).

226 Ito, T., Bulger, M., Kobayashi, R. & Kadonaga, J. T. Drosophila NAP-1 is a core histone chaperone that functions in ATP-facilitated assembly of regularly spaced nucleosomal arrays. *Molecular and cellular biology* **16**, 3112-3124 (1996).
227 Aguilar-Gurrieri, C. *et al.* Structural evidence for Nap1-dependent H2A-H2B deposition and nucleosome assembly. *EMBO J* **35**, 1465-1482, doi:10.15252/embj.201694105 (2016).
228 Chen, X. *et al.* Histone Chaperone Nap1 Is a Major Regulator of Histone H2A-H2B Dynamics at the Inducible GAL Locus. *Molecular and cellular biology* **36**, 1287-1296, doi:10.1128/MCB.00835-15 (2016).
229 McQuibban, G. A., Commisso-Cappelli, C. N. & Lewis, P. N. Assembly, remodeling, and histone binding capabilities of yeast nucleosome assembly protein 1. *J Biol Chem* **273**, 6582-6590 (1998).
230 Andrews, A. J., Chen, X., Zevin, A., Stargell, L. A. & Luger, K. The histone chaperone Nap1 promotes nucleosome assembly by eliminating nonnucleosomal histone DNA interactions. *Molecular cell* **37**, 834-842, doi:10.1016/j.molcel.2010.01.037 (2010).
231 Shintomi, K. *et al.* Nucleosome assembly protein-1 is a linker histone chaperone in Xenopus eggs. *Proceedings of the National Academy of Sciences of the United States of America* **102**, 8210-8215, doi:10.1073/pnas.0500822102 (2005).
232 Mosammaparast, N., Del Rosario, B. C. & Pemberton, L. F. Modulation of histone deposition by the karyopherin kap114. *Molecular and cellular biology* **25**, 1764-1778, doi:10.1128/MCB.25.5.1764-1778.2005 (2005).
233 Belotserkovskaya, R. *et al.* FACT facilitates transcription-dependent nucleosome alteration. *Science* **301**, 1090-1093, doi:10.1126/science.1085703 (2003).
234 Orphanides, G., Wu, W. H., Lane, W. S., Hampsey, M. & Reinberg, D. The chromatin-specific transcription elongation factor FACT comprises human SPT16 and SSRP1 proteins. *Nature* **400**, 284-288, doi:10.1038/22350 (1999).
235 Mahapatra, S., Dewari, P. S., Bhardwaj, A. & Bhargava, P. Yeast H2A.Z, FACT complex and RSC regulate transcription of tRNA gene through differential dynamics of flanking nucleosomes. *Nucleic acids research* **39**, 4023-4034, doi:10.1093/nar/gkq1286 (2011).
236 Heo, K. *et al.* FACT-mediated exchange of histone variant H2AX regulated by phosphorylation of H2AX and ADP-ribosylation of Spt16. *Molecular cell* **30**, 86-97, doi:10.1016/j.molcel.2008.02.029 (2008).
237 Gursoy-Yuzugullu, O., Ayrapetov, M. K. & Price, B. D. Histone chaperone Anp32e removes H2A.Z from DNA double-strand breaks and promotes nucleosome reorganization and DNA repair. *Proceedings of the National Academy of Sciences of the United States of America* **112**, 7507-7512, doi:10.1073/pnas.1504868112 (2015).
238 Tyler, J. K. Chromatin assembly. Cooperation between histone chaperones and ATP-dependent nucleosome remodeling machines. *European journal of biochemistry* **269**, 2268-2274 (2002).
239 Torigoe, S. E., Urwin, D. L., Ishii, H., Smith, D. E. & Kadonaga, J. T. Identification of a rapidly formed nonnucleosomal histone-DNA intermediate that is converted into chromatin by ACF. *Molecular cell* **43**, 638-648, doi:10.1016/j.molcel.2011.07.017 (2011).
240 Chang, L. *et al.* Histones in transit: cytosolic histone complexes and diacetylation of H4 during nucleosome assembly in human cells. *Biochemistry* **36**, 469-480, doi:10.1021/bi962069i (1997).
241 Tyler, J. K. *et al.* Interaction between the Drosophila CAF-1 and ASF1 chromatin assembly factors. *Molecular and cellular biology* **21**, 6574-6584 (2001).

242 Burgess, R. J. & Zhang, Z. Histone chaperones in nucleosome assembly and human disease. *Nature structural & molecular biology* **20**, 14-22, doi:10.1038/nsmb.2461 (2013).
243 Annunziato, A. T. & Seale, R. L. Histone deacetylation is required for the maturation of newly replicated chromatin. *J Biol Chem* **258**, 12675-12684 (1983).
244 Brownlee, P. M., Meisenberg, C. & Downs, J. A. The SWI/SNF chromatin remodelling complex: Its role in maintaining genome stability and preventing tumourigenesis. *DNA repair* **32**, 127-133, doi:10.1016/j.dnarep.2015.04.023 (2015).
245 Liu, Z. Q. & Yang, P. C. Construction of pET-32 alpha (+) Vector for Protein Expression and Purification. *North American journal of medical sciences* **4**, 651-655, doi:10.4103/1947-2714.104318 (2012).
246 Froger, A. & Hall, J. E. Transformation of plasmid DNA into E. coli using the heat shock method. *J Vis Exp*, 253, doi:10.3791/253 (2007).
247 Serrano, M., Lin, A. W., McCurrach, M. E., Beach, D. & Lowe, S. W. Oncogenic ras provokes premature cell senescence associated with accumulation of p53 and p16INK4a. *Cell* **88**, 593-602 (1997).
248 Fox, R. M., Hanlon, C. D. & Andrew, D. J. The CrebA/Creb3-like transcription factors are major and direct regulators of secretory capacity. *The Journal of cell biology* **191**, 479-492, doi:10.1083/jcb.201004062 (2010).
249 Abmayr, S. M., Yao, T., Parmely, T. & Workman, J. L. Preparation of nuclear and cytoplasmic extracts from mammalian cells. *Curr Protoc Pharmacol* **Chapter 12**, Unit12 13, doi:10.1002/0471141755.ph1203s35 (2006).
250 Mahmood, T. & Yang, P. C. Western blot: technique, theory, and trouble shooting. *North American journal of medical sciences* **4**, 429-434, doi:10.4103/1947-2714.100998 (2012).
251 White, C. L., Suto, R. K. & Luger, K. Structure of the yeast nucleosome core particle reveals fundamental changes in internucleosome interactions. *EMBO J* **20**, 5207-5218, doi:10.1093/emboj/20.18.5207 (2001).
252 Hamiche, A., Kang, J. G., Dennis, C., Xiao, H. & Wu, C. Histone tails modulate nucleosome mobility and regulate ATP-dependent nucleosome sliding by NURF. *Proceedings of the National Academy of Sciences of the United States of America* **98**, 14316-14321, doi:10.1073/pnas.251421398 (2001).
253 Assrir, N., Filhol, O., Galisson, F. & Lipinski, M. HIRIP3 is a nuclear phosphoprotein interacting with and phosphorylated by the serine-threonine kinase CK2. *Biological chemistry* **388**, 391-398, doi:10.1515/BC.2007.045 (2007).
254 Chou, C. C. & Wang, A. H. Structural D/E-rich repeats play multiple roles especially in gene regulation through DNA/RNA mimicry. *Molecular bioSystems* **11**, 2144-2151, doi:10.1039/c5mb00206k (2015).
255 Keller, D. M. *et al.* A DNA damage-induced p53 serine 392 kinase complex contains CK2, hSpt16, and SSRP1. *Molecular cell* **7**, 283-292 (2001).
256 Mao, P. *et al.* A basic domain in the histone H2B N-terminal tail is important for nucleosome assembly by FACT. *Nucleic acids research* **44**, 9142-9152, doi:10.1093/nar/gkw588 (2016).
257 Basnet, H. *et al.* Tyrosine phosphorylation of histone H2A by CK2 regulates transcriptional elongation. *Nature* **516**, 267-271, doi:10.1038/nature13736 (2014).
258 Monroy, M. A. *et al.* SNF2-related CBP activator protein (SRCAP) functions as a coactivator of steroid receptor-mediated transcription through synergistic interactions with CARM-1 and GRIP-1. *Molecular endocrinology* **17**, 2519-2528, doi:10.1210/me.2003-0208 (2003).

259 Szerlong, H. *et al.* The HSA domain binds nuclear actin-related proteins to regulate chromatin-remodeling ATPases. *Nature structural & molecular biology* **15**, 469-476, doi:10.1038/nsmb.1403 (2008).
260 Aravind, L. & Landsman, D. AT-hook motifs identified in a wide variety of DNA-binding proteins. *Nucleic acids research* **26**, 4413-4421 (1998).
261 Wong, M. M., Cox, L. K. & Chrivia, J. C. The chromatin remodeling protein, SRCAP, is critical for deposition of the histone variant H2A.Z at promoters. *J Biol Chem* **282**, 26132-26139, doi:10.1074/jbc.M703418200 (2007).
262 Cai, Y. *et al.* The mammalian YL1 protein is a shared subunit of the TRRAP/TIP60 histone acetyltransferase and SRCAP complexes. *J Biol Chem* **280**, 13665-13670, doi:10.1074/jbc.M500001200 (2005).
263 Kanemaki, M. *et al.* TIP49b, a new RuvB-like DNA helicase, is included in a complex together with another RuvB-like DNA helicase, TIP49a. *J Biol Chem* **274**, 22437-22444 (1999).
264 Queval, R., Papin, C., Dalvai, M., Bystricky, K. & Humbert, O. Reptin and Pontin oligomerization and activity are modulated through histone H3 N-terminal tail interaction. *J Biol Chem* **289**, 33999-34012, doi:10.1074/jbc.M114.576785 (2014).
265 Hanson, P. I. & Whiteheart, S. W. AAA+ proteins: have engine, will work. *Nature reviews. Molecular cell biology* **6**, 519-529, doi:10.1038/nrm1684 (2005).
266 Jonsson, Z. O., Jha, S., Wohlschlegel, J. A. & Dutta, A. Rvb1p/Rvb2p recruit Arp5p and assemble a functional Ino80 chromatin remodeling complex. *Molecular cell* **16**, 465-477, doi:10.1016/j.molcel.2004.09.033 (2004).
267 Boyer, L. A. & Peterson, C. L. Actin-related proteins (Arps): conformational switches for chromatin-remodeling machines? *BioEssays : news and reviews in molecular, cellular and developmental biology* **22**, 666-672, doi:10.1002/1521-1878(200007)22:7<666::AID-BIES9>3.0.CO;2-Y (2000).
268 Smith, A. P. *et al.* Histone H2A.Z regulates the expression of several classes of phosphate starvation response genes but not as a transcriptional activator. *Plant physiology* **152**, 217-225, doi:10.1104/pp.109.145532 (2010).
269 Deal, R. B., Topp, C. N., McKinney, E. C. & Meagher, R. B. Repression of flowering in Arabidopsis requires activation of FLOWERING LOCUS C expression by the histone variant H2A.Z. *The Plant cell* **19**, 74-83, doi:10.1105/tpc.106.048447 (2007).
270 Schulze, J. M., Wang, A. Y. & Kobor, M. S. YEATS domain proteins: a diverse family with many links to chromatin modification and transcription. *Biochemistry and cell biology = Biochimie et biologie cellulaire* **87**, 65-75, doi:10.1139/O08-111 (2009).
271 Zimmermann, K. *et al.* Targeted disruption of the GAS41 gene encoding a putative transcription factor indicates that GAS41 is essential for cell viability. *J Biol Chem* **277**, 18626-18631, doi:10.1074/jbc.M200572200 (2002).
272 Heisel, S., Habel, N. C., Schuetz, N., Ruggieri, A. & Meese, E. The YEATS family member GAS41 interacts with the general transcription factor TFIIF. *BMC molecular biology* **11**, 53, doi:10.1186/1471-2199-11-53 (2010).
273 Ding, X. *et al.* GAS41 interacts with transcription factor AP-2beta and stimulates AP-2beta-mediated transactivation. *Nucleic acids research* **34**, 2570-2578, doi:10.1093/nar/gkl319 (2006).
274 Goto, A., Fukuyama, H., Imler, J. L. & Hoffmann, J. A. The chromatin regulator DMAP1 modulates activity of the nuclear factor B (NF-B) transcription factor Relish in the Drosophila innate immune response. *J Biol Chem* **289**, 20470-20476, doi:10.1074/jbc.C114.553719 (2014).

275 Choi, J., Heo, K. & An, W. Cooperative action of TIP48 and TIP49 in H2A.Z exchange catalyzed by acetylation of nucleosomal H2A. *Nucleic acids research* **37**, 5993-6007, doi:10.1093/nar/gkp660 (2009).
276 Jha, S., Shibata, E. & Dutta, A. Human Rvb1/Tip49 is required for the histone acetyltransferase activity of Tip60/NuA4 and for the downregulation of phosphorylation on H2AX after DNA damage. *Molecular and cellular biology* **28**, 2690-2700, doi:10.1128/MCB.01983-07 (2008).
277 Nano, N. & Houry, W. A. Chaperone-like activity of the AAA+ proteins Rvb1 and Rvb2 in the assembly of various complexes. *Philosophical transactions of the Royal Society of London. Series B, Biological sciences* **368**, 20110399, doi:10.1098/rstb.2011.0399 (2013).

8 APPENDIX

8.1 List of publications

Latrick CM, Marek M, Ouararhni K, Papin C, Stoll I, Ignatyeva M, Obri A, Ennifar E, Dimitrov S, Romier , Hamiche A.

Molecular basis and specificity of H2A.Z-H2B recognition and deposition by the histone chaperone YL1.

Nat Struct Mol Biol. 2016 Apr;23(4):309-16. doi: 10.1038/nsmb.3189.

Print-out of the publication is attached at the end of this doctoral thesis.

Ignatyeva M., Shuaib M., Hamiche A. (2017);

Identification and characterization of HIRIP3 as a novel histone H2A chaperone – in preparation

Ignatyeva M., Hamiche A. (2017);

Cryo-EM structure of SRCAP complex functional domain – in preparation

8.2 List of conferences

"From Functional Genomics to Systems biology" conference, EMBL Heidelberg, Germany, 12 - 15 November 2016.

Ignatyeva M. "HIRIP3 interacts with H2A/H2B histone dimers *in vivo*."

Abstracts book of EMBO conference 'From Functional Genomics to Systems biology', 188 (2016).

9 PUBLICATION PRINT-OUT

nature structural & molecular biology

Molecular basis and specificity of H2A.Z–H2B recognition and deposition by the histone chaperone YL1

Chrysa M Latrick[1,5], Martin Marek[2,5], Khalid Ouararhni[1,5], Christophe Papin[1], Isabelle Stoll[1], Maria Ignatyeva[1], Arnaud Obri[1], Eric Ennifar[3], Stefan Dimitrov[4], Christophe Romier[2] & Ali Hamiche[1]

H2A.Z, a widely conserved histone variant, is evicted from chromatin by the histone chaperone ANP32E. However, to date, no deposition chaperone for H2A.Z is known in metazoans. Here, we identify YL1 as a specific H2A.Z-deposition chaperone. The 2.7-Å-resolution crystal structure of the human YL1–H2A.Z–H2B complex shows that YL1 binding, similarly to ANP32E binding, triggers an extension of the H2A.Z αC helix. The interaction with YL1 is, however, more extensive and includes both the extended acidic patch and the entire DNA-binding surface of H2A.Z–H2B. Substitution of only four amino acid residues of H2A is sufficient for the formation of an H2A.Z-like interface specifically recognized by YL1. Collectively, our data reveal the molecular basis of H2A.Z-specific recognition by YL1 and shed light on the mechanism of H2A.Z transfer to the nucleosome by the ATP-dependent chromatin-remodeling complexes SRCAP and P400–TIP60.

The evolutionarily conserved histone variant H2A.Z controls major nuclear events, including transcription and DNA repair, and is essential in flies and mice[1–5]. The H2A.Z nucleosomal crystal structure has revealed an expansion of the conserved acidic patch, owing to residues in the αC helix, a region required for *Drosophila* viability and interactions with ANP32E and Swr1 (refs. 4,6–8).

In yeast, the ATP-dependent chromatin-remodeling complex SWR1 exchanges canonical H2A with H2A.Z by using proteins Chz1, SWR1 and SWC2; SWC2 also recruits Swr1 to the nucleosome-free region[9–16]. Chz1 delivers H2A.Z to the SWR1 complex, where both SWR1 and SWC2 bind and participate in the exchange reaction[17,18]. However, how SWC2 functions remains unclear.

In humans, the P400–TIP60 complex and the Snf2-related CBP-activator protein (SRCAP) complex share compositional and functional similarities with SWR1 (ref. 19). ANP32E, a vertebrate-specific component of the P400–TIP60 complex facilitates H2A.Z eviction by recognizing a single glycine in the H2A.Z αC helix, thereby specifically discriminating H2A.Z from other H2A family members[7]. The SRCAP and P400–TIP60 complexes share core platform proteins: YL1, DMAP1, TIP49a, TIP49b, BAF53a and GAS41 (ref. 19).

Here, we set out to identify the human H2A.Z-deposition chaperone and investigated the mammalian SWC2 homolog, YL1, whose function was previously unknown. We found that YL1 specifically chaperones H2A.Z and deposits it into nucleosomes. The crystal structure of the acidic N-terminal domain (YL1 ZID) bound to the human H2A.Z–H2B dimer reveals extensive interactions between YL1 and H2A.Z, thus leading to a two-fold extension of the αC helix. We validated the importance of these interactions through both *in vivo* and *in vitro* experiments and showed that four residues define the specificity of H2A.Z with YL1. Finally, we showed that YL1 binding to H2A.Z is essential for the ATP-dependent exchange and identified YL1 as the major candidate involved in the final step of H2A.Z nucleosomal deposition.

RESULTS

YL1 N-terminal acidic domain directly binds H2A.Z–H2B

We have previously identified an acidic protein in the H2A.Z soluble complex (**Supplementary Fig. 1a–d** and ref. 7), YL1, the homolog of yeast SWC2 (ref. 17). To investigate this interaction further, we established a stable HeLa cell line expressing N-terminally FLAG-hemagglutinin (HA) epitope-tagged human YL1 (e-YL1) and then purified e-YL1 (**Fig. 1a**). Mass spectrometry analysis identified H2A.Z and H2B, and subunits of both the SRCAP and P400–TIP60 complexes associated with the e-YL1 complex (**Supplementary Fig. 1e**), results in agreement with previously published work[19]. Immunoblotting analysis confirmed the presence of H2A.Z in this complex but did not detect ANP32E or H2A (**Fig. 1b**).

YL1 exhibits three well-defined domains: an aspartate- and glutamate-rich N-terminal domain, a central DNA-binding domain, and a C-terminal proline-rich domain (**Fig. 1c** and **Supplementary Fig. 2a**). GST pulldowns with baculovirus-purified full-length glutathione S-transferase (GST)-tagged YL1 as bait showed that YL1 binds H2A.Z–H2B dimers but not H2A–H2B dimers (**Fig. 1d**). Only the N-terminal acidic domain (amino acids 1–110) of YL1 was required for binding (**Fig. 1e**). We further identified amino acids 1–69 as being sufficient for binding and termed this region the H2A.Z-interacting

[1]Equipe Labélisée Ligue Contre le Cancer, Département de Génomique Fonctionnelle et Cancer, Institut de Génétique et Biologie Moléculaire et Cellulaire (IGBMC), Illkirch, France. [2]Département de Biologie Structurale Intégrative, IGBMC, Illkirch, France. [3]Architecture et Réactivité de l'ARN, Université de Strasbourg, Institut de Biologie Moléculaire et Cellulaire du CNRS, Strasbourg, France. [4]Département Différenciation et Transformation Cellulaire, Institut Albert Bonniot, Grenoble, France. [5]These authors contributed equally to this work. Correspondence should be addressed to A.H. (hamiche@igbmc.fr) or C.R. (romier@igbmc.fr).

Received 28 September 2015; accepted 10 February 2016; published online 14 March 2016; doi:10.1038/nsmb.3189

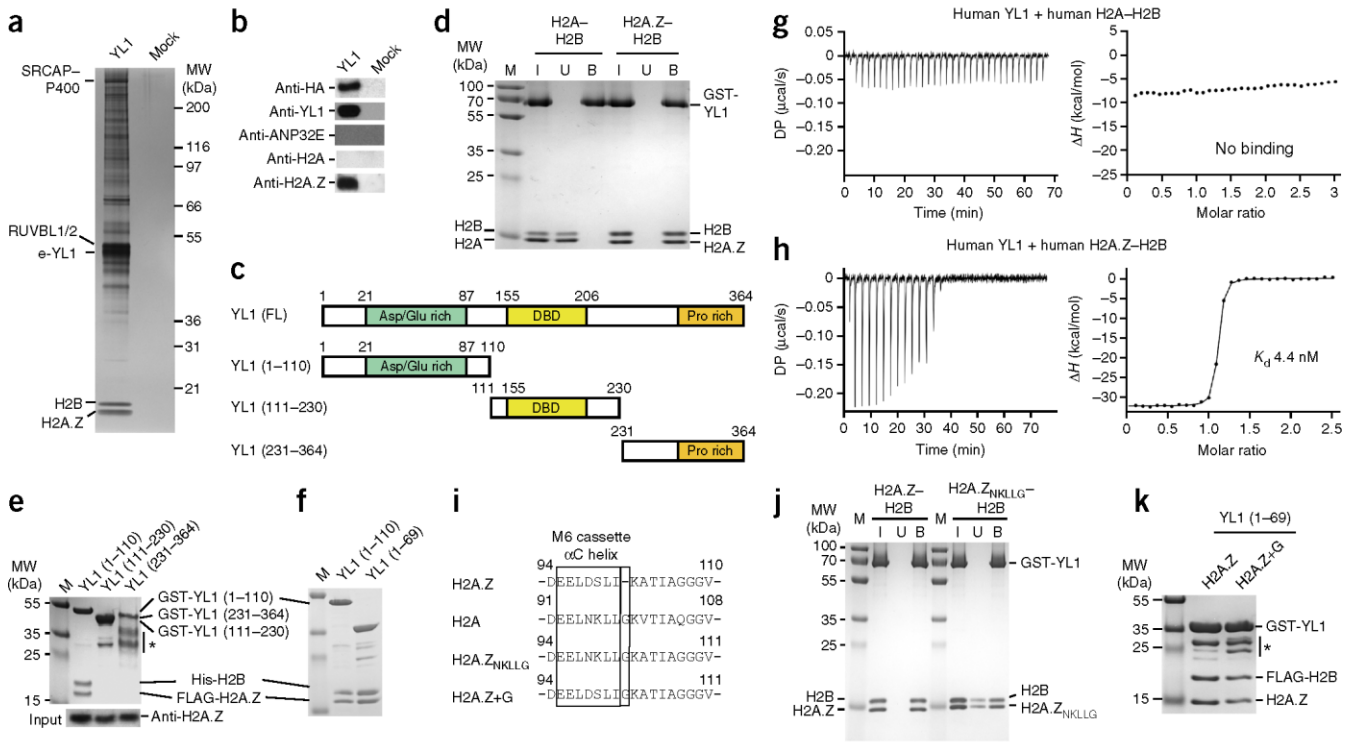

Figure 1 Human YL1 is an H2A.Z–specific binding protein. (**a**) Silver staining of e-YL1 and control (mock) complexes isolated from HeLa cells stably expressing e-YL1 or from naive HeLa cells, respectively. (**b**) Western blotting analysis of the e-YL1 complex and mock purifications shown in **a**. Each purification was probed for the presence of the tagged protein (anti-HA) as well as for YL1, ANP32E, H2A and H2A.Z. (**c**) Schematic representation of conserved regions of YL1: the aspartate- and glutamate-rich region (green), DNA-binding domain (DBD, yellow) and the proline-rich region (orange) are indicated. FL, full length. (**d**) GST pulldown assay with GST-tagged full-length YL1 and H2A–H2B and H2A.Z–H2B dimers. I, input; U, unbound; B, bound. (**e**) Top, GST pulldown assay as in **d**, with various YL1 constructs. Asterisk, degradation products. Bottom, western blot against H2A.Z in input. (**f**) GST pulldown assay for YL1 constructs 1–110 and 1–69 with H2A.Z–H2B. (**g**) ITC profiles of the titration of the human YL1 ZID (YL1 residues 1–69) with human H2A–H2B. Left, raw titration data of YL1 (1–69) injected into H2A–H2B. DP, power differential. Right, integrated heat measurements for the titration of YL1 with H2A–H2B. (**h**) ITC profiles of the titration of the human YL1 ZID (YL1 residues 1–69) with human H2A.Z–H2B. Left, raw titration data of YL1 (1–69) injected into H2A.Z–H2B. Right, integrated heat measurements for the titration of YL1 with H2A.Z–H2B. (**i**) Sequence alignment of the M6 cassettes of H2A.Z, H2A, the mutant H2A.Z$_{NKLLG}$ and the mutant H2A.Z+G. (**j**) GST pulldown assay with GST-tagged full-length YL1 and the H2A.Z–H2B and H2A.Z$_{NKLLG}$–H2B dimers. I, input; U, unbound; B, bound. (**k**) Purified coexpressed GST–YL1 ZID–H2A.Z–H2B complexes containing WT H2A.Z or mutant H2A.Z+G. In H2A.Z+G, an additional glycine was inserted at the end of the canonical H2A.Z αC helix, as found in H2A (G98). In gels throughout figure, molecular weight (MW) is indicated in kDa; M, marker. Asterisk, degradation products.

domain (YL1 ZID) (**Fig. 1f**). Using isothermal titration calorimetry (ITC), we observed no binding to H2A–H2B dimers (**Fig. 1g**), and we measured a K_d of 4.4 nM between the YL1 ZID and H2A.Z–H2B dimers (**Fig. 1h** and **Supplementary Table 1**).

Next, to determine the region of H2A.Z recognized by YL1, we used a candidate approach and focused on the H2A.Z αC helix (**Fig. 1i**), which is part of the M6 cassette (amino acids 89–110; human numbering) required for H2A.Z function[4,7,17,20] and contains the determinants for H2A.Z-specific interaction with ANP32E[7]. We performed a series of *in vitro* GST-pulldown experiments with YL1 and our H2A.Z$_{NKLLG}$-swapped mutant, in which the H2A.Z αC helix was substituted with the sequence of conventional H2A (**Fig. 1i**). In contrast to ANP32E, YL1 retained most of its ability to interact with the H2A.Z$_{NKLLG}$–H2B dimer (**Fig. 1j**) and was also able to bind mutant H2A.Z–H2B dimer[7] in which a single glycine was inserted in H2A.Z at the position of H2A G98 (**Fig. 1k**).

Structural basis of H2A.Z recognition by YL1

To shed light on the molecular basis of H2A.Z recognition by YL1, we solved the crystal structure of the YL1 ZID–H2A.Z–H2B complex. We cocrystallized the human YL1 ZID domain with an H2A.Z–H2B dimer in which the unstructured N-terminal tails of both histones had been removed. We collected a full data set at 2.7-Å resolution (**Table 1**) and solved the structure of the complex by molecular replacement, using the H2A.Z–H2B dimer taken from the structure of the H2A.Z nucleosome as a model. The initial electron density was sufficient for us to build the major parts of the YL1 protein and to modify the H2A.Z and H2B structures when necessary. We refined this initial model to 2.7-Å resolution through several cycles of model building and refinement (**Table 1**).

The ternary complex structure reveals that the YL1 ZID interacts extensively with the H2A.Z–H2B histone dimer, covering a substantial region of the dimer (**Fig. 2a**). The YL1 ZID contains two α-helices (αN1 and αN2) in its N-terminal region. The rest of the YL1 ZID does not adopt any specific secondary structure but makes substantial interactions with the histone dimer (**Fig. 2a** and **Supplementary Fig. 2b**).

YL1 binding to H2A.Z–H2B shares similarities but also has unique features compared with those of ANP32E. First, like ANP32E, YL1 binds to the same α3–αC region of H2A.Z, causing the same extension of the H2A.Z αC helix (**Fig. 2a–c** and **Supplementary Fig. 2b**). Although the C terminus of H2A.Z (docking domain) was also included in the construct used for crystallization, this region is not defined in the electron density and, owing to the extension of

Table 1 Data collection and refinement statistics

	Human YL1 ZID–H2A.Z–H2B
Data collection[a]	
Space group	$P2_1$
Cell dimensions	
a, *b*, *c* (Å)	36.12, 150.68, 96.61
α, β, γ (°)	90.00, 91.47, 90.00
Resolution (Å)	50–2.70 (2.75–2.70)[b]
R_{merge}	0.147 (0.700)
$I / \sigma I$	14.35 (1.97)
Completeness (%)	99.8 (97.6)
Redundancy	6.0 (5.4)
Refinement	
Resolution (Å)	44.25–2.70
No. reflections	26,955
R_{work} / R_{free}	0.177 / 0.243
No. atoms	
Protein	7,168
Water	7
B factors	
Protein	56.13
Water	36.73
r.m.s. deviations	
Bond lengths (Å)	0.01
Bond angles (°)	1.18

[a]Two crystals were used for data collection. Both data sets were processed independently, and the data were merged at the scaling step. [b]Values in parentheses are for highest-resolution shell.

the H2A.Z αC helix, cannot adopt the nucleosomal conformation required for essential interactions with the H3–H4 pair. We termed this region of YL1 interacting with the H2A.Z α3–αC region the ZID middle region 1 (ZIDM1).

Interestingly, the interface between the YL1 ZIDM1 and H2A.Z is more extensive than the ANP32E ZIDM1–H2A.Z interface, encompassing the YL1 αN2 helix and its immediate neighboring residues (**Fig. 3a,b** and **Supplementary Fig. 3a–c**). First, YL1 ZIDM1 contributes four hydrophobic residues—F29, Y30, Y34 and F37—to this interface (**Fig. 3a**). These residues form a hydrophobic core with H2A.Z L86, I90, I100 and I104, and H2B I61 and F65, which have been shown to be involved in interaction with ANP32E ZIDM1. Specifically, the side chains of YL1 F29, Y34 and F37 occupy nearly identical positions as those of ANP32E ZIDM1 M222, L218 and L221, respectively (**Supplementary Fig. 3b**).

The major exception concerns YL1 Y30, which is inserted more deeply at the interface at a position not occupied by any ANP32E residue. In addition, the YL1 Y30 side chain hydroxyl interacts directly with the carboxyl of H2A.Z D97 (N94 in H2A), which is part of the extended acidic patch of this variant[8] (**Fig. 3b**). The H2A.Z D97 carboxyl further interacts with the H2A.Z K101 side chain, which in turn binds to YL1 ZIDM1 D27. Such a network of hydrogen bonds is YL1 specific. In contrast, the hydrogen bond between H2A.Z T103 and H2B R72 observed in the ANP32E–H2A.Z–H2B structure is also conserved in the YL1–H2A.Z–H2B structure (**Fig. 3a**). H2A.Z residues K101, T103 and I104 are able to form the interactions described only because of the extension of the H2A.Z αC helix.

The parallel between YL1 and ANP32E extends further because YL1 also binds at the second anchoring point of ANP32E to the H2A.Z–H2B dimer (**Fig. 3c**). We termed this second anchoring point of the YL1 ZID the ZID middle region 2 (ZIDM2). Specifically, the interactions between YL1 ZIDM2 and H2A.Z–H2B involve interaction of the YL1 D43 carboxyl with the hydroxyls of S55 and S56 from H2B. Furthermore, the YL1 D45 carboxyl interacts with the side chain of H2A.Z R80 and the main chain of H2B I54. Finally, the side chain of Y46 from YL1 forms hydrophobic interactions with the side chains Y42 and M59 of H2B (**Fig. 3c**). These interactions are similar to those observed with ANP32E ZIDM2 and cannot account for H2A.Z-specific recognition[7].

We observed other interactions between YL1 ZIDM2 and H2A.Z–H2B. First, the T38 side chain of YL1 forms a hydrogen bond with the K57 side chain of H2B. Second, the YL1 E39 carboxyl forms a hydrogen bond with the H2A.Z T82 side chain (**Fig. 3c**). Interestingly, if the YL1 T38–H2B K57 interaction cannot account for specificity, the YL1 E39–H2A.Z T82 interaction is specific for H2A.Z, and T82 of this variant is an isoleucine in H2A (**Fig. 2c**). Of note, similar interactions have been observed with ANP32 ZIDM2: the hydroxyl of Y220 of ANP32E interacts with the K57 side chain of H2B, and the carboxyl of ANP32E residue D228 contacts the H2A.Z T82 side chain[7].

However, the YL1 ZID interacts much more extensively with the H2A.Z–H2B dimer than does ANP32E. After the YL1 ZIDM2, the C-terminal region of the YL1 ZID (YL1 ZIDC) follows the path of the DNA-binding groove of the H2A.Z–H2B dimer, entirely covering the DNA-binding surface of the histone pair (**Fig. 3d** and **Supplementary Fig. 3c,d**). The binding at this interface involves both hydrogen bonds and the formation of hydrophobic interactions. This interface involves residues 52 to 65 of the YL1 ZIDC and mostly residues from H2A.Z, although we also observed some interactions with H2B (**Fig. 3d**). Importantly, none of these interactions appeared to have a role in the specific recognition of H2A.Z. In contrast, YL1 ZIDC binding to the H2A.Z–H2B dimer prevents this dimer from binding DNA, both by steric hindrance and by changing the electrostatic potential of the DNA-binding surface (**Supplementary Fig. 3d**).

One surprising result of our structural analysis concerned the YL1 ZID N-terminal domain (YL1 ZIDN). This region, which encompasses residues 1–24 of YL1, is the most conserved region of the YL1 ZID (**Supplementary Fig. 1f**). In our structure, it is formed by a small extended peptide (residues 9–15) followed by the αN1 helix (residues 16–24). However, in the crystal, the YL1 ZIDN does not interact with the H2A.Z–H2B dimer bound to the rest of the YL1 ZID but instead contacts a symmetry-related YL1 ZID–H2A.Z–H2B complex. This contact includes a dimerization of both YL1 ZIDN αN1 helices and a specific interaction between the YL1 ZIDN and the symmetry-related H2A.Z–H2B dimer (**Supplementary Fig. 4a**).

Inspection of this latter interaction between the YL1 ZIDN and the H2A.Z–H2B dimer showed that the ZIDN interacts almost exclusively with H2A.Z. Notably most conserved YL1 ZIDN residues are found at this interface with the H2A.Z–H2B dimer (**Fig. 3e**). Specifically, we observed three major features at this interface. First, the fully conserved R10 of YL1 interacts with the acidic patch of H2A.Z in a manner highly reminiscent of the arginine anchor mechanism observed for the LANA peptide, the RCC1, CENP-C and Sir3 proteins, and the PCR1 complex bound to the nucleosome[21–25] (**Fig. 3e** and **Supplementary Fig. 4b**).

Second, at the heart of the ZIDN-H2A.Z interface, H2A.Z G92 provides specificity for this variant, because an asparagine at this position, as observed in H2A and the other H2A variants, affects binding (**Fig. 3e** and **Supplementary Fig. 4b**). Finally, we also observed a conformational change of the C terminus of the H2A.Z α2 helix and of the following L2 loop. Specifically, the H2A.Z α2 helix unfolds by one turn at its C terminus and, together with the L2 loop, adopts a specific conformation that contributes to the interaction of H2A.Z with YL1 αN1, notably bringing H2A.Z K74 into a position where its

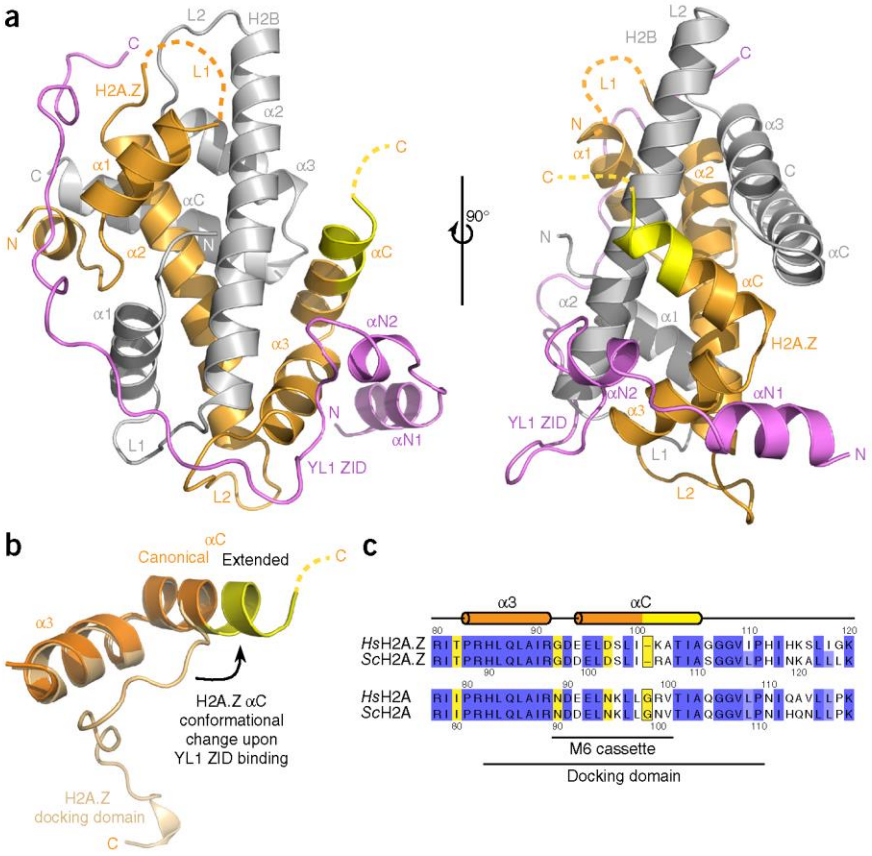

Figure 2 Human YL1 ZID extensively interacts with human H2A.Z–H2B and extends the H2A.Z αC helix. (**a**) Ribbon representations of the crystal structure of human YL1 ZID (violet) bound to the H2A.Z–H2B histone pair (orange and gray, respectively). The views are related by a 90° rotation from each other along the vertical axis. After YL1 ZID binding, the αC helix of H2A.Z doubles in length (extension colored in yellow; the H2A.Z C-terminal docking domain not seen in the density is shown as a dashed yellow line). (**b**) Conformational change of the H2A.Z αC helix after YL1 ZID binding. The extension of the H2A.Z αC helix prevents the C-terminal part of H2A.Z (docking domain; not seen in electron density) from adopting a conformation compatible with H3–H4 binding in the nucleosome. (**c**) Alignment of the sequences of the α3–αC region of H2A.Z (top) and of H2A (bottom) from human (*Hs*) and yeast (*Sc*), displayed with features identical to those of the YL1 sequences in **b**. Residues involved in the specific recognition of H2A.Z over H2A by YL1 are highlighted in yellow.

side chain can interact with the carboxyl of E22 (**Fig. 3e**,**f** and **Supplementary Fig. 4c**).

In light of this observed dimerization within the crystal, we analyzed the propensity of the YL1 ZID–H2A.Z–H2B complex to homodimerize. However, analytical ultracentrifugation of this complex unambiguously showed that it is a trimer with 1:1:1 stoichiometry (**Supplementary Fig. 5a**). We concluded that the observed dimerization is most probably due to crystal packing. Yet, considering the conserved interface between the YL1 ZIDN and H2A.Z and its specific features, we next asked whether this interface might be conserved within the same YL1 ZID–H2A.Z–H2B complex in solution. Using our structural data, we constructed a model of this trimer in which the YL1 ZIDN interacts with the same H2A.Z–H2B dimer as does the rest of the YL1 ZID, through amino acid interactions identical to those observed in the crystal structure. The analysis showed that such a trimer could be formed without causing steric clashes and would require only a rotameric change in H2A.Z R91 and repositioning of YL1 ZID residues E24, E25 and E26 (**Supplementary Fig. 5b**,**c**). These glutamate residues are less well defined in our electron density, thus suggesting that they form a hinge region. In support of this possibility, in *Saccharomyces cerevisiae*, additional residues are inserted between the equivalent residues of human E24 and E26, separating the ZIDN from the rest of the ZID (**Supplementary Fig. 1f**).

Biochemical characterization of the YL1–H2A.Z–H2B interaction

To further characterize the importance of the interactions between YL1 and the H2A.Z–H2B dimer, we studied the different interfaces through YL1 mutations and characterized the interactions between mutant YL1 and H2A.Z–H2B by coexpression and ITC measurements. We created several mutants of YL1 targeting the different interfaces: m1 (F29A Y30A Y34A F37A) for YL1 ZIDM1; m2 (D43A E45A Y64A) for YL1 ZIDM2; m1m2 (combination of mutants m1 and m2) for YL1 ZIDM; ΔC1 (residues 1–59) and ΔC2 (residues 1–49) for YL1 ZIDC; and ΔN (residues 27–69) for YL1 ZIDN (**Fig. 4a**).

Coexpression of these mutants with the H2A.Z–H2B pair showed that in the case of the m1 and m2 mutants the interaction was substantially weakened, whereas the double mutant m1m2 almost completely lost interaction with YL1 ZID (**Fig. 4b**). In contrast, ΔC1 and ΔC2 mutants were not impaired in their interaction with H2A.Z after coexpression and affinity purification (**Fig. 4c**). However, the subsequent purification step of these complexes by size-exclusion chromatography revealed a dissociation of the YL1 ΔC1 and ΔC2 mutants from H2A.Z–H2B, thus demonstrating the instability of these complexes. Finally, we also observed a weakened interaction in the case of YL1 mutant ΔN, thus demonstrating the participation of the YL1 ZIDN in overall H2A.Z–H2B recognition (**Fig. 4b**).

We then analyzed the binding of YL1 ZID mutants m1, m2, m1m2, ΔN and ΔC2 to the H2A.Z–H2B pair by ITC. We found that, consistently with the results of the coexpression experiments, mutants m1, m2, m1m2, ΔN and ΔC2 formed weaker interactions with the dimer, and the strength of the interaction varied by mutant (K_d values of 266, 317, 1,610, 192 and 730 nM, respectively, compared with 4.4 nM for wild-type H2A.Z; **Supplementary Table 1** and **Supplementary Fig. 6**).

We further complemented our analysis by expressing the YL1 mutants m1, m2, m1m2 and ΔN in in HeLa cells and purifying the resulting complexes (e-YL1 m1, e-YL1 m2, e-YL1 m1m2 and e-YL1 ΔN complexes). In contrast to wild-type YL1 (WT), all mutants (m1, m2, m1m2 and ΔN) were strongly impaired in their capacity to bind to the H2A.Z–H2B dimer (**Fig. 4d**). We conclude that the YL1 ZID domain is the minimal YL1 module essential for specific H2A.Z–H2B dimer recognition *in vivo* and that YL1 ZIDN also participates in this recognition.

We next extended this study to the yeast SWC2 ZID (residues 1–101) by investigating its interaction with yeast H2A.Z (HTZ1)–H2B (HTB1). We created three mutants of yeast SWC2 ZID, on the basis of our human YL1 mutants and our sequence alignment: m1 (I63A L65A L66A F67A), m2 (D73A D75A F76A) and ΔN (residues 46–101) (**Supplementary Fig. 5d**). Coexpression of the SWC2 ZID, HTZ1 and HTB1 proteins led to complex formation (**Supplementary Fig. 5e**).

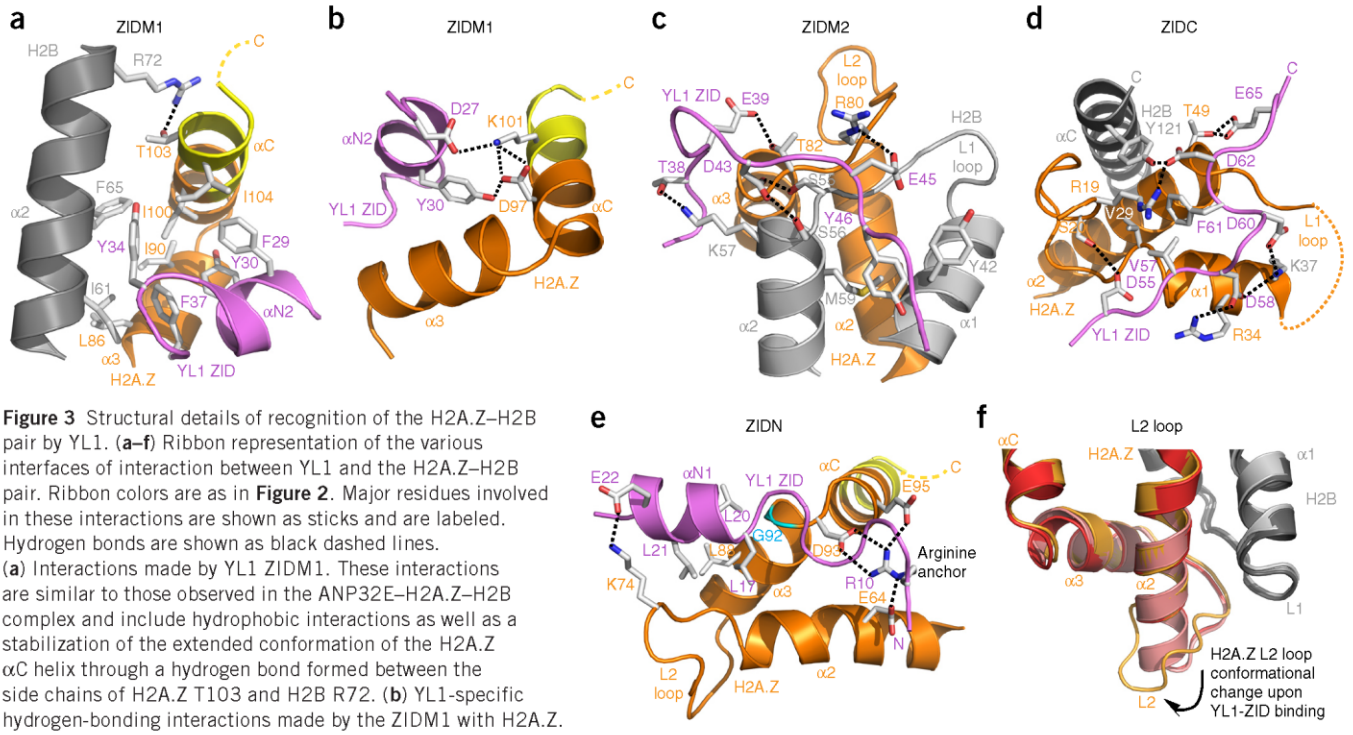

Figure 3 Structural details of recognition of the H2A.Z–H2B pair by YL1. (**a–f**) Ribbon representation of the various interfaces of interaction between YL1 and the H2A.Z–H2B pair. Ribbon colors are as in **Figure 2**. Major residues involved in these interactions are shown as sticks and are labeled. Hydrogen bonds are shown as black dashed lines. (**a**) Interactions made by YL1 ZIDM1. These interactions are similar to those observed in the ANP32E–H2A.Z–H2B complex and include hydrophobic interactions as well as a stabilization of the extended conformation of the H2A.Z αC helix through a hydrogen bond formed between the side chains of H2A.Z T103 and H2B R72. (**b**) YL1-specific hydrogen-bonding interactions made by the ZIDM1 with H2A.Z. (**c**) Interactions made by YL1 ZIDM2. These interactions are similar to those observed in the ANP32E–H2A.Z–H2B complex. (**d**) Interactions made by YL1 ZIDC. A nearly equivalent number of hydrophobic and hydrogen-bonding interactions are made at this interface, which cannot discriminate between H2A and H2A.Z. (**e**) Interactions made by YL1 ZIDN. These include an arginine anchor, as observed for the binding of the nucleosome to several transcription and epigenetic effectors. (**f**) Superposition of the H2A.Z α2 helix–L2 loop region from the YL1 ZID–H2A.Z–H2B complex (orange), the ANP32E ZID–H2A.Z–H2B complex (red) and the nucleosome (light red), and of the H2B α1 helix–L1 loop region of the same complexes (various grays). A conformational change of the H2A.Z L2 loop is apparent in the YL1 ZID–H2A.Z–H2B complex, which requires unfolding of one turn of the H2A.Z α2 helix at its C terminus.

The m1 and m2 mutants, similarly to the human YL1 mutants, strongly affected the interaction with HTZ1–HTB1. However, in contrast to human YL1, mutant ΔN had no strong negative effect on binding to yeast histones (**Supplementary Fig. 5e**), thus suggesting that there are some dissimilarities between the human and yeast systems.

To investigate these differences, we performed cross-species coexpression experiments between the human YL1 and yeast SWC2 and H2A.Z (HTZ1)–H2B (HTB1) components. Our results showed that human YL1 and yeast SWC2 displayed similar specificities toward human H2A.Z–H2B and yeast HTZ1–HTB1, including the specific

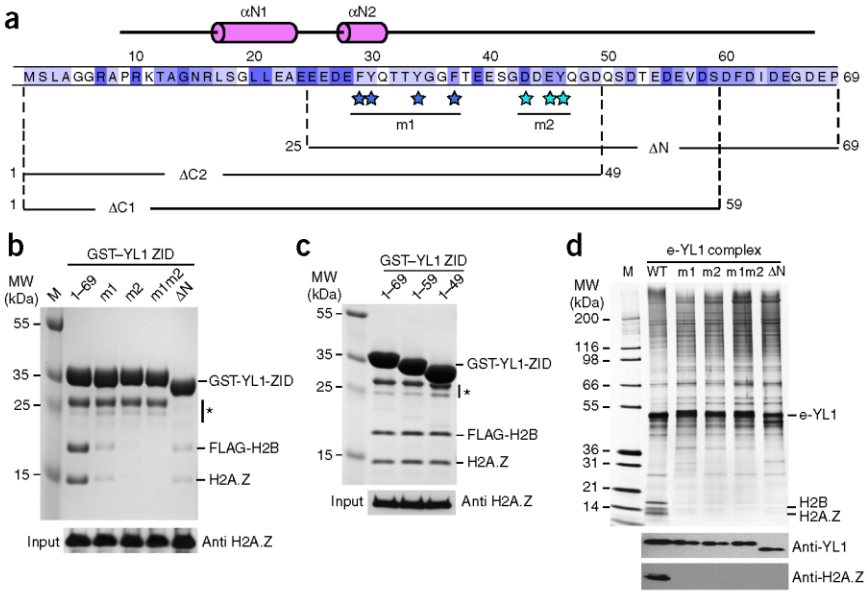

Figure 4 Binding between YL1 and H2A.Z involves extensive interactions in YL1. (**a**) Sequence of human YL1 ZID from alignment in **Supplementary Figure 1f**. Asterisks below the alignment indicate residues mutated in either mutant m1 (dark blue) or mutant m2 (light blue). Mutant YL1 ΔN was generated by deletion of the N-terminal region of YL1 (amino acids 1–25). Mutant YL1 m1 (F29A Y30A Y34A F37A) targeted the H2A.Z αC–binding region of YL1, mutant YL1 m2 (D43A E45A Y46A) targeted the first DNA-binding region of YL1, and mutant YL1 m1m2 (F29A Y30A Y34A F37A D43A E45A Y46A) included both m1 and m2 mutations. In mutant YL1 ΔC1 (amino acids 1–59), half of the YL1 region covering the H2A.Z–H2B DNA-binding region was removed, whereas in mutant YL1 ΔC2 (amino acids 1–49), this region was completely removed. (**b**) Top, GST pulldown of GST–YL1 ZID and H2A.Z–H2B complexes with WT H2A.Z and the indicated YL1 mutants. Bottom, western blot against H2A.Z in input. Asterisks, degradation products. (**c**) As in **b**, with the ΔC1 and ΔC2 YL1 mutants and WT H2A.Z–H2B. (**d**) Top, silver staining of FLAG-HA–purified e-YL1 WT and mutant (m1, m2, m1m2 and ΔN) complexes from HeLa cells. Bottom, western blot against YL1 and H2A.Z. MW, molecular weight; M, marker.

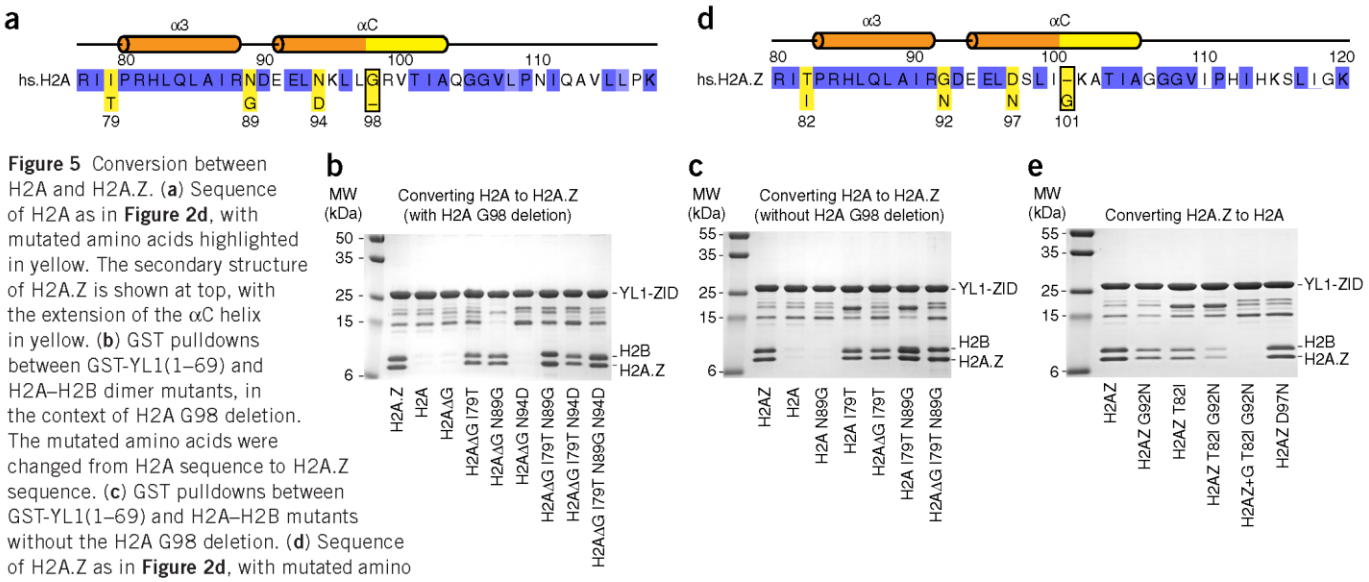

Figure 5 Conversion between H2A and H2A.Z. (**a**) Sequence of H2A as in **Figure 2d**, with mutated amino acids highlighted in yellow. The secondary structure of H2A.Z is shown at top, with the extension of the αC helix in yellow. (**b**) GST pulldowns between GST-YL1(1–69) and H2A–H2B dimer mutants, in the context of H2A G98 deletion. The mutated amino acids were changed from H2A sequence to H2A.Z sequence. (**c**) GST pulldowns between GST-YL1(1–69) and H2A–H2B mutants without the H2A G98 deletion. (**d**) Sequence of H2A.Z as in **Figure 2d**, with mutated amino acids highlighted in yellow. The secondary structure of H2A.Z is shown at top, with the extension of the αC helix in yellow. (**e**) GST pulldowns of GST-YL1(1–69) with H2A.Z–H2B mutants. The mutated amino acids were changed from H2A.Z sequence to H2A sequence. MW, molecular weight.

requirement of their N-terminal region (ZIDN) for proper binding to human histones but not to yeast histones (**Supplementary Fig. 5f,g**). We concluded that, despite their homology, human and yeast histones may have evolved to accommodate different functions.

Molecular basis of H2A.Z-specific recognition by YL1

To understand in depth the molecular basis of H2A.Z recognition by YL1, we further deleted or swapped specific H2A.Z and H2A amino acid residues and searched for a set of mutations that would either enable YL1 to bind to the H2A mutants or would disrupt the YL1 interaction with H2A.Z. We initially concentrated on generating mutations in H2A. Because our structural analysis had identified three residues of H2A.Z (H2A.Z T82 (H2A I79), G92 (H2A N89) and D97 (H2A N94)) that are important for YL1 binding to the H2A.Z–H2B dimer, in addition to the missing glycine in the H2A.Z αC helix, we substituted (or deleted) single or multiple amino acid residues of H2A with the respective H2A.Z amino acids (ΔG98, I79T, N89G and N94D). We studied YL1 binding to the H2A–H2B pairs bearing various combinations of mutations in H2A, first through protein coexpression experiments and then through ITC.

We first analyzed single mutations in H2A. Bearing in mind that residue G98 is present only in the H2A αC helix, we deleted it and analyzed the binding of YL1 to the mutant H2A ΔG98–H2B dimer (**Fig. 5a,b**). In this case, we observed no binding (**Fig. 5b**). We also observed the same result with the H2A N89G mutant (**Fig. 5c**). In strong contrast, the single point mutant H2A I79T showed interaction with YL1 (**Fig. 5c**), thus indicating that this mutant is important for creating an appropriate interface for binding.

Furthermore, we observed that double mutants H2A ΔG98 I79T, H2A ΔG98 N89G, and H2A I79T N89G, but not H2A ΔG98 N94D, showed binding, thus demonstrating the additive effect of the mutations and the importance of the ΔG98 and N89G mutations in overall binding. Notably, the binding of H2A I79T N89G was as strong as that of H2A.Z (**Fig. 5b,c**). In contrast, the triple mutants H2A ΔG98 I79T N89G and H2A ΔG98 I179T N94D and the quadruple mutant H2A ΔG98 I79T N89G N94D exhibited results similar to those observed with the double mutants in terms of increased binding (**Fig. 5b,c**).

We next complemented these analyzes with ITC measurements. As expected from our coexpression experiments, the single I79T mutation led to binding to YL1 in the high-nanomolar range (**Supplementary Fig. 6** and **Supplementary Table 1**). Interestingly, all other single mutants (ΔG98, N89G and N94D) induced binding, albeit in the micromolar range. More strikingly, the multiple mutants resulted in increased YL1 binding, and the K_d values for the mutant H2A–H2B pairs decreased steadily with increasing numbers of amino acid residues substituted in H2A, culminating with the quadruple mutant H2A ΔG98 I79T N89G N94D, which showed a K_d of 5.6 nM, a value almost identical to the K_d of 4.4 nM observed for the H2A.Z–H2B pair (**Supplementary Fig. 6** and **Supplementary Table 1**). We therefore concluded that all four studied residues contribute to the overall specific binding of YL1 to H2A.Z–H2B.

Finally, we made several single and multiple point mutants of H2A.Z, in which we substituted amino acid residues important for YL1 binding with the respective H2A residues. All mutants except H2A.Z D97N showed weaker binding (**Fig. 5d,e**). Importantly, the binding of YL1 was completely abrogated with the triple mutant H2A.Z G101 T82I G92N, a result in agreement with our crystal structure and the H2A-substitution experiments.

YL1 is an H2A.Z histone-deposition chaperone

Finally, we asked whether human YL1 acts in H2A.Z–H2B deposition or eviction. First, we analyzed in detail the ability of YL1 to selectively deposit H2A.Z–H2B dimers on an $(H3–H4)_2$ tetrameric particle (tetrasome) and to generate nucleosomes[7,26]. For a control, we also assayed the ability of YL1 to favor the deposition of H2A–H2B. First, we assembled $(H3–H4)_2$ tetrasomes incubated with increasing amounts of YL1–H2A.Z–H2B or YL1–H2A–H2B complexes for 30 min and then analyzed the deposition of histones onto DNA by electrophoretic mobility shift assay (EMSA) (**Fig. 6a**). Under these conditions, we observed no deposition of H2A–H2B to form nucleosomes (lanes 7–9). However, we observed a substantial amount of deposition of H2A.Z–H2B dimers by EMSA (lanes 4–6). We then tested the capacity of YL1 to evict H2A.Z from the nucleosome by adding YL1 alone to the H2A.Z nucleosomes in solution. For a

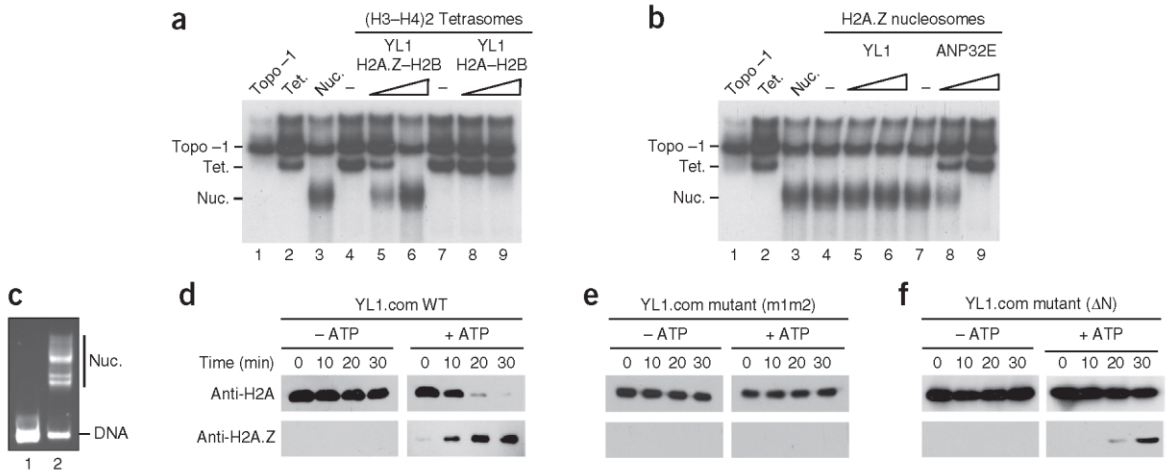

Figure 6 YL1 deposits H2A.Z–H2B dimers, and the YL1 complex exchanges H2A.Z–H2B. (**a**) Nucleosome deposition assay. Lane 1, DNA topoisomer–1 (topo –1); lane 2, tetrasomes (tet.) with two H3–H4 dimers bound; lane 3, preformed nucleosomes (nuc.); lanes 4–6, addition of increasing amounts of YL1 with H2A.Z–H2B dimer to tetrasomes; lanes 7–9, addition of increasing amounts of YL1 with H2A–H2B dimers to tetrasomes. (**b**) Histone eviction assay. Lane 1, DNA topoisomer –1; lane 2, reconstituted tetrasomes; lane 3, reconstituted nucleosomes; lanes 4–6, addition of increasing amounts of YL1 to H2A.Z nucleosomes; lanes 7–9, addition of increasing amounts of ANP32E to H2A.Z nucleosomes. (**c**) Ethidium bromide stain of reconstituted nucleosomes used in **d**–**f**. (**d**) Exchange assay. Samples are wild-type YL1 complex purified from HeLa cells and incubated with reconstituted H2A nucleosomes for increasing periods of time in the absence or presence of ATP. Western blots for the presence of H2A or H2A.Z in the nucleosomes. (**e**) Exchange assay as in **d**, but with YL1-mutant m1m2 complex purified from HeLa cells. (**f**) Exchange assay as in **d**, but with YL1 ΔN complex purified from HeLa cells.

control, we also assayed ANP32E for its ability to evict H2A.Z–H2B dimers from the nucleosome under the same conditions (**Fig. 6b**, lanes 7–9). Even at very high concentrations, YL1 was unable to evict H2A.Z from the nucleosome (**Fig. 6b**, lanes 4–6), thus showing that YL1 is a histone chaperone specific for H2A.Z deposition.

We next asked whether YL1 might facilitate H2A.Z exchange in an ATP-dependent manner when incorporated into the SRCAP and P400–TIP60 complexes. We carried out *in vitro* experiments, using e-YL1 complexes (WT, m1m2 and ΔN mutants) purified from HeLa cells (as described in **Fig. 4d**). We assembled conventional H2A nucleosomes onto 256-bp 5S DNA (**Fig. 6c**), immobilized them on magnetic beads and incubated them for different times with equivalent amounts of e-YL1 complex, or mutant e-YL1 m1m2 or e-YL1 ΔN complexes, in the presence or absence of ATP. The incubation of immobilized H2A nucleosomes resulted in rapid, highly efficient removal of H2A and deposition of H2A.Z after addition of ATP to the reaction (**Fig. 6d**). In contrast, the e-YL1-mutant complexes either were unable to exchange H2A for H2A.Z, in the case of the e-YL1 m1m2 complex (**Fig. 6e**), or were able to only very weakly exchange H2A for H2A.Z, in the case of the e-YL1 ΔN complex (**Fig. 6f**).

DISCUSSION

Here, we showed that YL1 acts as a deposition-and-exchange histone chaperone specific for H2A.Z. The crystal structure of human YL1 (YL1 ZID) in complex with an H2A.Z–H2B dimer reveals an extension of the αC helix of H2A.Z after binding to YL1, a structural feature similar to those in ANP32E and SWR1. However, in contrast to ANP32E, YL1 does not rely solely on the αC helix for binding and instead forms extensive interactions with the DNA-binding groove.

Through extensive mutational analysis, we identified the key residues involved in binding and specificity on H2A.Z. Mutation of only four amino acids on H2A—ΔG98, I79T, N89G and N94D—resulted in tight binding. The corresponding subset of these mutations on H2A.Z, G101, T82I and G92N indeed disrupted binding. Interestingly, whereas deletion of G98 on H2A was necessary for a complete restoration of binding, the insertion of a glycine into H2A.Z did not destroy binding, in stark contrast with results for ANP32E. These results indicate that the other amino acids have critical roles in both the stability and specificity of binding.

Whereas human YL1 and yeast SWC2 show a strong sequence conservation, and both are likely to be involved in the same types of deposition or exchange events, we presented evidence that speciation has occurred, because the SWC2 ZIDN was dispensable for yeast HTZ1–H2B binding but not for human H2A.Z–H2B binding. It is possible that this speciation might have affected the function of the YL1 and SWC2 proteins.

Finally, we observed that YL1 copurified with both the SRCAP–YL1 and P400–TIP60 complexes, but ANP32E was excluded from the YL1 complex. The implications of this specialization of the human system remain to be explored.

In conclusion, our study establishes the molecular basis and specificity of H2A.Z recognition by the histone-deposition chaperone YL1 and provides a framework for the investigation of the H2A.Z deposition-and-exchange pathway. Our findings also offer insights into the roles of YL1 in mediating histone transactions that regulate gene expression and genome integrity.

METHODS

Methods and any associated references are available in the online version of the paper.

Accession codes. Coordinates and structure factors have been deposited in the Protein Data Bank under accession codes PDB 5FUG.

Note: Any Supplementary Information and Source Data files are available in the online version of the paper.

ACKNOWLEDGMENTS

This work was supported by institutional funds from the Centre Nationale de la Recherche Scientifique (CNRS, France), the Institut National de la Santé et de la Recherche Médicale (INSERM, France), the Université de Strasbourg

(UDS) and the Université de Grenoble Alpes and by grants from the Ligue Nationale Contre le Cancer Equipe Labellisée (A.H.), the Fondation ARC pour la Recherche sur le Cancer (C.R.), the UDS Institute for Advanced Study (USIAS) (A.H.), IdEX Attractivité UDS (C.R.), the French National Research Agency (ANR; VariZome, contract ANR-12-BSV8-0018-01; Nucleoplat, contract NT09_476241), the French National Cancer Institute (INCA) (INCa_4496 and INCa_4454), la Fondation pour la Recherche Medicale, the French Infrastructure for Integrated Structural Biology (FRISBI; ANR-10-INSB-05-01) and by Instruct as part of the European Strategy Forum on Research Infrastructures (ESFRI). We thank the members of the European Synchrotron Radiation Facility/European Molecular Biology Laboratory joint structural biology group and staff of the synchrotron SOLEIL for use of beamline facilities and for help during data collection. We thank S. Tan (Pennsylvania State University) for fruitful discussions, C. Birck (IGBMC) for help with biophysical characterization and C. Da Veiga for help with ITC experiments.

AUTHOR CONTRIBUTIONS

C.M.L., M.M. and K.O. contributed equally to this work. C.M.L. performed complex purification and characterization, designed and analyzed the human mutants and contributed to the text. K.O. performed complex purification, chromatin assembly and eviction assays and analysis of yeast mutants. C.P. and A.O. built constructs and performed preliminary complex purification. I.S. generated baculovirus constructs and performed purification. M.I. performed preliminary pulldown assays. C.R. and M.M. solved the YL1 ZID–H2A.Z–H2B structure and designed the mutants. E.E. and M.M. performed the ITC experiments. S.D. provided important reagents. A.H., C.R. and S.D. designed experiments, analyzed data and wrote the paper.

COMPETING FINANCIAL INTERESTS

The authors declare no competing financial interests.

1. Larochelle, M. & Gaudreau, L. H2A.Z has a function reminiscent of an activator required for preferential binding to intergenic DNA. *EMBO J.* **22**, 4512–4522 (2003).
2. Raisner, R.M. *et al.* Histone variant H2A.Z marks the 5′ ends of both active and inactive genes in euchromatin. *Cell* **123**, 233–248 (2005).
3. Papamichos-Chronakis, M., Watanabe, S., Rando, O.J. & Peterson, C.L. Global regulation of H2A.Z localization by the INO80 chromatin-remodeling enzyme is essential for genome integrity. *Cell* **144**, 200–213 (2011).
4. Clarkson, M.J., Wells, J.R., Gibson, F., Saint, R. & Tremethick, D.J. Regions of variant histone His2AvD required for *Drosophila* development. *Nature* **399**, 694–697 (1999).
5. Faast, R. *et al.* Histone variant H2A.Z is required for early mammalian development. *Curr. Biol.* **11**, 1183–1187 (2001).
6. Hong, J. *et al.* The catalytic subunit of the SWR1 remodeler is a histone chaperone for the H2A.Z-H2B dimer. *Mol. Cell* **53**, 498–505 (2014).
7. Obri, A. *et al.* ANP32E is a histone chaperone that removes H2A.Z from chromatin. *Nature* **505**, 648–653 (2014).
8. Suto, R.K., Clarkson, M.J., Tremethick, D.J. & Luger, K. Crystal structure of a nucleosome core particle containing the variant histone H2A.Z. *Nat. Struct. Biol.* **7**, 1121–1124 (2000).
9. Mizuguchi, G. *et al.* ATP-driven exchange of histone H2AZ variant catalyzed by SWR1 chromatin remodeling complex. *Science* **303**, 343–348 (2004).
10. Kobor, M.S. *et al.* A protein complex containing the conserved Swi2/Snf2-related ATPase Swr1p deposits histone variant H2A.Z into euchromatin. *PLoS Biol.* **2**, E131 (2004).
11. Krogan, N.J. *et al.* A Snf2 family ATPase complex required for recruitment of the histone H2A variant Htz1. *Mol. Cell* **12**, 1565–1576 (2003).
12. Luk, E. *et al.* Stepwise histone replacement by SWR1 requires dual activation with histone H2A.Z and canonical nucleosome. *Cell* **143**, 725–736 (2010).
13. Wu, W.H. *et al.* N terminus of Swr1 binds to histone H2AZ and provides a platform for subunit assembly in the chromatin remodeling complex. *J. Biol. Chem.* **284**, 6200–6207 (2009).
14. Yen, K., Vinayachandran, V. & Pugh, B.F. SWR-C and INO80 chromatin remodelers recognize nucleosome-free regions near +1 nucleosomes. *Cell* **154**, 1246–1256 (2013).
15. Luk, E. *et al.* Chz1, a nuclear chaperone for histone H2A.Z. *Mol. Cell* **25**, 357–368 (2007).
16. Ranjan, A. *et al.* Nucleosome-free region dominates histone acetylation in targeting SWR1 to promoters for H2A.Z replacement. *Cell* **154**, 1232–1245 (2013).
17. Wu, W.H. *et al.* Swc2 is a widely conserved H2AZ-binding module essential for ATP-dependent histone exchange. *Nat. Struct. Mol. Biol.* **12**, 1064–1071 (2005).
18. Zhou, Z. *et al.* NMR structure of chaperone Chz1 complexed with histones H2A.Z-H2B. *Nat. Struct. Mol. Biol.* **15**, 868–869 (2008).
19. Cai, Y. *et al.* The mammalian YL1 protein is a shared subunit of the TRRAP/TIP60 histone acetyltransferase and SRCAP complexes. *J. Biol. Chem.* **280**, 13665–13670 (2005).
20. Jensen, K., Santisteban, M.S., Urekar, C. & Smith, M.M. Histone H2A.Z acid patch residues required for deposition and function. *Mol. Genet. Genomics* **285**, 287–296 (2011).
21. Barbera, A.J. *et al.* The nucleosomal surface as a docking station for Kaposi's sarcoma herpesvirus LANA. *Science* **311**, 856–861 (2006).
22. Makde, R.D., England, J.R., Yennawar, H.P. & Tan, S. Structure of RCC1 chromatin factor bound to the nucleosome core particle. *Nature* **467**, 562–566 (2010).
23. Armache, K.J., Garlick, J.D., Canzio, D., Narlikar, G.J. & Kingston, R.E. Structural basis of silencing: Sir3 BAH domain in complex with a nucleosome at 3.0 Å resolution. *Science* **334**, 977–982 (2011).
24. Kato, H. *et al.* A conserved mechanism for centromeric nucleosome recognition by centromere protein CENP-C. *Science* **340**, 1110–1113 (2013).
25. McGinty, R.K., Henrici, R.C. & Tan, S. Crystal structure of the PRC1 ubiquitylation module bound to the nucleosome. *Nature* **514**, 591–596 (2014).
26. Hamiche, A. & Richard-Foy, H. Characterization of specific nucleosomal states by use of selective substitution reagents in model octamer and tetramer structures. *Methods* **19**, 457–464 (1999).

ONLINE METHODS

Tandem affinity purification. The full-length human cDNA clone of YL1 (IMAGE 2958630) was purchased from Source Bioscience. The different full-length cDNAs were then cloned into the XhoI–NotI sites of the pREV-HTF retroviral vector[27] with standard techniques. e-H2A, e-H2A.Z and e-YL1 nuclear complexes and their respective mutants were purified by double immunoaffinity from human HeLa cells, as previously described[7]. Cell lines were obtained from the IGBMC cell culture facility and tested for mycoplasma contamination.

Mass spectrometry. Identification of proteins was carried out with an ion-trap mass spectrometer (ThermoFinnigan LTQ-Orbitrap Velos) or by the Taplin Biological Mass Spectrometry Facility (Harvard Medical School).

Antibodies. Antibodies used were as follows: monoclonal anti-FLAG M2 (Sigma); polyclonal anti-ANP32E (SAB2100124, Sigma); anti-HA 3F10 (Roche); monoclonal anti-YL1 (EXM10001, Epigex); and monoclonal anti-H2A.Z (EXM10007, Epigex). Validation for all commercial antibodies for western blotting is available on the manufacturers' websites . Rabbit polyclonal anti-H2A.Z and anti-H2A were generated by S.D. Original images of blots used in this study can be found in **Supplementary Data Set 1**.

Histones. Human histones were PCR amplified and cloned into a homemade bicistronic pET28b vector. H2B was cloned at the NdeI–BamHI sites of pET28b in frame with an N-terminal histidine tag, whereas FLAG-tagged H2A was cloned at the EcoRI–NotI sites. Human H2A.Z and its mutants were cloned at the EcoRI–NotI sites in frame with an N-terminal FLAG tag. The coding sequences of H2A.Z and H2A were mutated with Megaprime PCR to produce mutants. Histones were coexpressed with the different GST-YL1 or His-SWC2 constructs in BL21-CodonPlus-RIL (Stratagene) and purified as previously described[28]. Nontagged human recombinant wild-type or mutant core histones (H2A, H2A.Z, H2B, H3 and H4) were individually expressed in BL21-CodonPlus-RIL (Stratagene), purified and reconstituted as octamers or tetramers as previously described[29,30].

Preparation of recombinant YL1 and SWC2. The full-length and deletion mutants of YL1 were PCR amplified from pCMV-YL1 (Source Bioscience) and cloned into the pGEX-4X.1 vector (GE Healthcare) for bacterial expression and the pFastBac-GST vector (Invitrogen) for baculovirus expression. Yeast SWC2 was PCR amplified from yeast genomic DNA and inserted with NdeI and BamHI restriction sites in the pnEA-tH[31], which adds an N-terminal histidine tag followed by a thrombin-cleavage site. GST- and histidine-fusion proteins were purified by standard methods.

Purification of GST- and histidine-fusion complexes expressed in bacteria. GST- or histidine-fused YL1 and its mutants were coexpressed with H2A or H2A.Z (WT or mutant) and H2B in *Escherichia coli* strain BL21-CodonPlus-RIL-pLysS (Stratagene) at 22 °C with multiexpression bicistronic vectors, as previously described[7,28]. The soluble proteins were purified on glutathione Sepharose 4B beads (Amersham) or Ni-NTA agarose beads (Qiagen) with standard methods. Briefly, GST- or histidine-fusion proteins were incubated on either glutathione Sepharose or Ni-NTA agarose beads for 4 h at 4 °C in TGN buffer (20 mM Tris, pH 7.65, 3 mM $MgCl_2$, 0.1 mM EDTA, 10% glycerol, and 0.01% NP-40) containing 500 mM NaCl. Beads were then washed extensively in TGN containing 500 mM NaCl. Bound proteins were eluted either with 10 mM glutathione or with 250 mM imidazole. Samples were fractionated on SDS-PAGE and stained by colloidal blue.

In-gel histone deposition and eviction assay. Assays of histone H2A.Z deposition/eviction in the presence of the histone chaperone YL1 were performed with a negatively supercoiled DNA topoisomer −1 prepared from the 360-bp human α-satellite DNA[28]. This fragment was purified from an EcoRI digestion of the plasmid pBSK360, ^{32}P end-labeled, and circularized in the presence of ethidium bromide[26]. For the deposition assay, increasing amounts of recombinant YL1, mixed with stoichiometric amounts of H2A.Z–H2B or H2A–H2B dimers, were incubated with $(H3–H4)_2$ tetrasome particles reconstituted on negatively supercoiled human α-satellite DNA corresponding to topoisomer −1. Tetrasomes (1 μM) were incubated with increasing amounts (1 μM and 2 μM) of either YL1–H2A.Z–H2B or YL1–H2A–H2B for 30 min at 37 °C. For the eviction assays, recombinant H2A.Z octamers were reconstituted on negatively supercoiled human α-satellite DNA corresponding to topoisomer −1 with the salt jump method[26] and a histone to DNA ratio $r_w = 0.5$. Nucleosome substrates (1 μM) were then incubated with two different amounts of GST-YL1 (5 μM or 10 μM) for 30 min at 37 °C in 20 mM Tris-HCl, pH 7.5, 50 mM NaCl, 3 mM $MgCl_2$ and 0.01% BSA. The reaction products were analyzed on 4.5% native polyacrylamide gel in 1× TG (0.025 M Tris-HCl and 0.192 M glycine), run at room temperature for 2 h 45 min at 120 V. Control tetrasomes were assembled on circular DNA according to the salt jump method as previously described[26].

Histone eviction and exchange assay on bead-bound nucleosomes. The 256-bp fragment containing a sea urchin 5S RNA gene was gel-purified from an EcoRI digest of plasmid pLV405–10 (ref. 32) and PCR amplified to generate a biotinylated DNA fragment. The 3′-biotinylated 256-bp 5S DNA fragment was used to generate either H2A or H2A.Z mononucleosomes by the salt jump dialysis method[26]. For eviction assays, 50 ng of H2A.Z or H2A mononucleosomes was immobilized onto Dynabeads M-280 (Dynal) and then incubated with increasing amounts of either WT or mutant (m1, m2 or ΔN) YL1 complexes (2.5 μM, 5 μM and 10 μM) for 30 min at 37 °C. The bound protein–DNA complexes were purified with a magnetic particle concentrator (Dynal) by three washes with 20 mM Tris-HCl, pH 7.65, 150 mM NaCl, 3 mM $MgCl_2$, and 10% glycerol. The nucleosomes bound to the beads were directly eluted in SDS electrophoresis loading buffer and run on a 12% SDS PAGE gel, transferred to a PVDF membrane and blotted with either anti-H2A or anti-H2A.Z antibodies. For exchange assays, 50 ng of H2A mononucleosomes was immobilized onto Dynabeads M-280 (Dynal) and then incubated or not with increasing amounts of e-YL1 complex (2 μl, 4 μl and 8 μl) for 30 min at 37 °C. The bound protein–DNA complexes were purified with a magnetic particle concentrator (Dynal) by three washes with 20 mM Tris-HCl, pH 7.65, 150 mM NaCl, 3 mM $MgCl_2$, and 10% glycerol. The nucleosomes bound to the beads were directly eluted in SDS electrophoresis loading buffer and run on a 12% SDS PAGE gel, transferred to a PVDF membrane and blotted with either anti-H2A or anti-H2A.Z antibodies.

Preparation of recombinant YL1–H2A.Z–H2B complexes. The various constructs used were amplified by standard PCR procedures and inserted via NdeI and BamHI restriction sites in pET-MCN multiexpression vectors[31] pnEA-tH (YL1 constructs), which encodes an N-terminal histidine tag followed by a thrombin-cleavage site, and pnCS (H2A.Z and H2B constructs), which encodes either no tag or an N-terminal FLAG tag. For the H2A–H2B or H2A.Z–H2B pairs, further concatenation of the pnCS vectors was carried out to obtain a single vector coexpressing both partners, as previously described[31]. All complex subunits were coexpressed by cotransforming *E. coli* BL21(DE3) cells (Novagen) with pnEA-tH and pnCS vectors, as well as the pRare2 vector (Novagen). Cells were grown in 2× LB at 37 °C to an absorbance of 0.3 at 600 nm, and the temperature was then switched to 25 °C. Growth was then allowed to proceed until cells reached an absorbance of 0.8–1.0 at 600 nm. Expression was induced by addition of a final concentration of 1 mM isopropyl-β-D-thiogalactopyranoside (Euromedex), and cells were further grown overnight at 25 °C. Cells were collected by low-speed centrifugation, resuspended in buffer A (10 mM Tris-HCl, pH 8.0, and 200 mM NaCl) and lysed by sonication. The soluble fraction recovered by high-speed centrifugation was mixed with Talon resin (Clontech). After 1 h incubation, the supernatant was removed, and the resin was washed extensively with buffer A. The complex was then eluted from the resin by cleavage of the histidine tag with bovine thrombin (MP Biomedicals) overnight at 4 °C. For analytical purification, a second step of affinity purification was carried out against the FLAG-tagged H2B subunit with anti-FLAG M2 Affinity Gel purified immunoglobulin beads (Sigma). For the large-scale cultures, the supernatant was recovered and applied onto a gel-filtration column (HiLoad 16/60 Superdex 75, Amersham Pharmacia) equilibrated with buffer A and 2 mM DTT (Euromedex). The purified proteins were concentrated with Microsep 10K Omega centrifugal filters (Pall Filtron) to a final concentration of 12 mg/ml, as assayed with a Bio-Rad protein assay (Bio-Rad).

Crystallization and data collection. For crystallization attempts, various constructs of YL1 were used: 1–110 (full N-terminal domain), 1–92 (highly conserved N-terminal region) and 1–69 (ZID domain). Only the ZID-domain construct yielded crystals, thus suggesting that the longer constructs impaired

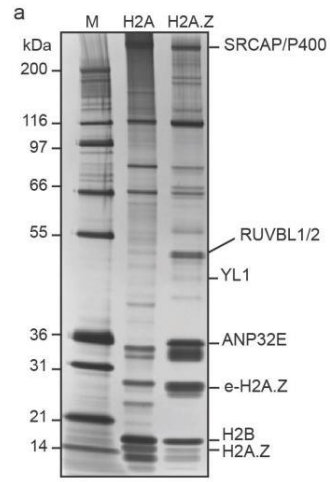

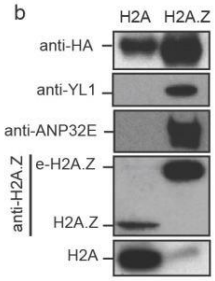

c

e-H2A.com			
Entry	Proteins	Peptides	
P78527-1	PRKDC	196	DNA repair
P09874	PARP1	58	
P13010	XRCC5	45	
P12956	XRCC6	43	
Q08945	SSRP1	31	FACT.com
Q9Y5B9	SUPT16H	48	
Q9Y265-1	RUVBL1	2	
Q9Y230	RUVBL2	3	
P55209	NAP1L1	17	histone chaperones
Q99733	NAP1L4	10	
Q13547	HDAC1	10	
P11021	HSPA5	11	
P11142-1	HSPA8	10	
P68431	H3	15	histones
P62807	H2B	27	
P0C0S8	H2A	29	
P0C0S8	H2A.Z	3	
P62805	H4	16	

d

e-H2A.Z.com			
Entry	Proteins	Peptides	
Q9Y4A5-1	TRRAP	221	p400/TIP60.com
Q96L91-2	EP400	107	
Q9H0E9-3	BRD8	31	
Q9NV56	MRGBP	4	
Q9H2F5-1	EPC1	21	
Q52LR7	EPC2	20	
Q92993-2	TIP60	15	
Q9NXR8-1	ING3	16	
Q15014	MRGX	3	
Q9UBU8	MRG15	3	
O95619	GAS41	6	SRCAP.com
Q9NPF5	DMAP1	32	
Q9Y265-1	RUVBL1	25	
Q9Y230	RUVBL2	29	
Q15906	YL1	11	
O96019-1	ACTL6A	17	
O43257	ZNHIT1	5	
Q6ZRS2-2	SRCAP	71	
Q9GZN1	ACTR6	7	
Q05BQ5-3	MBTD1	8	
P11142-1	HSPA8	23	DNA repair
P78527-1	PRKDC	81	
Q01831	XPC	7	
P49916-2	LIG3	6	
P52701-2	MSH6	3	
P43246	MSH2	5	
P18887	XRCC1	6	
P13010	XRCC5	17	
P12956	XRCC6	21	
P54727	RAD23B	7	
Q9BTT0	ANP32E	12	histone chaperones
P55209	NAP1L1	2	
Q99733	NAP1L4	1	
P68431	H3	3	histones
P62807	H2B	28	
P62805	H4	5	
P0C0S5	H2A.Z	32	

e

Entry	Protein	Peptides	
Q9Y4A5-1	TRRAP	80	p400/TIP60.com
Q96L91-2	EP400	54	
Q9H0E9-3	BRD8	11	
Q9NV56	MRGBP	1	
Q9H2F5-1	EPC1	11	
Q52LR7	EPC2	10	
Q92993-2	TIP60	6	
Q9NXR8-1	ING3	4	
Q15014	MRGX	3	
Q9UBU8	MRG15	3	
O95619	GAS41	10	SRCAP.com
Q9NPF5	DMAP1	15	
Q9Y265	RUVBL1	22	
Q9Y230	RUVBL2	27	
Q15906	YL1	11	
O96019-1	ACTL6A	14	
O43257	ZNHIT1	3	
Q6ZRS2-2	SRCAP	33	
Q9GZN1	ACTR6	5	
Q05BQ5-3	MBTD1	5	
P11142-1	HSPA8	18	DNA repair
P78527-1	PRKDC	52	
P49916-2	LIG3	3	
P52701-2	MSH6	26	
P43246	MSH2	23	
P13010	XRCC5	8	
P12956	XRCC6	8	
P62807	H2B	2	
P0C0S5	H2A.Z	3	

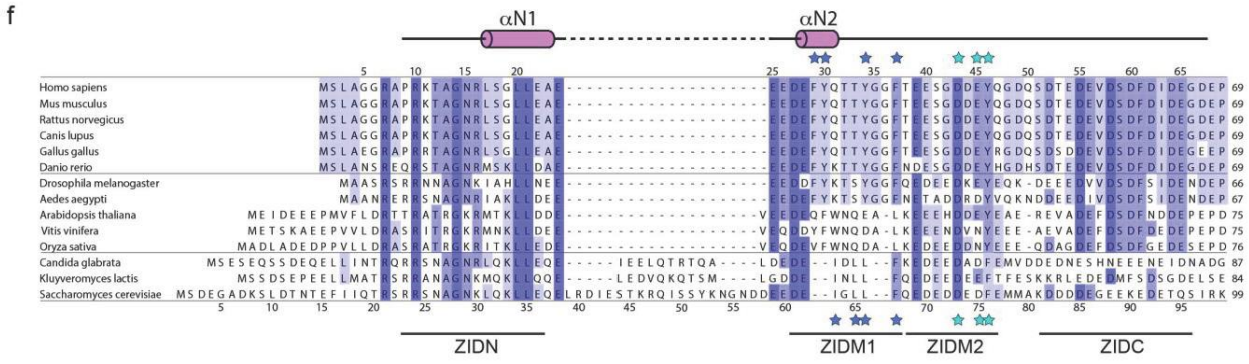

Supplementary Figure 1

YL1 specifically associates with the H2A.Z complex.

a) Silver staining of proteins associated with double immuno-affinity (FLAG-HA) purified e-H2A.com and e-H2A.Z.com complexes.
b) Western blotting analysis of the e-H2A.com and e-H2A.Z.com complexes shown in (a). Each complex was probed for the presence of the tagged protein (anti-HA) as well as for YL1, ANP32E, H2A and H2A.Z.
c) Mass spectrometry identification of additional proteins associated with e-H2A.com shown in (a). For each identified protein the number of unique peptides is given.
d) Mass spectrometry identification of additional proteins associated with e-H2A.Z.com shown in (a). For each identified protein the number of unique peptides is given.
e) Mass spectrometry identification of additional proteins associated with e-YL1.com shown in Figure 1a. For each identified protein the number of unique peptides is given.
f) Alignment of the YL1–ZID sequences from vertebrates, insects, plants and fungi. Conservation of the residues is represented by shades of blue. Numbering above and underneath the sequences corresponds to YL1 sequences from human and *S. cerevisiae* (yeast SWC2), respectively. Secondary structure elements of human YL1, as seen in the structure, are displayed above the alignment (helices, cylinders; coils, lines). The various regions of the YL1–ZID described in the text are indicated (ZIDN, ZIDM1, ZIDM2, ZIDC). Stars above and underneath the alignment mark residues of human YL1 and yeast SWC2 that were mutated in our study: m1 mutant (dark blue), m2 mutant (light blue), and m1m2 mutant (combination of m1 and m2 mutants).

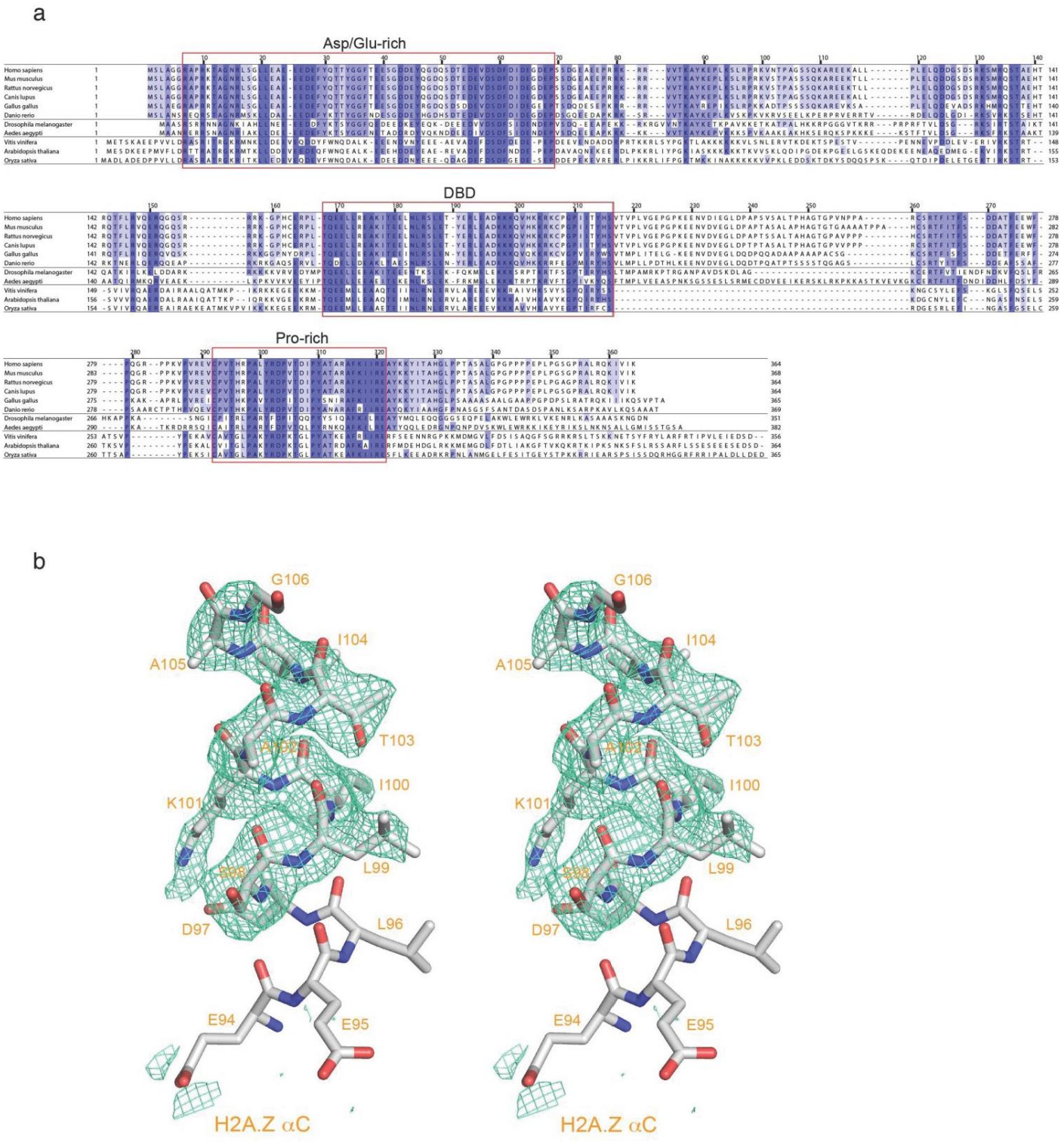

Supplementary Figure 2

Alignment of full-length YL1 and stereo view of the elongated αC helix.

a) Sequences of YL1 proteins from different organisms have been aligned. For clarity, fungi sequences have not been included since they are twice as long as their other homologs. See alignment of the YL1–ZID region in **Supplemental Figure 1f** for incorporation of the fungi sequences. Conservation is shown with different hues of blue (strong, dark blue; weak, light blue). Red boxes highlight the three main regions conserved throughout evolution (fungi display similar conservation patterns as those shown on this figure). Numbering above the sequences corresponds to the human protein.

b) Stereo view of the Fo–Fc simulated-annealing omit map contoured at 2.5 σ of H2A.Z elongated αC helix in the YL1–ZID–H2A.Z–H2B complex. Residues spanning the end of the canonical plus the extended part of the αC helix were removed prior to simulated-annealing.

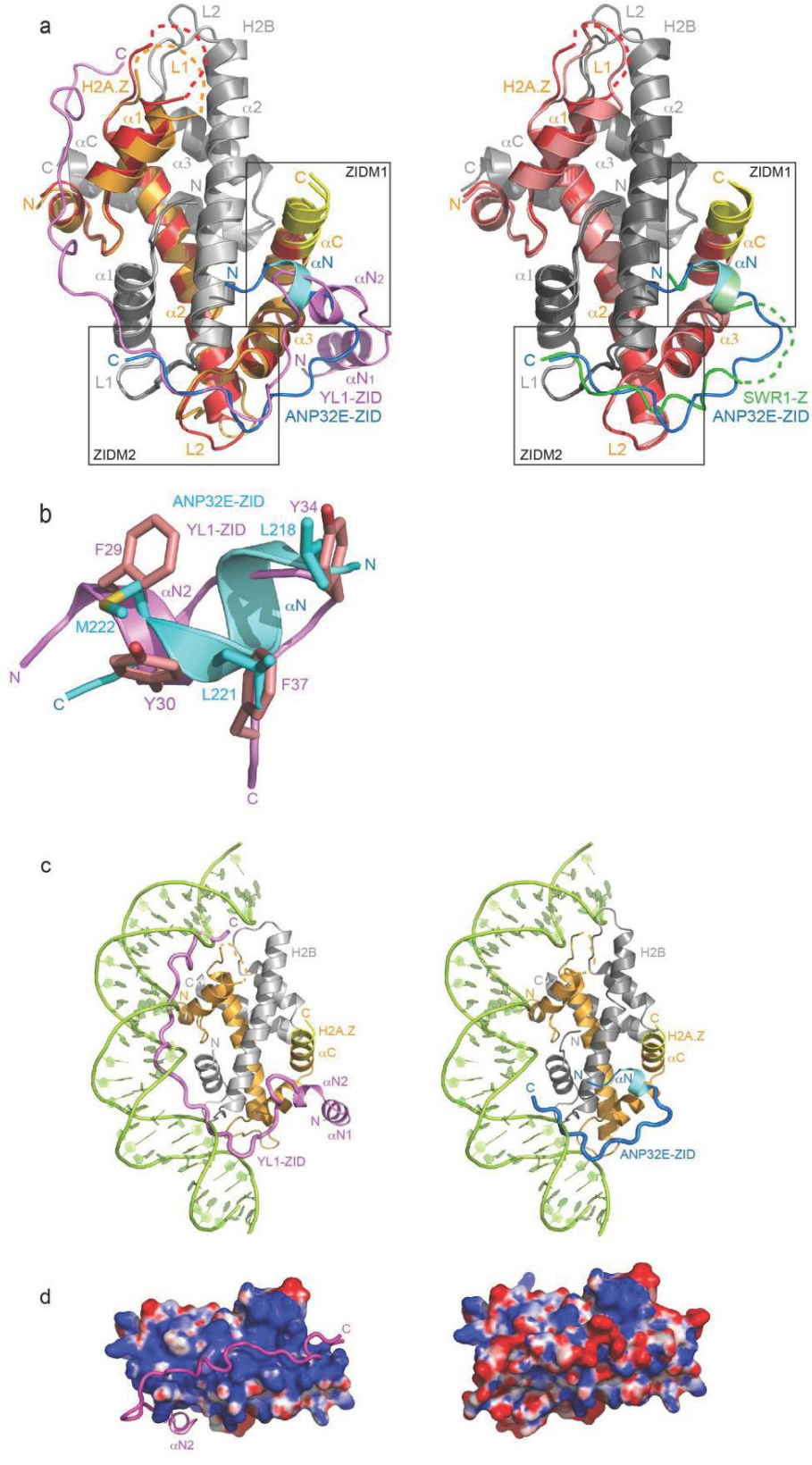

Nature Structural & Molecular Biology: doi:10.1038/nsmb.3189

Supplementary Figure 3

Human YL1, human ANP32E and yeast SWR1 all extend the αC helix, but only YL1 entirely covers the H2A.Z–H2B DNA-binding surface.

a) Superposition of (left) human YL1–ZID–H2A.Z–H2B (colored violet, orange and light gray, respectively) and human ANP32E–ZID–H2A.Z–H2B (colored blue, red and gray, respectively) complexes and of (right) human ANP32E–ZID–H2A.Z–H2B (colored blue, red and gray, respectively) and yeast SWR1–Z–H2A.Z–H2B (colored green, light red and dark gray, respectively) complexes. The common regions of interaction between YL1, ANP32E and SWR1 with the H2A.Z–H2B pair are boxed and labeled (ZIDM1 and ZIDM2). All H2A.Z histone chaperones extend H2A.Z αC helix, but only YL1 interacts extensively with the variant histone pair. In addition, YL1 binds to H2A.Z α3–αC region with a different conformation that ANP32E and SWR1, these latter chaperones showing high structural similarity.
b) Superposition of YL1 αN2 (violet) and ANP32E (blue) αN helices. The side chains of the hydrophobic residues of these helices that form hydrophobic interactions with the same set of hydrophobic residues from H2A.Z and H2B are shown as sticks. These hydrophobic residues from the histone chaperones occupy the same positions explaining that despite their difference in composition and the antiparallel orientation of the YL1 αN2 and ANP32E αN helices, they have the same effect in favoring H2A.Z αC helix extension. The only exception concerns YL1 Y30 that occupies a unique position and forms an YL1-specific hydrogen bonding network with residues from YL1 and H2A.Z.
c) Ribbon representation of (left) the superposed human YL1–ZID–H2A.Z–H2B (colored violet, orange and light gray, respectively) complex and H2A.Z–H2B histone pair (not shown) bound to a nucleosomal DNA region (green) and (right) the superposed human ANP32E–ZID–H2A.Z–H2B (colored blue, red and gray, respectively) complex and H2A.Z–H2B histone pair (not shown) bound to a nucleosomal DNA region (green). The C-terminal region of the YL1–ZID completely covers the H2A.Z–H2B DNA-binding surface.
d) Surface electrostatic potential of the DNA-binding region of the H2A.Z–H2B histone dimer (–5 k_BT, 5 k_BT; k_B, Boltzmann constant; blue: positive, red: negative). Left: The H2A.Z–H2B dimer displays a highly positive electrostatic potential in its DNA binding groove. The YL1–ZID binding to the H2A.Z–H2B dimer is displayed as ribbon. Right panel: Same as left, but with YL1–ZID included in the surface electrostatic potential calculation. Upon binding, the YL1–ZID not only covers the DNA-binding region of the H2A.Z–H2B dimer, but completely changes the electrostatic potential displayed on this face of the complex, rendering it more negative and thus, repulsive for DNA interactions.

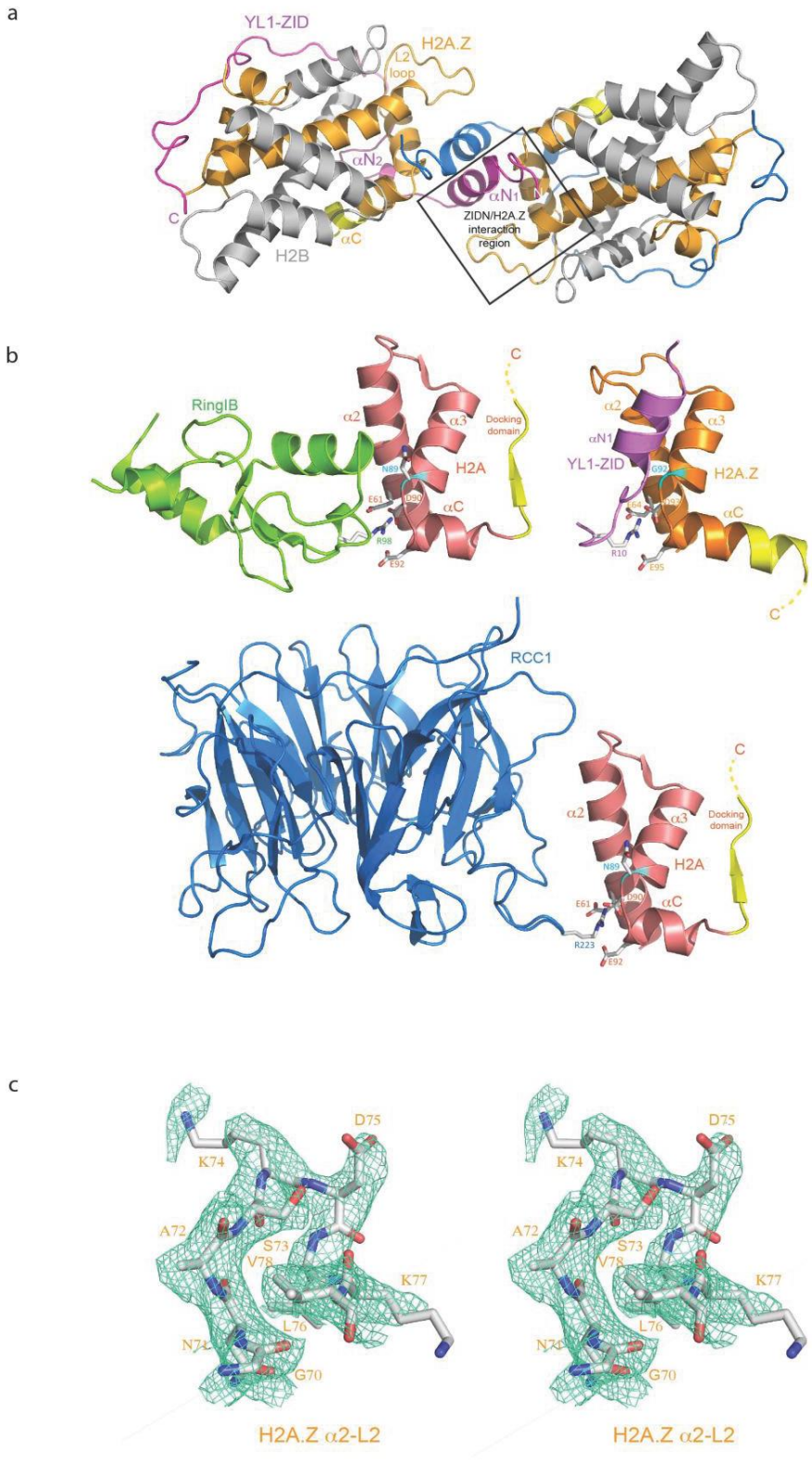

Nature Structural & Molecular Biology: doi:10.1038/nsmb.3189

Supplementary Figure 4

YL1 ZIDN has the ability to interact with H2A.Z–H2B through an arginine anchor feature.

a) Dimer of the YL1–ZID–H2A.Z–H2B complex observed in the crystal, where dimerization occurs through stacking of YL1 αN1 helices. At this dimeric interface, the N-terminal region of the YL1–ZID (ZIDN) from one complex interacts with the H2A.Z–H2B pair from a symmetry-related YL1–ZID–H2A.Z–H2B complex. This interaction between the ZIDN and the H2A.Z–H2B pair includes an arginine anchor, where an YL1 arginine binds to the acidic patch pocket of H2A.Z. This interaction is reminiscent of interactions made by several transcription and epigenetic effectors when bound to the nucleosome. In addition, ZIDN conserved residues are involved in this interaction that is only possible due to the presence of H2A.Z-specific G92 (an asparagine in H2A), enabling YL1–ZIDN to lay onto H2A.Z.
b) Examples of arginine anchor features. Upper left: RingIB (from PCR1 complex) binding to the H2A nucleosome (PDB code 4R8P). Bottom: RCC1 binding to the H2A nucleosome (PDB code 3MVD). Upper right: YL1–ZIDN binding to H2A.Z (this study). The position of H2A N89 and equivalent H2A.Z G92 are displayed, showing that the presence of a bulkier side chain at this position affects the way of binding of the effectors to H2A/H2A.Z.

c) Stereo view of the Fo–Fc simulated-annealing omit map contoured at 2.5 σ of H2A.Z α2 helix C-terminus and L2 loop in the YL1–ZID–H2A.Z–H2B complex. Residues spanning this region were removed prior to simulated-annealing.

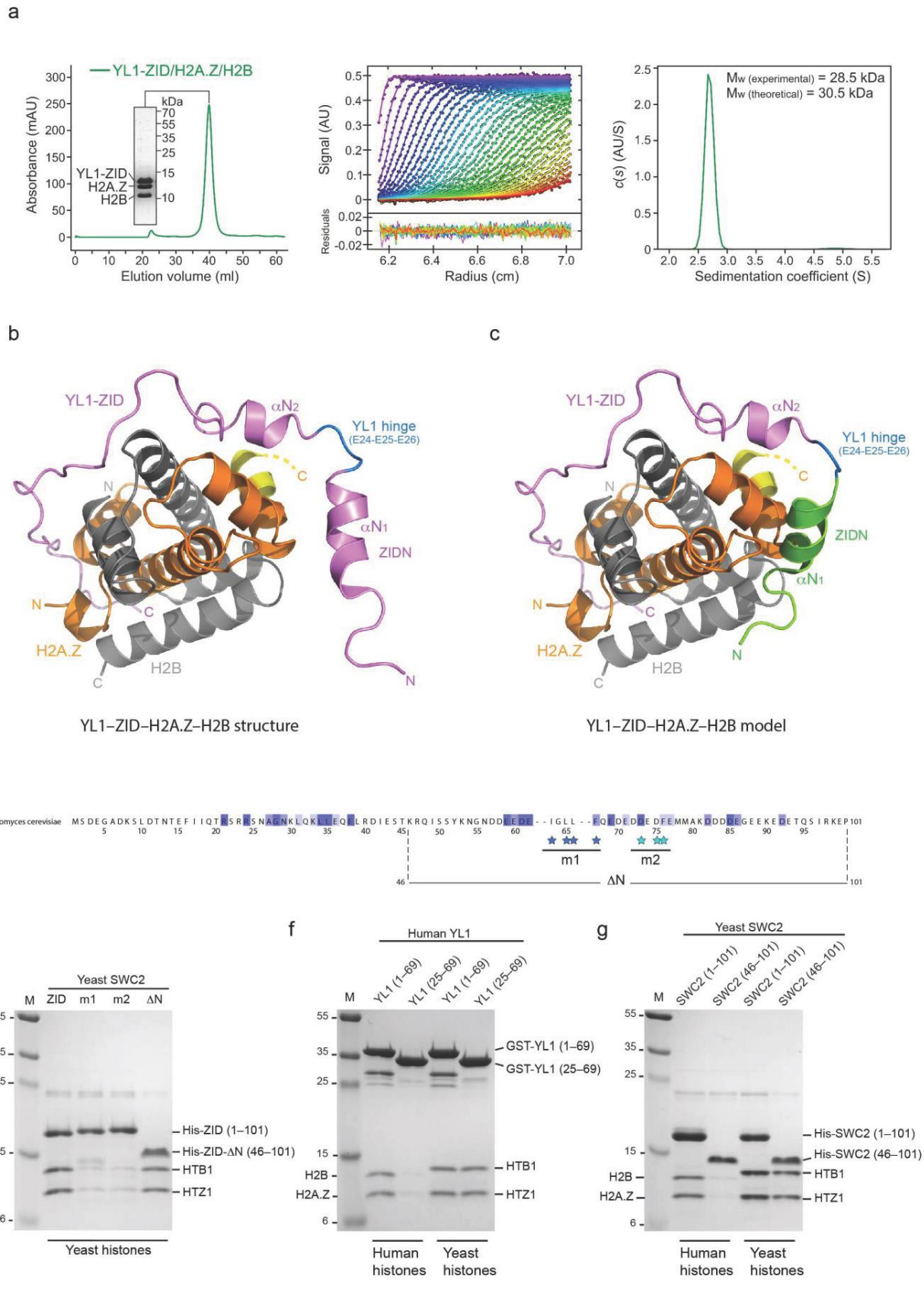
a
YL1-ZID/H2A.Z/H2B
Absorbance (mAU)
Elution volume (ml)
kDa
YL1-ZID
H2A.Z
H2B
Signal (AU)
Residuals
Radius (cm)
Mw (experimental) = 28.5 kDa
Mw (theoretical) = 30.5 kDa
c(s) (AU/S)
Sedimentation coefficient (S)
b
YL1-ZID
αN2
YL1 hinge
(E24-E25-E26)
αN1
ZIDN
H2A.Z
H2B
YL1–ZID–H2A.Z–H2B structure
c
YL1-ZID
αN2
YL1 hinge
(E24-E25-E26)
ZIDN
αN1
H2A.Z
H2B
YL1–ZID–H2A.Z–H2B model
d
Saccharomyces cerevisiae
m1
m2
ΔN
e
Yeast SWC2
M
ZID
m1
m2
ΔN
His-ZID (1–101)
His-ZID-ΔN (46–101)
HTB1
HTZ1
Yeast histones
f
Human YL1
YL1 (1–69)
YL1 (25–69)
GST-YL1 (1–69)
GST-YL1 (25–69)
H2B
H2A.Z
Human histones
Yeast histones
g
Yeast SWC2
SWC2 (1–101)
SWC2 (46–101)
His-SWC2 (1–101)
His-SWC2 (46–101)

Supplementary Figure 5

YL1 ZID–H2A.Z–H2B is monomeric in solution, and the YL1 and SWC2 N-terminal regions (ZIDN) are required for proper binding to human H2A.Z but not to yeast HTZ1.

a) Size exclusion chromatography purification profile on a Superdex 200 16/60 (left) and analytical ultracentrifugation (AUC) data of the YL1–ZID–H2A.Z–H2B complex. This analysis shows that the YL1–ZID–H2A.Z–H2B complex is monomeric in solution.

b) Ribbon representation of the YL1–ZID–H2A.Z–H2B complex as observed in the structure (left; ZIDN colored violet in a position interacting with a symmetry-related H2A.Z–H2B dimer) and of the model of the YL1–ZID–H2A.Z–H2B complex (right; ZIDN colored green interacting with the same H2A.Z–H2B dimer than the rest of the YL1–ZID domain). The model was created by modeling the ZIDN onto the H2A.Z–H2B dimer recognized by the rest of the YL1–ZID and using the mode of binding observed when it binds to a symmetry-related H2A.Z–H2B dimer. The model was then refined to obtain correct stereochemistry. This procedure showed that only the position of YL1–ZID residues E24, E25 and E26 (colored blue), which are part of the hinge region between YL1–ZID αN1 and αN2 helices, need to be moved to adapt to the new ZIDN conformation.

c) Sequence of yeast SWC2–ZID from alignment in figure 2b. Stars below the alignment indicate the residues mutated in either mutant m1 (dark blue) or mutant m2 (light blue). Mutant SWC2-ΔN was made by deletion of the N-terminal region of SWC2 (deletion of amino acids 1–45), including the αN1 helix. Mutant SWC2-m1 (I63A L65A L66A F67A) targeted the H2A.Z αC binding region of YL1 and mutant SWC2-m2 (D73A D75A F76A) targeted the first DNA-binding region of SWC2.

d) His-pulldowns with yeast His–SWC2–ZID and HTZ1/HTB1 complexes using WT HTZ1 and the indicated SWC2 mutants. The interaction between SWC2 and HTZ1–HTB1 is strongly affected by the m1 and m2 mutations but not by deletion of the N-terminal region (ΔN).

e) GST-pulldowns with human GST–YL1–ZID (1–69) or GST–YL1–ZID–ΔN (25–69) and human H2A.Z–H2B or yeast HTZ1–HTB1 dimers. The interaction between human YL1 and histones is dependent of its N-terminal region (ZIDN) for proper binding to human H2A.Z–H2B but not to yeast HTZ1–HTB1.'*', degradation products.

f) His-pulldowns with yeast His–SWC2–ZID (1–101) or His–SWC2–ZID–ΔN (46–101) and human H2A.Z–H2B or yeast HTZ1–HTB1 dimers. The interaction between yeast SWC2 and histones is dependent of its N-terminal region (ZIDN) for proper binding to human H2A.Z–H2B but not to yeast HTZ1–HTB1.

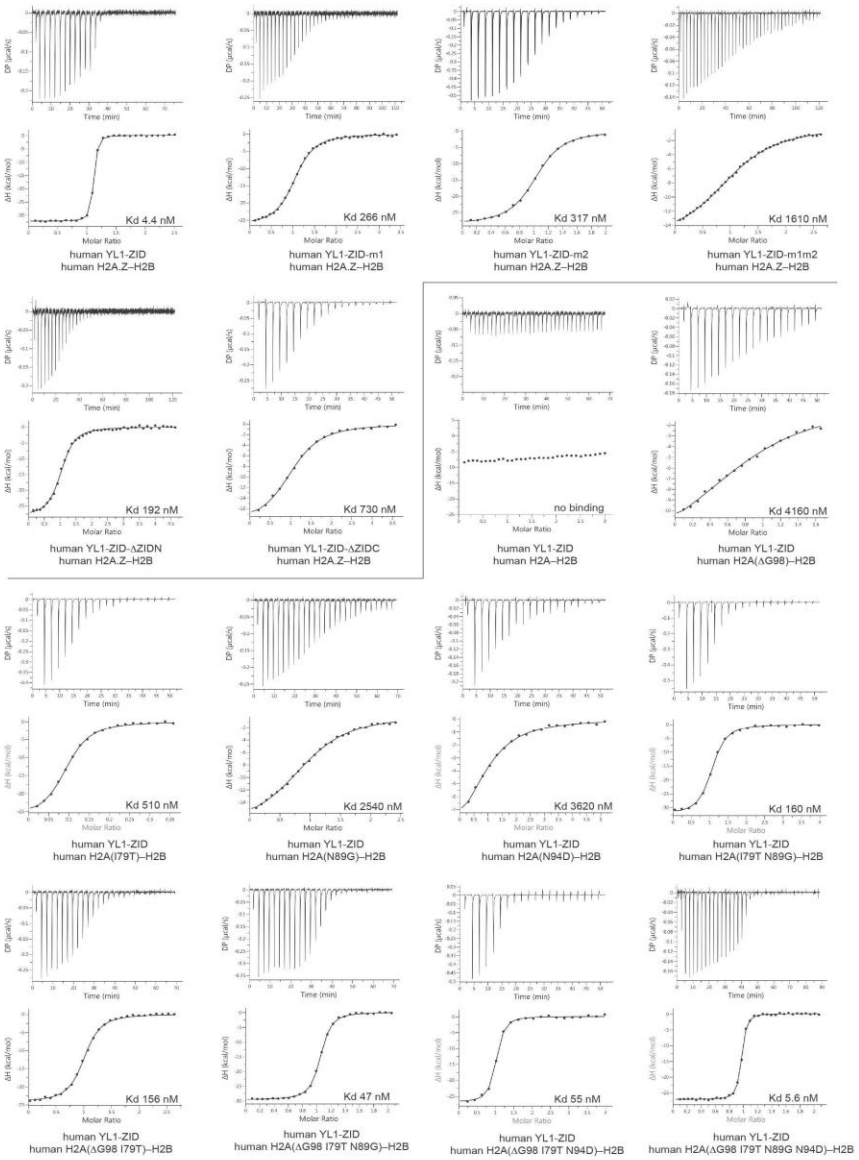

Supplementary Figure 6

ITC data.

ITC profiles of the titration of the human YL1–ZID (YL1 residues 1–69) by human H2A.Z–H2B and H2A–H2B pairs. The name of the proteins and mutants used are indicated underneath the data. For all experiments: top panel: raw titration data of YL1 (1–69) injected into H2A(.Z)–H2B. Bottom panel: integrated heat measurements for the titration of YL1 with H2A(.Z)–H2B.

Supplementary Table 1. Binding and thermodynamic parameters obtained from ITC experiments.

YL1 construct	Histone pair	Kd (nM)	ΔG (kcal.mol^{-1})	ΔH (kcal.mol^{-1})	−TΔS (kcal.mol^{-1})	N
YL1*	H2A.Z–H2B	4.4 ± 0.2	−11.4	−32.3 ± 0.1	20.9	1.07
YL1	H2A–H2B	no binding				
YL1-m1	H2A.Z–H2B	266 ± 9	−9.0	−26.6 ± 0.1	17.7	1.05
YL1-m2	H2A.Z–H2B	317 ± 11	−8.8	−28.8 ± 0.1	19.9	1.01
YL1-m1m2	H2A.Z–H2B	1610 ± 40	−7.9	−16.2 ± 0.1	8.3	1.11
YL1-ΔN	H2A.Z–H2B	192 ± 11	−9.2	−28.4 ± 0.3	19.3	1.02
YL1-ΔC	H2A.Z–H2B	730 ± 41	−8.4	−19.0 ± 0.3	10.6	1.05
YL1	H2A(ΔG98)–H2B	4160 ± 407	−7.4	−14.8 ± 0.7	7.4	0.89
YL1	H2A(I79T)–H2B	510 ± 28	−8.6	−26.8 ± 0.3	18.3	0.93
YL1	H2A(N89G)–H2B	2540 ± 114	−7.6	−18.1 ± 0.3	10.4	0.98
YL1	H2A(N94D)–H2B	3620 ± 540	−7.4	−10.7 ± 1.0	3.3	0.96
YL1	H2A(ΔG98 I79T)–H2B	156 ± 8	−9.3	−24.2 ± 0.1	14.9	0.98
YL1	H2A(I79T N89G)–H2B	160 ±9	−9.3	−32.4 ± 0.3	23.1	0.99
YL1	H2A(ΔG98 I79T N89G)–H2B	47 ± 2	−10.0	−29.7 ± 0.1	19.7	1.02
YL1	H2A(ΔG98 I79T N94D)–H2B	55 ± 6	−9.9	−26.9 ± 0.2	17.0	0.93
YL1	H2A(ΔG98 I79T N89G N94D)–H2B	5.6 ± 0.4	−11.3	−27.2 ± 0.1	16.0	0.94

* YL1 corresponds to human YL1–ZID (1–69). Histone pairs are human pairs deleted from their unstructured N-termini.

Nature Structural & Molecular Biology: doi:10.1038/nsmb.3189

Maria IGNATYEVA

Identification et caractérisation de HIRIP3 comme nouveau chaperon d'histone H2A

Résumé

Le génome des cellules eucaryotes est empaqueté dans la chromatine, dont l'établissement et la maintenance nécessitent des processus d'assemblage et de remodelage. Ce travail de thèse a été consacré à la caractérisation de deux facteurs de la machinerie d'assemblage de la chromatine

Le premier facteur étudié dans ce travail était HIRIP3, un homologue mammifère de la levure H2A.Z chaperon Chz1. Nous voulions vérifier si HIRIP3 est une chaperon d'histone par elle-même. Pour commencer, nous avons décrit l'interaction de HIRIP3 avec les histones *in vivo*. Ensuite, nous avons étudié la spécificité structurale de cette interaction *in vitro*. Nous avons caractérisé HIRIP3 comme une nouvelle chaperon d'histone H2A qui utilise le motif CHZ pour sa fonction.

La deuxième partie de ce travail a été axée sur le complexe de remodelage de la chromatine SRCAP. Nous avons cherché à décoder son réseau d'interaction et à décrire ses sous-complexes. Nous avons reconstitué le complexe de base YL1, SRCAP, TIP49A, TIP49B et H2A.Z / H2B en utilisant le système d'expression chez baculovirus. Notre protocole nous a permis de purifier un complexe de base adapté aux futures études structurelles par microscopie cryo-électronique.

Mots clés :
Epigénétique, chromatine, chaperon d'histone

Résumé en anglais

The genome of eukaryotic cells is packaged into chromatin, which establishment and maintenance require mechanisms of assembly and remodelling. This thesis work was dedicated to the characterization of two factors of chromatin assembly machinery.

The first factor studied in this work was HIRIP3, a mammalian homologue of yeast H2A.Z chaperone Chz1. We aimed to test whether HIRIP3 is a histone chaperone by itself. At first, we established HIRIP3 interaction with histones *in vivo*. After then, we studied the structural specificity of this interaction *in vitro*. We have characterized HIRIP3 as a novel H2A histone chaperone that utilizes the CHZ motif for its function.

The second part of this work was focused on SRCAP chromatin remodelling complex. We aimed to decipher its interaction network and to describe its sub-complexes. We have reconstituted YL1, SRCAP, TIP49A, TIP49B and H2A.Z/H2B core complex using baculovirus expression system. Our protocol allowed us to purify core complex suitable for future structural studies by cryo-electron microscopy.

Keywords :
Epigenetics, chromatin, histone chaperone